The Dissertation Committee for Andrew Jason Bowling certifies that this is

the approved version of the following dissertation:

Imaging the Cytoplasmic Domain of the Rosette

Cellulose-synthesizing Terminal Complex

Committee:

_____
R. Malcolm Brown, Jr., Supervisor

_____
David Vandenbout

_____
Jerry Brand

_____
Alan Lloyd

_____
Stanley Roux

Imaging the Cytoplasmic Domain of the Rosette

Cellulose-synthesizing Terminal Complex

by

Andrew Jason Bowling, B.S.

Dissertation

Presented to the Faculty of the Graduate School of

the University of Texas at Austin

in Partial Fulfillment

of the Requirements

for the Degree of

Doctor of Philosophy

The University of Texas at Austin

August 2005

For Jenna, Drew, and Owen

Acknowledgments

It is impossible to thank everyone who helped make this dissertation possible, but here I go anyway. I would like to thank Richard Santos for all of his help in the lab: cultures, equipment, supplies, and more. I would like to thank Dr. Dwight Romanovicz for all of his support, both moral and technical. I would like to thank Dr. Jin Nakashima for dropping everything to work with me whenever the need arose. I would like to thank David Nobles for all of his excellent conversations and suggestions. I would also like to thank Zack Barnes for being a great sounding-board. I would like to thank Dr. David Vanden Bout for allowing me to attend his group meetings, letting me use his AFM, and for all of his good advice. I would like to thank Dr. Malcolm Brown for getting me into microscopy in the first place, then bearing with me for seven years, and lately, for all of his hard work getting this dissertation read and corrected while trying to relax in Aspen! My love and appreciation go to my parents, John and LaDona Bowling for their loving patience and support, and my brother, Dan, for listening to all my rambling and nodding in the right places; and to my grandparents, Dale and Carol Bowling for their love and unflagging belief in the importance of education, and James and Mary Steinbrink for their love and their belief in good old-fashioned hard work. And finally, this dissertation would not be possible without the support of Jenna, Drew, and Owen, without which I would be totally lost.

Imaging the Cytoplasmic Domain of the Rosette Cellulose-synthesizing Terminal Complex

A new technique for imaging terminal cellulose-synthesizing complexes in isolated plasma membrane sheets was developed. Protoplasts bound to poly-L-lysine-coated substrates were burst in a sonicator bath. This process served to partially extract the plasma membrane, allowing the imaging of cellulose microfibrils through holes in the plasma membrane and the tracing of these cellulose microfibrils back to rosette terminal complexes. Using this new technique, the cytoplasmic domain of the rosette terminal complex was imaged. This domain appears to be hexagonal. A new model of the complete rosette cellulose-synthesizing terminal complex includes the hexagonal geometry of the cytoplasmic domain. This new technique effectively augments freeze-fracture data in providing new data about the structure-function of the cellulose-synthesizing terminal complex.

Table of Contents

List of Figures and Tables

Introduction

Cellulose is the major structural component of plant cell walls. This natural biopolymer is synthesized by a rather simple polymerization of two glucose units; however, the crystallization is a much more complex biophysical process resulting in the formation of a metastable arrangement of glucan chains in the microfibril. The formation of this metastable product is due to the presence of a highly ordered multi-enzyme complex which simultaneously polymerizes up to 1200 glucan chains in some systems (Itoh, 1989; Itoh *et al.*, 1983; Brown, 1996).

Initially, I was interested in the structural features of the metastable cellulose I microfibril, and my early investigations centered upon the microscopic analysis of the degradation of crystalline cellulose from the gram negative bacterium *Acetobacter xylinum* (Bowling *et al.*, 2001; Appendix 1). Significant strain is locked into the cellulose microfibrils during their biosynthesis. Because of the complex structural features of the crystalline phase of cellulose, it became all the more obvious that the biosynthetic apparatus, the terminal complex, was indeed a complicated structure itself. Until this study, the only structural data about the terminal complex had come from freeze-fracture. While freeze fracture was sufficient to prove the presence of an organized terminal complex, it could not answer questions about the organization of the catalytic component of cellulose synthase. With the successful cloning of the gene for cellulose synthase (Saxena *et al.*, 1990; Pear *et al.*, 1990), it became obvious that the cellulose synthase is composed of a hydrophobic region with 6 transmembrane segments and a globular catalytic domain. Thus, the catalytic region of the terminal complex is

1

located in the cytoplasm, not in the hydrophobic interior of the plasma membrane as revealed by the freeze-fracture technique. This cytoplasmic domain has only been observed in thin sections of the giant marine alga *Boergesenia* (Kudlicka *et al.*, 1987) but has never been observed for rosette terminal complexes from vascular plants.

The cellulose synthesizing complex was originally hypothesized by Roelofsen (1958) to be a multimeric component at the end of a growing microfibril. Hints at this were shown by Robards (1969) in sectioned materials examined by transmission electron microscopy (TEM); however, the first concrete evidence came from the studies of Brown and his colleagues using the technique of freeze-fracture (Brown and Montezinos, 1976; Mueller and Brown, 1980). From 1976 until 1999, the evidence that terminal complexes synthesize cellulose had been largely circumstantial, relying on the association of ordered arrays of particles with microfibril impressions. In 1999, Kimura *et al.* used the freeze-fracture replica-labeling (FFRL) technique to demonstrate for the first time that the catalytic region of cellulose synthase was indeed a member of the rosette terminal complex.

Over the years, the structure of the terminal complex has been of great interest and debate. To this day, freeze fracture has been the method of choice for imaging terminal complexes; however, the data generated by this technique is limited to the hydrophobic interior of the lipid bilayers. As the bilayers of biological membranes are split apart during the freeze-fracture process, the hydrophobic regions of transmembrane proteins are cleaved. For this reason, only cross-sectional images of the transmembrane regions of transmembrane proteins can be generated by this technique. Furthermore,

because cellulose microfibrils exist on the exterior of plant cells and not in the hydrophobic interior of the bilayer, only microfibril impressions can be seen in these replicas, not the actual microfibrils.

Recently, new data regarding the number and types of cellulose synthase enzymes which must be present in a single terminal complex have been reported (Doblin *et al*., 2002; Scheible and Pauly, 2004; Saxena and Brown, 2005; Somerville *et al*., 2004). Furthermore, various other proteins have been hypothesized to be associated with the cytoplasmic domain of the terminal complex (Delmer, 1999; Somerville *et al*., 2004). CesA genes are predicted to have several transmembrane regions and a large cytoplasmic domain; however, as mentioned above, the only proof of this large cytoplasmic domain has come from thin-sections of the marine alga *Boergesenia* (Kudlicka *et al*., 1987). This organism has large linear terminal complexes which can reach almost one micron in length and which synthesize microfibrils having nearly 1200 glucan chains (Brown, 1996). These linear terminal complexes were found to protrude approximately 35 nm into the cytoplasm of the cell. The success of this study was possible due to the large size of these linear terminal complexes. Because rosette terminal complexes are approximately 25 nm in diameter and are thought to synthesize only 36 glucan chains, the successful visualization of rosette terminal complexes by thin-sectioning is unlikely. For these reasons, the cytoplasmic domain of rosette terminal complexes from vascular plants has never been directly imaged. Therefore, we decided to investigate whether the rosette terminal complex does indeed have a large cytoplasmic component, as predicted by

genetic analysis of individual CesA sequences and implied by evidence gained from analysis of linear terminal complexes.

Because neither sectioning nor freeze-fracture has a reasonable chance to yield images of the cytoplasmic domain of intact rosette terminal complexes, a different technique was sought and developed. In order for nascent cellulose microfibrils to be extruded to the exterior of a cell, active rosette terminal complexes must be located in the plasma membrane. Therefore, a procedure was utilized in the current study for the isolation of patches of plasma membrane by binding cells to surfaces coated with poly-L-lysine (Heuser, 2000, Mazia *et al.*, 1975). The fact that terminal complexes make a large, microscopically identifiable product was used originally to identify terminal complexes based on their association with microfibril impressions (Brown and Montezinos, 1976; Mueller and Brown, 1980). By selecting an organism which is actively synthesizing a large amount of cellulose at the time that the plasma membrane sheets are isolated, the chances of finding a cellulose microfibril and tracing it back to its terminus are increased. Therefore, the selection of the organism to use is critical to this investigation.

During this long process of trying to find the ideal organism, the isolation of plasma membranes from *Boergesenia* was attempted based on the fact that the alga has very large terminal complexes. Also, *Boergesenia* has correspondingly large microfibrils which aid in locating these structures under the electron microscope (see Appendix 2). Furthermore, when wounded, this organism spontaneously re-organizes its cytoplasmic organelles into many spherical aplanospores. These aplanospores begin to synthesize cellulose very soon after they have formed. Unfortunately, it was found that these

4

nascent aplanospores also secrete an isotropic coating which prevents the isolation of plasma membranes by attaching them to a poly-L-lysine coated surface.

Another organism tested was fibers from *Gossypium hirsutum.* Cotton fibers are known to synthesize large quantities of nearly pure cellulose during the deposition of the secondary cell wall. The transition from primary cell wall deposition to secondary wall deposition occurs at characteristic intervals for *in vitro*-cultured cotton ovules (usually at 14 days post-anthesis) (Seagull, 1990). In 2000, Feng and Brown published a technique for the growth of submerged-fibers on *in vitro*-cultured cotton ovules. The walls of these submerged fibers are more easily accessible to wall-degrading enzymes because they are fully hydrated. In contrast, even living cotton fibers from the surface of the ovule in contact with air requires the use of vacuum infiltration to allow wall-degrading enzymes to coat the fibers and begin to degrade the cell walls (Gould *et al.*, 1986). As the long fibers become weaker due to the removal of the cell walls, they begin to break apart. Because each cotton fiber has only one nucleus, and that nucleus is located in the base of the epidermal cell of the seed coat, the pieces of cotton fiber which break away are anucleate. These anucleate structures are therefore termed cytoplasts, not protoplasts. Plasma membrane sheets were isolated from these cotton cytoplasts and found to have ordered arrays of cortical microtubules. Unfortunately, these cytoplasts had lost the ability to synthesize cellulose during the rather lengthy isolation procedure, and they were not useful starting materials for our investigation (see Appendix 3).

Plasma membrane sheets were isolated from *Arabidopsis* suspension culture cells (see Appendix 4). These isolated plasma membrane sheets were not capable of

synthesizing cellulose *in vitro*; however, intact protoplasts were able to generate new cellulose microfibrils soon after removal from the wall-degrading enzyme solution. These plasma membrane sheets were analyzed by TEM. Although cellulose microfibrils could be seen after the treatment of plasma membrane sheets with chloroform/methanol to remove the lipids, no cellulose microfibrils could be seen under untreated plasma membrane sheets.

Ultimately, an ideal organism was found which allowed the exploration of new technical approaches towards the problem of identifying the cytoplasmic domains of terminal complexes. Success was finally achieved when protoplasts were produced from suspension-cultured tobacco BY-2 cells which were used to isolate plasma membrane sheets. The development of a new technique to visualize the cytoplasmic domains of rosette terminal complexes has provided further evidence for the presence of a large cytoplasmic component to the rosette terminal complex as predicted by the protein sequencing data.

Cellulose

Cellulose is a highly crystalline homopolymer of beta 1,4-linked glucose residues. Each glucose residue is rotated 180 degrees with respect to its intra-chain neighbors, making the unit cell cellobiose instead of glucose (Gardner and Blackwell, 1974). Although cellulose can exist in at least four different crystalline allomorphs (cellulose I-IV), in nature cellulose chains crystallize almost exclusively into the cellulose I allomorph. This allomorph is characterized by having a parallel arrangement of the glucan chains.

Cellulose II, on the other hand, has an anti-parallel arrangement of glucan chains. When cellulose I is dissolved and reprecipitated, the result is cellulose II. This is indicative of the fact that cellulose II is actually the most thermodynamically stable form of cellulose (Ranby, 1952; Brown, 1996). In fact, based on this information, if beta-1,4 glucans were to be synthesized individually by a single catalytic subunit of cellulose synthase, the resulting product would be a folded chain cellulose II molecule. Taking this one step further, we can see that it is the molecular scaffolding of many cellulose synthase enzymes into one terminal complex which is responsible for the fact that 180 billion tons of cellulose I are synthesized each year (Delmer, 1999). Therefore, elucidation of the structure of the terminal complex could have profound effects on our understanding of this extremely commercially valuable biopolymer.

Just as the presence of multiple cellulose synthase enzymes in a single terminal complex gives rise to the predominance of the cellulose I allomorph, the shape of the terminal complex itself determines the cross-sectional shape of the cellulose microfibrils generated by that terminal complex (Brown, 1996). In bacteria and some algae, linear terminal complexes predominate. The cross-sections of the microfibrils generated by these linear terminal complexes are correspondingly rectangular. In vascular plants, the shape of the terminal complexes is hexagonal.

Cellulose microfibril data

Each rosette is thought to synthesize an elementary microfibril of 36 glucan chains, meaning that each of the six subunits of the rosette synthesize 6 glucan chains (Herth,

1983; Reiss *et al*., 1984; Delmer, 1999; Kimura *et al*., 1999; Perrin 2001; Doblin *et al*.,

2002). These elementary fibrils are usually stated as being approximately 3-3.5 nm in

diameter (Herth, 1983; Jarvis, 2003; Somerville *et al*., 2004). However, one group has

used solid-state NMR spectroscopy to measure the diameter of elementary fibrils from

onion and quince and found them to be 2 nm (Ha *et al*., 1998). This diameter is

indicative of 10-15 glucan chain elementary fibrils. It is uncertain whether these 2 nm

fibrils are being made by the subunits of the terminal complex or by the entire terminal

complex.

Imaging terminal complexes by freeze-fracture

Terminal complexes were first identified by their association with the ends of cellulose

microfibril impressions by the then new technique of freeze-fracture. The first terminal

complexes were discovered in the green alga *Oocystis* (Brown and Montezinos, 1976).

Shortly thereafter, rosette terminal complexes were discovered in *Zea mays* (Mueller and

Brown, 1980). Since that time, many researchers have imaged terminal complexes from

a wide variety of sources (Brown, 1996). Rosette terminal complexes from vascular

plants are approximately 24 nm in diameter and are composed of six 8 nm subunits

(Mueller and Brown, 1980; Rudolph and Schnepf, 1988; Rudolph *et al*., 1989; Kimura *et

al*., 1999). The hexagonal rosette structure of the terminal complex in vascular plants is

very appealing to many researchers, especially because elementary fibrils (the product of

a single terminal complex) are reported to contain 36 glucan chains (Somerville *et al*.,

2004, Saxena and Brown, 2005). These facts gave rise to the theory that each of the six

rosette subunits must synthesize six glucan chains. Several recent reviews have been

published with diagrams indicating that six glucan chains evolve from each of the six

members of the rosette (Perrin, 2001; Doblin *et al*., 2002). Relatively little thought or

credence has been given to the possibility that the rosette TC, found only in the

hydrophobic interface of the plasma membrane, may only be an exit pore and that the real

cellulose-synthesizing machinery may be located in the cytoplasm below the rosette TC.

One reason for this neglect may be the simple fact that the cytoplasmic domain of the

terminal complex has so rarely been seen (Robards, 1969; Kudlicka *et al*., 1987).

Relatively recently, the cellulose synthase enzyme (CesA) has been demonstrated to be a

part of the rosette terminal complex through immunolabeling of freeze-fracture replicas

(Kimura *et al*., 1999).

Images of terminal complexes by sectioning

Freeze-fracture is not the only method of visualizing terminal complexes, just the most

convenient. Although almost all published studies of terminal complexes have been done

by freeze-fracture, terminal complexes have been imaged, although rarely, in sectioned

material (Kudlicka *et al*., 1987). In this study, terminal complexes in regenerated

Boergesenia forbesii protoplasts were imaged by thin sectioning. First, grazing sections

of the plasma membrane were studied and terminal complexes were observed to be

directly associated with microfibrils. The terminal complexes had a size that was

comparable to what had been previously been reported by freeze-fracture. After terminal

complexes had been identified by their direct association with microfibrils, terminal

complexes were located in cross-sections of the plasma membrane. The terminal complexes were found to extend 30-40 nm into the cytoplasm. This is one of the only studies to date showing the cytoplasmic component of the terminal complex; however, one early study found particles associated with the outer surface of the plasma membrane which were thought to play a role in cellulose assembly (Robards, 1969). Repeating this finding in an organism with rosette terminal complexes, such as vascular plants, is very unlikely due to the fact that the 25 nm rosette terminal complexes are only a fraction of the size of the giant linear terminal complexes found in *Boergesenia*.

Synthesis of beta-glucans *in vitro*

The synthesis of cellulose *in vitro* has been plagued with problems of all types for many years. A recent report of the synthesis of cellulose in vitro reports a 20% yield of beta-1,4 glucans (Lai-Kee-Him, *et al*., 2002). In this study, detergent-solubilized membrane fractions of suspension-cultured cells were treated with UDPG and found to synthesize some cellulose. When these preparations were viewed with negative staining and electron microscopy, particles could be seen associated with the growing tips of these in vitro-grown microfibrils. Although not specifically reported, the particle in the published figure measure approximately 60 nm in diameter. In another, unrelated study, detergent-solubilized membrane fractions were purified by affinity chromatography with CesA antibodies. When incubated with UDPG, these affinity-isolated microsomes synthesized a fibrillar product. When this product was imaged by TEM, 50-60 nm particles were found associated with the tips of microfibrils. Taken together, these findings indicate that

the terminal complex is more than just the rosette seen by freeze-fracture (W. Laosinchai, unpublished results; Saxena and Brown, 2005).

The study of cell cortices

The isolation of plasma membrane sheets by binding cells to poly-L-lysine coated surfaces was first reported by Mazia *et al*. (1975) for the study of cortical granules in sea urchin eggs, but first applied to plant cells by Marchant (1978) for the study of cortical microtubules in the alga *Mougeotia*. Soon after that, cortical microtubules (Van der Valk *et al*., 1980) and coated vesicles (Van der Valk and Fowke, 1981) were found on plasma membrane sheets isolated from tobacco suspension culture cells. Patches of plasma membrane, isolated by binding cells to sticky surfaces and then shearing away the cell body, are called by several different names. These names include cell cortices, protoplast ghosts, plasma membrane ghosts, and plasma membrane sheets. In this document, I will refer to these specimens as plasma membrane sheets. Membrane sheets can (and have) been produced from isolated organelles and so it is important to explicitly state that the specimens imaged in this report are composed of plasma membrane. There are several methods for gluing cells to a surface; however, no difference has been noted between specimens prepared by different methods. An excellent review of the production of membrane sheets for study by TEM has been published by Heuser (2000).

Hirai *et al*. (1998) reported the synthesis of beta-glucans on plasma membrane sheets of tobacco BY-2. They were able to correlate microtubule orientation with that of in vitro-synthesized beta-glucans by fluorescence microscopy. This study indicated that

intact terminal complexes are present in membrane sheets. We therefore proposed to use this technique to image the cytoplasmic domain of the terminal complex.

Preparation of specimens for electron microscopy

The preparation of plasma membrane sheets for electron microscopy invariably involves dehydration of the specimen and giving contrast to the specimen. Several methods exist for dehydrating biological specimens. The simplest method for preparing specimens for electron microscopy is negative staining. Samples are applied to Formvar or carbon coated grids and a solution of heavy metal salts is applied. This dries down to a thin layer which surrounds and provides negative contrast to the specimen. Negative staining works particularly well for imaging macromolecular complexes, virus particles, and objects in a similar size range (Harris, 1997). Larger samples can be prepared by replication by evaporation of a thin metal film in high vacuum.

Many specimens to be imaged by scanning electron microscopy (SEM) are dehydrated by critical-point drying. First, water in the specimen is exchanged to ethanol usually by treatment with a graded series of ethanol to minimize specimen shrinkage/swelling. In the past, amyl acetate was used but most researchers have moved to the use of ethanol. This step is critical because ethanol, but not water, is soluble in liquid carbon dioxide. Next, the specimen, dehydrated in graded ethanol, is put into a high pressure chamber and the ethanol is exchanged for liquid carbon dioxide. Once complete solvent exchange has taken place, the liquid carbon dioxide is heated and pressurized such that the liquid carbon dioxide turns into a gas in a continuous fashion.

That is, the liquid/gas transition happens beyond the critical point for fluid-phase carbon dioxide. This method works very well for most specimens; however, specimens with a high lipid content can be extracted by the treatment with ethanol. That is, the liquid/gas transition happens beyond the critical point for fluid-phase carbon dioxide. There is literally never a surface tension force applied to the specimen. For plasma membrane sheets, however, the lengthy exposure to absolute ethanol required for this technique causes extensive extraction of lipids from the membranes themselves.

A second method for minimizing air-drying artifacts is to dehydrate the specimens in graded ethanol, followed by solvent exchange to hexamethyldisilazane (HMDS). This compound is a liquid at room temperature but it has a very low surface tension and a high rate of evaporation. The dehydration, exchange to HMDS, and air-drying can be carried out much more rapidly than the critical point drying process. This minimizes the loss of lipids. Critical point drying works better than HMDS on specimens with large interior void volumes, such as the highly vacuolated protoplasts used to create the plasma membrane sheets. Membrane sheets, however, do not have large void volumes like protoplasts do and as such are more easily preserved by the HMDS drying than critical point drying. Due to the solvent exchanges intrinsic to these methods of drying, they are not compatible with negative staining. Once specimens are dehydrated by one of the above techniques, they must be given contrast by coating the sample in a thin metal film.

A third method for dehydrating biological specimens involves quick-freezing the specimens either in a liquid cryogen such as nitrogen slush, liquid propane or ethane, or

13

by slamming the specimen against a copper or gold surface cooled to liquid nitrogen temperatures (Willison and Rowe, 1980). The rate of freezing must be high enough to form vitreous ice. If the rate of cooling is insufficient, cubic ice crystals will be formed. The size difference between liquid water and cubic ice causes the specimen to be damaged. Once a thin layer of vitreous ice has been formed around the specimen, it is transferred to a high vacuum apparatus. The temperature of the stage where the specimen is mounted is raised from liquid nitrogen temperature (-197 degrees) to between -120 and -80 degrees. A liquid nitrogen-cooled surface is then moved into close proximity to the specimen. In the presence of a high vacuum and a colder surface nearby, water molecules will sublime from the surface of the specimen and collect on the colder surface. This is process is known as freeze-etching and is a more controlled version of the process more generally known as freeze-drying. This entire process is termed the quick-freeze, deep-etch (QFDE) technique (Heuser, 1981). When the water has been completely sublimed from the specimen, the specimen is shadowed with metal and backed with carbon. The replica thus produced is then examined in the TEM.

Crystallization disruption by dye and physical factors

The bacterium *Acetobacter xylinum* synthesizes a pellicle of cellulose at the air-water interface. The addition of the cellulose-specific dye Tinopal to the culture medium has been shown to interfere with the crystallization of cellulose microfibrils (Haigler *et al.*, 1980; Cousins and Brown, 1997). In particular, the synthesis of the glucans and their crystallization into microfibrils becomes decoupled due to the interference of the dye

molecules. Furthermore, the rate of synthesis of cellulose speeds up, leading to the

conclusions that either the rate of cellulose synthesis is limited by the rate of the slowest

member of the terminal complex (Delmer, 1999) or that the crystallization process

proceeds more slowly than the actual polymerization itself.

Plant material: suspension cultures

Tobacco BY-2 suspension culture cells, shown in Figure 1 by interference contrast

microscopy, were used for the current course of study due to their ease of culture and

sample preparation. Also, the extremely rapid growth rate of BY-2 cells suggests that

they have thin cell walls (because they divide so quickly) and that they make a large

amount of cellulose nearly constantly in order to cover the new cells. It should be

possible to image terminal complexes by this method from any cell type from which

protoplasts can be isolated that have the ability to regenerate a new cell wall.

Biochemical and genetic data

The cellulose synthase enzyme is approximately 120 kD (Nakashima *et al*., 2003; Kimura

et al., 1999). It has been found that three different CesA proteins are required for the

synthesis of cellulose (Taylor *et al*., 2003; Somerville *et al*., 2004; Saxena and Brown,

2005). Furthermore, it has been found that at least two of these CesA proteins associate

with each other in an *in vitro* assay (Taylor *et al.*, 2003), indicating that they are probably

members of the same rosette terminal complex. The requirement of three different

proteins and the presence of six subunits in the terminal complex leads to the conclusion

that three homodimers are present in the terminal complex. The current hypothesis is that

36 of these homodimers must be present in each terminal complex in order to generate

the 36 glucan chain elementary fibril (Saxena and Brown, 2005; Scheible *et al*., 2001;

Perrin, 2001; Doblin *et al*., 2002). One estimate of the total molecular weight of a

terminal complex is 3 million daltons (Somerville *et al*., 2004).

These diverse facts add up to yield several possible schemes for rosette terminal

complexes. Each subunit of the terminal complex may be composed of six CesA

molecules, each synthesizing one glucan chain, for a total of 36 chains. Each subunit

may contain three CesA subunits, each synthesizing two glucan chains, for a total of 36

chains. Or each subunit may be one CesA, synthesizing two glucan chains, for a total of

12 chains. More structural data about the terminal complex is needed to narrow these

possibilities.

FFRL and immunocytochemistry

A technique for immunocytochemically labeling transmembrane proteins in replicas

generated by freeze-fracture has been reported (Fujimoto, 1995). In this technique,

freeze-fracture replicas are cleaned by application of 2.5% SDS. This treatment causes

all non-fractured bilayers to be removed from the replica, while only fractured

membranes are retained. This technique was used to confirm the presence of cellulose

synthase in terminal complexes (Kimura *et al*., 1999). With the knowledge that anti-

CesA antibodies label rosette terminal complexes, this same antibody was used in the

current study against plasma membrane sheets to identify the cytoplasmic domains of

terminal complexes.

Materials and Methods

Cell cultures

BY-2 suspension culture cells were grown in modified Linsmaer-Skoog medium (MLS) containing 3% sucrose, 370 mg/mL KH2PO4, 100 mg/mL myo-inositol, 1 mg/mL thiamine, and 0.2 mg/mL 2,4 D, pH 5.7. Cultures were kept in the dark on a gyratory shaker at 60 rpm and 28ºC. Two mL of culture medium containing cells were transferred to 100 mL fresh MLS medium in a 500 mL flask every 7 days in order to maintain a high growth rate (Nagata and Kumagai, 1999).

Protoplast production and isolation

BY-2 suspension culture cells were digested in a solution containing 1% (w/v) Onozuka RS cellulase, 0.1% pectolyase, 0.45 M mannitol, and 10 mM MES, pH 5.5. This digestion medium (DM) was made up in a 3x stock and diluted with suspension culture cells in MLS and attached to a rotisserie for 1.5 hours at 28ºC. Protoplasts were gently pelleted in a microfuge at approx. 500g, and the digestion medium was poured off. The protoplasts were resuspended in 1 mL of a heavy solution (solution C) containing 500 mM sucrose, 1 mM $CaCl_2$, and 5 mM MES-KOH, pH 6.0. This solution was transferred to a glass centrifuge tube and 1 mL of a lighter solution (solution B) containing 400 mM sucrose, 100 mM D-sorbitol, 1 mM $CaCl_2$, and 5 mM MES-KOH, pH 6.0 was carefully layered on top of the protoplasts. A light solution (solution A) consisting of 500 mM D-sorbitol, 1 mM $CaCl_2$, and 5 mM MES-KOH, pH 6.0, was layered on top of the solution B, and the tube was centrifuged for 5 minutes at 1000g in a clinical centrifuge. The

18

interface between the top two layers was collected and diluted in additional solution A, and spun again in a microfuge at ~500g. In order to increase the chances of visualizing cellulose microfibrils, protoplasts in solution A were gently pelleted as above and resuspended in MLS + 0.4 M sorbitol and allowed to regenerate for 15-20 minutes at 28°C on a shaker.

Preparation of "sticky" substrates for the production of membrane sheets

Several different substrates were found to be able to bind protoplasts tightly enough for the production of plasma membrane sheets. Standard microscope coverslips were rinsed in distilled, deionized water to remove any large debris (small fibers or glass chips) and placed into a coverslip staining jar filled with 50% sulfuric acid + 5% sodium dichromate. Coverslips were kept in this solution for as little as one week but up to several months. Coverslips were also cleaned with lens tissue, and then a drop of 0.1% poly-L-lysine was placed onto the glass for 1-2 minutes (PLL). The PLL was washed off in running deionized water and air-dried. Other glass coverslips were silanized by incubating clean coverslips in a 2% solution of 3-aminopropyl triethoxysilane (APTES) in dry acetone (stored over molecular sieve) for 30 minutes at room temp. Coverslips were rinsed in running deionized water and air-dried. Freshly-cleaved mica was also coated with PLL and APTES as described above for glass.

Preparation of membrane sheets

Aliquots of "regenerated" protoplasts were placed onto "sticky" substrates (acid-charged glass coverslips, PLL coated glass coverslips, freshly-cleaved mica squares, or APTES-coated glass and mica) for 1-2 minutes. The plasma membrane sheets were generated in one of two ways. The first method was initially developed by Seiji Sonobe and is therefore referred to in this document as the "Sonobe method" (Sonobe, 1990; Sonobe and Takahashi, 1994; Hirai *et al*., 1998). Substrates (grids or coverslips) with adhering protoplasts were plunged into a hypo-osmotic, microtubule-stabilizing lysis solution (50 mM PIPES, pH 7.0; 2 mM MgCl$_2$; 5 mM EGTA) and moved rapidly up and down (100-200 manual plunges) over ~30 seconds and then plunged into fixative (see below). In the second method, substrates with their bound protoplasts were plunged into a beaker of lysis solution (50 mM PIPES, pH 7.0; 2 mM MgCl$_2$; 5 mM EGTA) in a bath sonicator. The coverslip was vigorously moved up and down in the lysis solution for 10-20 seconds and then plunged immediately into a fixative solution of 4% formaldehyde, 1% glutaraldehyde, 50 mM cacodylate (pH ~7.4), and 2.5 mM CaCl$_2$. Membrane sheets were fixed for 30 min – 1 hour at room temperature (RT). The sheets were then dehydrated in a graded series of ethanol (70, 95, absolute – 5 min each) and hexamethyldisilazane (HMDS), then air-dried.

Replication of membrane sheets

The area of the coverslip with attached membrane sheets was excised with a diamond scribe. These fragments of coverslip were attached to the specimen table of a Rototilt

20

attachment with removable photographic double-stick tape and mounted in an Edwards

E306A high-vacuum evaporator. Four centimeters of 0.1 mm platinum wire was

evaporated from a graphite electrode located 8-10 cm above the specimen. Specimens

were rotated at ~5 revolutions per second and 75 degrees tilt (15 degrees from vertical.

Platinum was evaporated below 2×10^{-5} torr with the rough pump off to minimize any

vibrations. Specimens were backed with carbon at ~10 degrees from horizontal at full

speed rotation for 8-10 seconds. Replicas were floated off of the glass by immersing in

full strength (47%) hydrofluoric acid (HF). Replicas were collected from the surface of

the HF with a glass rod onto glass distilled water. Specimens were rinsed on glass-

distilled water 3 times and then cleaned with sulfochromic acid (5% sodium dichromate

in 50% sulfuric acid) for 10-60 minutes. Specimens were then rinsed on three changes of

glass-distilled water and collected on Formvar-covered 75 mesh copper grids and

examined in a Philips EM420 transmission electron microscope at 100 kV. Digital

images were captured with a Gatan Bioscan camera.

Creation of 3D anaglyphs

The goniometer stage of the TEM was tilted +/- 5 degrees (10 degrees total) and two

images were captured. The two images were labeled left and right based on which

direction the stage was tilted (i.e. which eye's view was being simulated). The images

were pasted into different layers using the GIMP (v 2.2), the opacity of the overlaying

images was decreased, and particles from the background were carefully matched. The

images were then cropped to be exactly the same size (areas where the two images were

not overlapped were cut off). The images were converted from grayscale to RGB. The blue and green channels were deleted from the left image (to generate a red image) and the red channel was deleted from the right image (to generate a blue-green image). When these images are viewed with the correct glasses (with the red lens over the left eye), each eye sees only one of the images (left or right) and the human brain assembles these views into a three dimensional image.

Immunocytochemical labeling of plasma membrane sheets

Plasma membrane sheets were prepared on TEM grids by the Sonobe technique. Plasma membrane sheets were fixed in 4% formaldehyde, 0.1% glutaraldehyde, 2.5 mM $CaCl_2$, and 100 mM cacodylate for 45 minutes at RT. Grids were rinsed in PBS followed by distilled water. Specimens were quenched for 30 minutes in 50 mM glycine in PBS. Specimens rinsed in PBS and then blocked for 2 hours at 37ºC in 5% normal goat serum (Sigma Chemical). Grids were incubated in anti-CesA antibody raised against transgenically-expressed cellulose synthase catalytic subunit from cotton (Kimura *et al*., 1999) in blocking solution overnight (16 hrs) at 4ºC. Next, grids were washed vigorously, and then incubated with goat anti-rabbit conjugated to 10 nm gold particles for 2 hours at RT. After treatment with the secondary antibody, grids were washed in washing buffer, then PBS, and fixed for 10 minutes in 2% glutaraldehyde. And finally, grids were rinsed in PBS, followed by distilled water. Grids were then dehydrated in graded ethanol followed by HMDS and replicated as usual.

Detection of polysaccharides with the PATAg technique

Plasma membrane sheets were treated with the PATAg (periodic acid-thiocarbohydrazide-Ag proteinate) reagent following the method of Roland and Vian (1991). Plasma membranes were prepared on carbon coated nickel grids by the Sonobe method and fixed for 1.5 hours in 4% formaldehyde, 1% glutaraldehyde. Grids were then rinsed in distilled water then incubated for 5 minutes in 1% periodic acid and immediately again rinsed in distilled water. Grids were incubated in 0.2% thiocarbohydrazide (TCH) in 20% acetic acid for 6 hours at RT in the dark. Grids were rinsed in graded acetic acid (10% for 10 minutes, 5% for 5 minutes, and 2% for 5 minutes) and distilled water for 10 minutes. Finally, grids were incubated in 1% silver proteinate (Roques) for 30 minutes in the dark. Grids were then dehydrated and shadowed as usual.

Results

Cellulose crystallization, but not polymerization, is inhibited by the binding of the plasma membrane to a poly-L-lysine coated surface

In order to determine whether the binding of the plasma membrane to a PLL-coated surface affects the synthesis and/or crystallization of cellulose, intact BY-2 protoplasts were either glued to coverslips with poly-L-lysine or allowed to float freely in an Eppendorf tube and allowed to regenerate for one hour in osmotically-adjusted culture medium. Protoplasts regenerated free in solution synthesized microfibrils on their upper (Figure 2A) and lower surfaces (Figure 2B). Protoplasts which were stuck to a glass substrate regenerated cellulose microfibrils on their upper surfaces (Figure 2C), however, they secreted a non-fibrillar product between the cell body and the glass surface (Figure 2D). The images of the lower surfaces look sharper than the images of the upper surfaces because the lower surface is in direct contact with the coverslip surface. An epi-fluorescence microscope was used to generate these images. For this reason, the area directly in contact with the coverslip is the first area of the sample illuminated by the excitation light and it is also the closest to the objective lens. In order to image the upper surface, however, one must focus through the entire cell (15-20 micrometers) both to illuminate and collect light from the specimen. Thus, the area between the plasma membrane and PLL was too constricted for the secretion of cellulose in the form of microfibrils, and it is hypothesized that the glucan chains simply collapsed into a semi-amorphous form of cellulose at these loci.

Lysis of protoplasts to plasma membrane sheets prohibits true membrane sheet formation

The terminal complex is known to be a highly labile structure. Therefore, in order to generate images which were as close as possible to the native state, protoplasts were bound to glass or grids and lysed directly with fixative. The cross-linking of the protoplasts by the fixative was so rapid and extensive that the protoplasts could not be torn away from the substrate and thus no plasma membrane sheets were isolated by this technique. Instead, only the outer surfaces of protoplasts were imaged by this "fixative lysis" technique. This fact is indicative of the extremely fast and complete fixation that this fixative causes in these specimens and therefore that it is highly likely that plasma membrane sheets treated with this fixative are very close to the native state. Although the overall structure of these protoplasts has been somewhat distorted by the rough treatment of the cells with the fixative, the surface of the protoplasts can be seen to be very smooth and covered by a fine network of microfibrils (Figures 3A and 3D). With the TEM, these structures could be mistaken for membrane sheets (Figure 3A), however, when these sheets are viewed with SEM they can easily be seen to be intact protoplasts (Figures 3B and 3C). Vesicles can be seen attached to the protoplast surface under the cellulose microfibril network. It is unclear whether these vesicles are fusing with the membrane or budding off the membrane.

Imaging the external surface of protoplasts

Isolated BY-2 protoplasts were allowed to regenerate a cell wall, fixed with glutaraldehyde, and post-fixed with osmium tetroxide while free in solution (on a rotisserie). These protoplasts were then bound to a glass coverslip with PLL and dehydrated with graded ethanol and HMDS. Coverslips were moved slowly and gently to minimize the displacement of cellulose microfibrils from the surface of the protoplasts (Williamson *et al.*, 1977). In Figure 4A and B, cellulose microfibrils can be seen on the surface of protoplasts. The surface of the membrane looks very smooth, unlike that seen on the inner surface of plasma membrane sheets. Cellulose microfibrils can be seen to aggregate, forming large microfibrillar bundles in Figure 4B. In Figures 4C and D cellulose microfibrils appear to terminate.

Negative-stained membrane sheets

Membrane sheets were prepared on poly-L-lysine treated, carbon-coated, 300 mesh electron microscope grids by plunging repeatedly and rapidly into a hypo-osmotic medium 100-200 times (Sonobe method). The membrane sheets thus produced were immediately plunged into a strong fixative. Following fixation, the grids were rinsed briefly in distilled water and negatively stained with either uranyl acetate (UA) or sodium silicotungstate (STA). Clathrin-coated pits and vesicles were easily recognizable on these negatively-stained sheets (Figure 5B). Also in this image, microtubules and ribosomes are clearly identifiable. Microtubules have the appearance of being doublets; however, negatively-stained microtubules from this and other similar images were

carefully measured and were found to be consistently 25 nm in diameter, the reported

diameter of microtubule singlets. Furthermore, while many microtubule bundles were

seen, no true microtubule doublets were seen in any of the subsequent plasma membrane

replicas.

Ultrastructure of the cell cortex of BY-2 protoplasts revealed by shadowing

Plasma membrane sheets were made by the Sonobe lysis method, dehydrated in graded

ethanol followed by HMDS, air-dried, and rotary shadowed with platinum/carbon at a

high angle (15-20 degrees from vertical). This method of sheet production is compatible

with both coverglasses and grids. Plasma membrane sheets produced on grids are

shadowed directly with platinum/carbon. Plasma membrane sheets produced on

coverglasses must be shadowed with platinum/carbon, backed with pure carbon to

strengthen the replica, floated onto hydrofluoric acid to dissolve the glass and release the

replica, and rinsed on distilled water before collection onto grids. Plasma membrane

sheets prepared by the Sonobe method show a large amount of adhering cortical cellular

structures (Figure 6A). Shadowed or replicated plasma membrane sheets allow the

visualization of cortical microtubules (Figures 6B and D), rough endoplasmic reticulum

(Figures 6A and B), and ribosomes (Figure 6C). Although some fibrillar structures can

be seen in Figure 6D, cellulose microfibrils remain largely undetected beneath the plasma

membrane.

Removal of lipids with chloroform/methanol allows visualization of cellulose microfibrils

In order to image the cellulose microfibrils which might be present under plasma membrane sheets, the lipid component of the plasma membrane sheets was removed. Plasma membrane sheets were made on carbon-coated grids from protoplasts which had been allowed to synthesize new microfibrils for 10-20 minutes. The grids were then immersed in 1:1 chloroform/methanol and gently agitated to remove lipids. After lipid removal, grids were rinsed several times in glass-distilled water and negatively stained with UA. Numerous cellulose microfibrils can be seen in Figure 7 (A-D). Vesicles (Figure 7B) and clumps/patches of protein aggregates (Figure 7C and D) can be seen atop the cellulose microfibrils. No globular structures could be found associated with the ends of cellulose microfibrils.

Immunocytochemical labeling of membrane sheets with anti-CesA antibodies

Plasma membrane sheets were made by the Sonobe method on Formvar/carbon-coated nickel grids and lightly fixed. These membrane sheets were incubated with anti-CesA antibodies to label the cellulose synthase component of the terminal complex. In Figure 8, 10 nm gold particles can be seen associated with 90-100 nm globular structures. Some gold particles are not associated with any discernible structure, however, those that are associated are almost exclusively associated with these 90-100 nm structures. The surface of the membrane sheets is visibly different from what is normally seen (Figure 6).

Occasionally, hints of cellulose microfibrils could be discerned attached to these CesA-labeled structures.

PATAg reagents do not label cellulose microfibrils under plasma membrane sheets

In Figure 9A, colloidal silver particles can be seen bound indiscriminately to the entire surface of the plasma membrane sheet. This membrane sheet is unstained and un-shadowed to increase the contrast difference between the specimen and the silver grains. In Figure 9B, the membrane sheets have been replicated and the replica has been treated with the PATAg reagents. A darkening of rough ER and vesicles can be observed; however, no silver grains can be discerned associated with the cellulose microfibril running through the center of this replica.

Ultrastructure of plasma membrane sheets prepared by sonication

Figure 10 shows the results of plasma membrane sheets generated by plunging coverslips with adhering protoplasts into a hypo-osmotic, microtubule-stabilizing solution in a bath-type sonicator. Coverslips were moved rapidly up and down in the lysis solution for 15-20 seconds while the sonicator was in operation. After lysis, the coverslips were immediately immersed in fixative solution. Total time from living protoplast to fixed specimen was approx. 30 seconds. The overall shape and features of the plasma membrane sheets is comparable with sheets prepared by the Sonobe method, however, significant improvements in the visualization the components of the cell cortex can be noted. The microtubules can be seen to be rounded and lie atop the plasma membrane.

Ribosomes can be seen surrounding the membrane sheets (Figures 10A-C). On closer

inspection, the surface of the membrane sheet itself has been altered by the sonication

(Figures 10E and F). An extensive network of rough endoplasmic reticulum can be seen

passing over (toward the cell interior) the plasma membrane-bound microtubules.

Clathrin-coated pits and vesicles can just be discerned in Figures 10E and F.

Exposure of plasma membrane sheets to sonication yields windows through which

cellulose microfibrils can be imaged

At higher magnification (Figure 11), the surface of the plasma membrane can be seen to

be much different from what was seen on membrane sheets prepared by the Sonobe

method (Figure 6). The membrane appears to have aggregated into a reticulate network.

Due to the extensive network of holes in the plasma membrane, cellulose microfibrils can

be visualized. This is shown at several magnifications in Figures 11A-C. An anaglyph

of these microfibrils running behind the plasma membrane was prepared and is shown in

Figure 11D.

The effect of secondary and tertiary fixations on plasma membrane sheet

ultrastructure

Plasma membrane sheets were prepared by sonication of coverslips with attached

protoplasts for 5 seconds and then fixed. The primary fixative was 4% formaldehyde, 1%

glutaraldehyde in 10 mM cacodylate buffer, pH 7.4, 2.5 mM $CaCl_2$. The secondary

fixative was 1% osmium tetroxide in distilled water. The tertiary fixative was 1% uranyl

acetate in distilled water. All membrane sheets show a continuous layer of plasma membrane. The cellulose microfibrils are completely occluded by this layer of membrane. Figures 12A and B were treated with the primary fixative only. The surface of the plasma membrane is intact but shows signs of vesiculation. Microtubules and clathrin-coated vesicles are recognizable. The membrane sheets shown in Figures 12C and D were treated with primary and secondary fixatives. The surface of the membrane sheet is granular but continuous. The structure of microtubules and especially clathrin-coated pits and vesicles is markedly improved from primary-only fixation specimens. Finally, the sheets in Figure 12E and F were fixed with primary, secondary, and tertiary fixatives. The surface of the membrane has areas of granular structure and areas of very smooth, fine structure. The structure of clathrin-coated vesicles is very distinct. All three specimens showed some areas where "windows" had been torn through the plasma membranes, exposing the cellulose microfibrils beneath (see Figure 12F for an example).

Cortical structures found on plasma membrane sheets

Membrane sheets made from protoplasts which have been allowed to regenerate cell walls for 15-20 minutes following the removal of cell wall degrading enzymes have a large number of plasma membrane-bound cortical microtubules. These microtubules frequently bundle together (Figure 13). Cross-bridges can be seen spanning the members of the bundles.

Surrounding each membrane sheet is a zone containing a large number of ribosomes and polysomes bound to the positively-charged PLL (14A). The ribosomes

are very similar in size, but they are not perfectly spherical and therefore show a small

variation in appearance depending on which side is in contact with the substrate. The

network of material often observed associated with the cytoplasmic side of the plasma

membrane-bound microtubules can be seen covered in particles identical in size and

shape to the ribosomes identified bound to the PLL (Figure 14B). For this reason, these

structures have been identified as rough endoplasmic reticulum.

Microtubule-oriented cellulose deposition

Occasionally, cellulose microfibril orientations can be seen to be remarkably similar to

that of neighboring plasma membrane-bound microtubules. In Figure 15A, cellulose

microfibrils can be seen as they pass out from under the edge of a plasma membrane

sheet. These microfibrils can be seen to be parallel to the adjacent microtubules present

on the plasma membrane. A bundle of plasma membrane-bound microtubule can be seen

in the center of this Figure 15B. Just below the microtubule bundle, a cellulose

microfibril can be seen to closely follow the microtubules, even changing direction

slightly to follow the curving edge of the microtubule ends. Similarly, in Figure 15C a

cellulose microfibril can be seen running parallel to a microtubule bundle. Additionally,

numerous clathrin-coated pits can be seen on the surface of this membrane sheet. In one

instance (Figure 15D), several cellulose microfibrils can be seen to be parallel to

membrane-bound microtubules as they pass out from under the edge of a membrane

sheet, similar to those seen in Figure 15A. However, the cellulose microfibrils can be

followed under the membrane sheet itself, where they appear to be trapped between the members of the microtubule bundle.

Three-dimensional anaglyph analysis of plasma membrane sheet ultrastructure

In order to better understand the three-dimensional nature of the membrane sheets, anaglyphs were made by tilting the goniometer stage of the TEM +/- 5 degrees (10 degrees total). These images must be viewed with red/blue (or red/cyan) glasses, with the red lens over the left eye. In Figure 16A, a bundle of plasma membrane-bound cortical microtubules can be seen along with several membrane-bound clathrin-coated vesicles. On the left a piece of rough endoplasmic reticulum can be seen lying atop a microtubule and spreading over an area of the plasma membrane. The surface of the membrane appears pebbled. In some places, many clathrin-coated vesicles appear to bud off from a small region (Figures 16C and D). Occasionally, as the cell body tears away the cellulose microfibrils which were wrapped around the cell tear through the delicate plasma membrane. This can be seen in the lower left of Figure 16C. Surrounding every plasma membrane sheet is an area of bound ribosomes and polysomes. Some of these can be seen in Figure 16C. Many highly-oriented plasma membrane-bound microtubules exist in the cell cortex of BY-2 protoplasts. Just interior to this plasma membrane-bound microtubule system is a large network of rough endoplasmic reticulum (Figure 16A, B and D). For the specimen shown in Figure 16D, the degree of sonication used to generate the sheets was reduced, the fixation was increased (to include osmium tetroxide and uranyl acetate as well as the standard aldehyde combination fixative), and a very thin

replica was produced. For these reasons, the structure of the plasma membrane surface, as well as the clathrin-coated vesicles, are markedly improved from that seen in the other images in this figure.

New evidence to support the presence of a cytoplasmic domain associated with rosette cellulose synthesizing complexes of tobacco BY-2 cells

Patches of plasma membrane were isolated on PLL-coated coverslips from protoplasts of tobacco BY-2 suspension culture cells. The plasma membrane was partially removed by the technique described in Chapter 5, allowing the imaging of cellulose microfibrils which were synthesized on the exterior of recovering protoplasts. These cellulose microfibrils were tracked back to their ends, and globular particles were found associated with these ends. It should be kept in mind that all of the images in this report are replicas of biological material. What is actually imaged by the electron beam are grains of platinum that have been deposited onto the specimen. The specimen itself has been removed from the replica by treatment with acid. All measurements of specimen replicas are subject to a certain amount of broadening due to the thickness of the platinum/carbon film. As a final note, the contrast of all of the following images has been reversed to be more naturally interpretable by the human brain.

The terminal complex replica in Figure 17 is roughly 50-55 nm in diameter and has a 7.5-8.5 nm microfibril attached to it. The cellulose microfibril can be seen to run under the remnants of the plasma membrane which have been partially extracted by the

sonication used to generate the sheets. Several other particles can be seen bound to the plasma membrane.

Figure 18 illustrates the manner in which terminal complexes were identified. In each image, cellulose microfibrils can be seen under the remnants of the plasma membrane. Terminal complexes (circled in yellow) were located and identified by their association with the ends of cellulose microfibrils.

A montage of terminal complexes, all at the same magnification, can be seen in Figure 19. All of these terminal complexes are similar in size and shape. Sixty measurements made over 30 different particles yielded an average size of 47 nm ±4.9 nm. In Figure 20, the most obviously hexagonal terminal complexes have been presented. All of these hexagonal terminal complexes are extremely similar in size. The replicas of terminal complexes in Figure 20, measured across their flat faces, average 59 nm across and have a standard deviation of ±3.2 nm. The average distance from point-to-point is 65 nm with a standard deviation of ±5.4 nm. A rotational analysis was performed on the hexagonal terminal complexes shown in Figure 20 (Figure 21). Each terminal complex was rotated 60 degrees and added to the previous image. The reinforcement of the hexagonal shape by adding images roated by 60 degrees proves that these particles are indeed truly hexagonal in shape. Terminal complexes having a more complicated substructure were also observed (Figure 22). These terminal complexes were consistently larger than the hexagonal terminal complexes.

Cortical microtubule bundles are frequently found associated with the inner surface of the plasma membrane (Figure 23).   The microtubules in this image have a

mean diameter of 26-28 nm, however, these measurements are not exact as the diameter of the microtubules can be seen to vary by a substantial amount over their length. Despite this uncertainty, their average diameter is in accordance with the known diameter of microtubules obtained through x-ray and electron crystallography (Nogales *et al.*, 1999; Amos, 2000). Furthermore, the microtubules in this image probably have many types of microtubule-associated proteins and motor proteins bound to them, increasing their apparent diameters and possibly accounting for some of the irregularity in their diameters. Since microtubules are circular in cross-section, the height of these microtubules is probably 25-30 nm. A hexagonal particle approximately 50 nm in diameter can be seen adjacent to the microtubule bundle. The particle appears slightly taller than the neighboring microtubule, perhaps 30-35 nm tall. Although it does not have a cellulose microfibril associated with it, based on its size and shape, it is likely to be a terminal complex.

Discussion

Cellulose crystallization, but not polymerization, is inhibited by the binding of the plasma membrane to a poly-L-lysine coated surface

Plasma membrane sheets are made by "gluing" protoplasts to coverslips and then shearing away the cell body, leaving only the piece of plasma membrane which was glued to the glass. This gluing effect must be very strong in order to overcome the shearing forces used to remove the cell body and cortical cytoplasm. It was thought that this gluing effect might be prohibiting the *in vitro* synthesis of crystalline cellulose microfibrils under membrane sheets. Protoplasts of both *Arabidopsis* and tobacco BY-2 cells produce cellulose almost immediately upon removal of the cell wall-degrading enzymes. Plasma membrane sheets isolated from these two experimental systems, however, are incapable of synthesizing cellulose when provided with UDPG. When intact BY-2 protoplasts were bound to glass coverslips with poly-L-lysine and incubated with osmotically-adjusted culture medium, they were unable to synthesize fibrillar glucans in the region between the cell and the glass (Figure 2D). Poly-L-lysine polypeptides have a positive charge at every lysine residue. Cells stick to surfaces coated with PLL because most cells have a net negative charge on the outer leaflet of their plasma membranes. When these negatively charged lipids adhere to a PLL-coated surface, they become immobilized in the plane of the bilayer and are therefore not mobile anymore. Terminal complexes have a cellulose synthase domain, but they must also possess a transmembrane domain where newly synthesized cellulose microfibrils are extruded to the outside of the cell. Cellulose microfibrils are non-compressible,

37

especially along their long axes. As more monomers are added to the growing chain, the terminal complex must move in the plane of the membrane, driven by the force of synthesis/crystallization of the glucan chains. If the lipids surrounding the terminal complex become immobilized by binding to a PLL-coated surface, the terminal complexes will not be able to move freely in the plane of the membrane. If crystallization happens inside the cell, near the site of synthesis, the force which builds up would most likely interfere with the polymerization of glucan chains. However, we have observed the build-up of amorphous, non-fibrillar material in the glass/membrane interface which seems to indicate that the polymerization of glucan chains is unaffected by the immobilization of terminal complexes. That is, the ability of glucans to crystallize into a microfibril is inhibited while the polymerization of glucans continues. One explanation of this observation is that the crystallization of the glucan chains into microfibrils may take place in the channel of the rosette itself, which is spatially separated from the site of polymerization, which takes place on the cytoplasmic face of the terminal complex. This may be a tool which will advance our knowledge of cellulose biosynthesis and crystallization in a manner similar to the analysis of dye-altered cellulose (Cousins and Brown, 1995; Cousins and Brown, 1997).

Another possibility is that the protoplasts are synthesizing callose in the zone adhered to the coverslip. Callose is normally non-fibrillar and is synthesized in response to wouding. If this is indeed what is happening, this technique may be an ideal experimental system for studying cell wounding *in vitro*.

Fixative lysis of protoplasts does not permit visualization of cell cortex

The ideal specimen for observing functional terminal complexes would be an isolated plasma membrane sheet that was capable of synthesizing cellulose *in vitro*. This sheet could be very rapidly fixed because the specimen would be very thin and since the cell had already been sheared away, there would be no physical disruption. As discussed above, the synthesis of cellulose *in vitro* by isolated plasma membrane sheets was not possible (see also Appendix 4). The next best alternative was to lyse protoplasts actively synthesizing cellulose with fixatives. When these plasma membrane sheets were replicated and imaged by TEM, the surface of the membrane sheets was much different than anything previously observed (Figure 3). Cellulose microfibrils could be observed on these membrane sheets in abundance. The surface of the membrane itself was markedly smoother than other membrane sheets. There was also a total lack of cortical microtubules. When these replicas were imaged by SEM, the true nature of these specimens was revealed. The combination fixative caused sufficient cross-linking within the protoplasts that the cells did not tear away and leave plasma membrane sheets. Intact protoplasts remained on the surface of the coverslip, distorted somewhat by the force of the spray itself.

Details of the cytoplasmic surface of membrane sheets revealed by negative staining

Plasma membrane sheets were prepared for negative staining by binding protoplasts directly to PLL-coated EM grids and plunging these grids into hypo-osmotic lysis solution 100-200 times very rapidly. The nearly grainless images obtainable with

negative staining and the ease of preparing negatively-stained specimens are what prompted favoring this preparation method over other more time-consuming and technically challenging procedures such as shadowing. As demonstrated in Figures 5A and B, negatively-stained plasma membrane sheets show many of the same features later seen with replicas. In particular, in Figure 5B several clathrin coated pits/vesicles can be easily identified. This image also shows ribosomes and a microtubule. The microtubule appears to be a doublet, however, measurements as well as comparison to images of replicas show that these "doublet" microtubules are actually singlets. Microtubules identical to the ones shown in Figure 5B have been reported previously (Van der Valk, 1980; Sonobe and Takahashi, 1994). This artifact may be an air-drying artifact, since specimens dehydrated with ethanol and HMDS did not show this effect. In order to prepare negatively-stained plasma membrane sheets, however, specimens must be air-dried. This causes flattening of specimen structures due to the surface tension of the drying water film. When microtubules are flattened, a central "trough" may result. This trough, when filled with negative stain, would result in a dark central region just as observed. It is also possible that the central cores of the microtubules are being filled with negative stain due to a charge affinity between the positively-charged uranyl acetate ions and the central core residues of the tubulin monomers.

UA also interacts with lipids and has been used for many years as a tertiary fixative for the preservation of lipids (Glauert and Lewis, 1998). Also, the inner surface of the plasma membrane sheet is not smooth so that different thicknesses of negative stain accumulate around structures present on this surface. This is most apparent when

observing the microtubule in Figure 5B. The microtubule appears to have a variable width over its length, while microtubules viewed in replicas have a very constant diameter. Negative stain works best when the structures to be given contrast are very solid (can survive air-drying with little deformation) and are spread on a very flat surface (usually Formvar films). For these reasons, platinum/carbon replicas were used for the bulk of this study.

Ultrastructure of plasma membrane sheets prepared by the Sonobe technique and shadowed with platinum/carbon

The drying of plasma membrane sheets by HMDS was found to preserve the structure of the membrane so well that cellulose microfibrils could not be discerned beneath the intact membrane. Large areas of some plasma membrane sheets are covered with cytoplasmic debris (Figure 6A). This debris is mostly composed of rough endoplasmic reticulum and vesicles of various sizes. On closer examination, bundles of cortical microtubules can be seen attached to the cytoplasmic surface of the plasma membrane (Figure 6B). Surrounding the exterior of the plasma membrane, numerous particles of a regular size can be seen adhered to the PLL (Figure 6C). These particles have been identified as ribosomes by their size and appearance. Their presence on structures thought to be rough endoplasmic reticulum was noted. There is a direct correlation between the particles density and proximity to a plasma membrane sheet, strongly suggesting that these particles were released from the protoplasts upon lysis. Due to the fact that cellulose microfibrils could not be imaged through these membrane sheets, techniques to remove

41

the membrane and/or to provide contrast to the cellulose present beneath the plasma membrane sheet were examined.

Removal of lipids with chloroform/methanol

Previous experiments demonstrated the presence of a large number of cellulose microfibrils on the surface of protoplasts of BY-2 after a brief recovery period (Figures 2, 3, and 4). However, no evidence of this extensive network of cellulose could be detected under plasma membrane sheets. Treatment of plasma membrane sheets with chloroform/methanol caused the lipid component of the plasma membrane sheets to be removed, allowing the cellulose microfibrils to be observed (Figure 7). Terminal complexes or globular structures could not be seen associated with the termini of cellulose microfibrils, due in part to the fact that extensive aggregation of proteins and generally low contrast of the specimen made tracing the cellulose microfibrils back to their termini extremely difficult.

When the lipids are removed from around transmembrane proteins, their hydrophobic regions are exposed. When the specimen is then immersed in water and negatively stained, the hydrophobic regions aggregate to exclude water. This aggregation makes the identification of terminal complexes exceedingly difficult.

Detergents were also tested for their ability to remove lipids, allowing the visualization of cellulose microfibrils and ultimately terminal complexes. Previous biochemical studies have shown that detergent extracts of plasma membranes can in some cases retain the ability to synthesize cellulose from UDPG. Furthermore, in several

cases these detergent-solubilized micelles have been imaged by TEM and shown to be associated with the growing tip of a cellulose microfibril (Lai-Kee-Him *et al*., 2002; Saxena and Brown, 2005). Previous work in this lab has also demonstrated by immunocytochemical indicates that these cellulose microfibril-associated globules contain cellulose synthase. SDS, CHAPS and Brij 58 were tested for the ability to remove lipids, allowing the imaging of cellulose microfibrils and, ultimately, terminal complexes associated with them. The use of any of these detergents caused the membrane sheets to separate from the substrate. All detergents contain a charged, hydrophilic region and a hydrophobic region. Since the attraction between the lipids of the plasma membrane and the PLL coating is electrostatic in nature, it is likely that the charged moiety of the detergents blocked and/or out-competed the bonds between the membrane sheet's negatively charged lipids and the PLL. It is also possible that the detergents caused the removal of the PLL from the surface of the glass.

Plasma membrane sheets labeled with anti-CesA antibodies

An alternate method for the identification of terminal complexes is immunocytochemical localization of cellulose synthase by anti-CesA antibodies. Structures of a consistent diameter appear to be recognized by the anti-CesA antibodies. These structures are 90-100 nm in diameter.   The use of blocking agents (BSA, gelatin, and goat serum) in the immunolabeling procedure increases the specificity of the labeling reaction, but these proteins also adhere to the surface of the plasma membrane sheets. Based on the broadening of features of known diameters (such as microtubules and ribosomes), this

layer is estimated to be 25-30 nm in thickness. The true diameter of these particles is therefore estimated to be 40-60 nm. Occasionally, gold particles can be seen not associated with any structure, but rather adhered to the surface of the plasma membrane sheet; however, gold particles are not seen associated with structures of other sizes. A chart showing the number and the size distribution of particles labeled by gold particles would lend statistical significance to this labeling experiment. However, the labeling of particles of a specific size on the cytoplasmic side of isolated plasma membrane sheets does imply the presence of the catalytic region of cellulose synthase, probably in the form of rosette terminal complexes as seen by the freeze-fracture replica-labeling technique (Kimura *et al.*, 1999).

Using the PATAg test for polysaccharides to visualize cellulose microfibrils under plasma membrane sheets

Cellulose microfibrils are present under plasma membrane sheets, as demonstrated by the chloroform/methanol extraction experiment. Terminal complexes are present in the plasma membrane sheets, as demonstrated by the CesA immunolabeling. The periodic acid-thiocarbohydrazide-silver proteinate (PATAg) test for polysaccharides was applied to plasma membrane sheets in order to give contrast to the cellulose microfibrils present under the membrane. The PATAg test involves oxidizing the vic-glycol moieties of polysaccharides (including cellulose) into aldehydes with periodic acid, reacting these aldehyde groups with thiocarbohydrazide, and then exposing the specimen to silver proteinate. Ideally, colloidal silver will be deposited at each vic-glycol, causing

polysaccharide-containing tissues to deflect electrons and look dark in the electron

microscope. Colloidal silver particles can be seen bound indiscriminately to the entire

surface of the plasma membrane sheet in Figure 9A. It is possible that the silver grains

are deposited over the glycosylated proteins and lipids naturally found in plant plasma

membranes. In Figure 9B, the membrane sheets have been replicated and the replica has

been treated with the PATAg reagents. A darkening of rough ER and vesicles can be

observed, however, no silver grains can be discerned associated with the membrane

sheets. Even the cellulose microfibril running through the center of Figure 9B shows no

silver accumulation. It should be noted that the PATAg test for polysaccharides is most

often performed on plastic-embedded sections of plant material. Furthermore, these

images are usually interpreted at relatively low magnification in a qualitative manner for

the presence of polysaccharides in cell walls. Furthermore, plant cells produce many

types of polysaccharides as well as glycosylated membrane proteins and lipids. This is

the most likely reason for the reaction seen in Figure 9A. In a section, the plasma

membrane would be in direct contact with the cell wall, which would be stained very

dark by the PATAg test and so the presence of sliver grains of the plasma membrane

would not be discernable. The replica shown in Figure 9B may not have any plasma

membrane present under areas where the topology of the membrane is relatively flat.

Researchers studying freeze fracture-replica labeling (FFRL) have demonstrated that

lipid bilayers are easily displaced from metal replicas and that only cleaved membrane

leaflets adhere to the metal through the direct association of the hydrophobic region of

the lipids with the metal replica. This would indicate that there is no cellulose or plasma

membrane for the PATAg reagents to react with under the replicas. Areas where

significant invaginations occur, such as rough endoplasmic fenestrae or vesicles, may be

retained by purely physical means.

Sonication of plasma membrane sheets yields improved ultrastructure and "windows" in the membrane through which cellulose microfibrils can be imaged

Plasma membrane sheets prepared by sonication show a different morphology than

membrane sheets prepared by the Sonobe method (Figures 6 and 10). Sonication cleans

surfaces in two ways simultaneously. First, sound waves passing through the liquid

sonication medium provide frictional energy to particles, causing them to be physically

dislodged from the surface to be cleaned. Secondly, sonication causes microcavitations

to occur. These microcavitations generate bubbles which form and collapse violently,

causing the water molecules in the vicinity to move rapidly. The movement of these

water molecules causes particles to be dislodged from the surface being cleaned.

Sonication of plasma membrane sheets causes the membrane surface to change from a

continuous sheet to a reticulated network (Figure 11). This network has enough holes to

permit the location and tracking of cellulose microfibrils beneath the membrane.

Because this technique does not rely on chemical or immunological methods of locating

cellulose, it should be applicable to any specimen where the ability to correlate

cytoplasmic structures with extracellular markers is necessitated.

Sonication of plasma membrane sheets, however, precludes the preparation of

plasma membrane sheets on TEM grids. The force of the sonication causes the rupture of

the support films used to span the grid holes. Therefore, all membrane sheets prepared by sonication must be viewed as replicas prepared on glass and removed by HF. For these reasons, it has not been possible to image sonicated plasma membrane sheets with negative staining, which must be done on a grid.

The effect of secondary and tertiary fixations on plasma membrane sheet ultrastructure

The effect of secondary fixation with osmium tetroxide and tertiary fixation with uranyl acetate was examined. The ultrastructure of plasma membrane sheets fixed in primary only; primary plus secondary; and primary, secondary, and tertiary fixatives were compared. In order to directly compare the effect of the fixation, all specimens were sonicated for exactly 5 seconds. All of the membrane sheets prepared by a 5 second sonication showed intact, non-vesiculated sheets. The plasma membrane sheets in Figures 12A and B have been fixed with primary (aldehyde) fixative only. Therefore, the only difference then between the sheets in this figure and those seen previously is the length of sonication. This indicates that it is the time of sonication which is responsible for the formation of holes and eventually the formation of the highly vesiculated, reticulate membrane structures which permit the observation of cellulose microfibrils. The inclusion of secondary fixation with osmium tetroxide improved the preservation of clathrin-coated vesicles; however, the addition of tertiary fixation in uranyl acetate had a dramatic effect on the preservation of the membrane surface structure as well as the ultrastructural preservation of clathrin-coated pits and vesicles. Clathrin triskelions self-

47

assemble on the inner surface of the plasma membrane. This self-assembly caused the

invagination of the plasma membrane and eventually the budding off of a clathrin-coated

vesicle. Thus, clathrin-coated pits are just a stage in the development of a clathrin-coated

vesicle. Because clathrin self-assembles on the plasma membrane, it seems logical that

clathrin must depend on the lipid bilayer for some of its structural integrity, at least in the

early stages of pit assembly. The generation of plasma membrane sheets by longer

sonication times generates membrane sheets with a reticulated surface. Obviously, this is

damaging to the bilayer and therefore may be distorting the clathrin-coated vesicles.

However, both osmium tetroxide and uranyl acetate are well known lipid fixatives

(Glauert and Lewis, 1998). The inclusion of both of these lipid-specific fixatives causes

a change in the preservation of the plasma membrane itself, and therefore its preservation

of the ultrastructure of the clathrin-coated vesicles is not surprising. In fact, the surface

of the plasma membrane of the specimens shown in Figure 12E and F is very similar to

what has been seen in animal cells (Aggeler and Werb, 1982; Heuser, 2000) and plant

cells (Willison and Cocking, 1975; Grout, 1975; Williamson *et al*., 1977) by the quick

freeze-deep etch technique. The main advantage being that this technique does not

require the use quick freezing devices or the use of a freeze etch apparatus.

Ribosomes and rough endoplasmic reticulum identification

Ribosomes have been identified based on their size, their great abundance, their close

proximity to plasma membrane sheets, and their similarity to structures reported

surrounding animal cells (Heuser, 2000). Rough endoplasmic reticulum has been

identified based on the fact that these structures appear to be largely covered by ribosomes.

Tobacco BY-2 cell cultures grow at a very fast rate (Nagata *et al*., 1992). The protoplasts used for study have been collected during the logarithmic phase of growth. These cells must have an extremely high rate of protein and lipid synthesis to keep up with this aggressive growth rate. The endoplasmic reticulum is known to be the site of lipid synthesis, with the rough endoplasmic reticulum being the site where proteins are made. A central paradigm of cell biology is that proteins are synthesized from mRNA on the rough endoplasmic reticulum, which then buds off vesicles which travel to the Golgi apparatus for further processing. It is possible that some proteins and lipids do not need any additional processing and so can be inserted directly into the plasma membrane from the endoplasmic reticulum. Perhaps in these cells, at this rate of growth, the streaming of vesicles to and from the Golgi apparatus to the plasma membrane is so rapid and constant that these structures have fused into one amalgamated structure which we see in these plasma membrane sheets prepared from cells at the log phase of growth. Then when the nutrients of the culture medium begin to run low these structures may separate into discrete entities once again. This hypothesis would be easily testable by making membrane sheets from cells from an older culture that are not in the logarithmic phase of growth. Can endoplasmic reticulum be seen directly fusing into the plasma membrane from these cells? Are there ribosomes on this structure or is it devoid of ribosomes?

Microtubule-oriented cellulose deposition

The direction of cellulose microfibrils determines the growth axis of plant cells. The direction of growth of plant cells is perpendicular to the direction of the cellulose microfibrils (Somerville *et al.*, 2005; Green, 1980). For this reason, the directed deposition of cellulose is a crucial part of plant morphogenesis. Cellulose deposition has long been hypothesized to be oriented by cortical microtubules. The plasma membrane sheet imaging technique developed here allows the simultaneous imaging of cortical structures such as microtubules and exoplasmic structures such as cellulose microfibrils. Furthermore, this technique allows the differentiation between cortical microtubule, i.e. microtubules present in the cell cortex but not actually bound to the plasma membrane, and plasma membrane-bound microtubules. One of the most influential pieces of evidence for the microtubule-controlled deposition of cellulose was captured using freeze fracture-freeze etch by Giddings and Staehelin (1991). In this study, the authors freeze-fractured cells of *Closterium* and etched the P fracture face. As water was lost from the cytoplasm, the plasma membrane sank down onto the cortical microtubules. On these replicas, rosette TCs could be seen between cortical microtubule impressions. The author's interpretation was that terminal complexes are guided between microtubule barriers.

The results of the current study, as seen in Figure 14, can be thought of as the opposite view of the microtubule/cellulose association from that seen by Giddings and Staehelin. They were looking from the outside in, while the newly developed technique in this dissertation looks from the inside out. Furthermore, Giddings and Staehelin

(1991) tried to compare terminal complex arrays with microtubule directions when what is really needed is a way to correlate cellulose microfibril deposition direction with cortical microtubule orientation. In the current study, cellulose microfibrils can be clearly seen where they pass out from under the membrane sheets. The direction these microfibrils are oriented was found to be parallel to that of adjacent microtubules bound to the plasma membrane. Furthermore, because of the perforation of the plasma membranes, cellulose microfibrils were seen under the plasma membrane sheet running parallel to plasma membrane-bound microtubules (Figures 15B and C). In one instance (Figure 15D), cellulose microfibrils can be seen to travel between microtubules, just as hypothesized by Giddings and Staehelin (1991). A more comprehensive comparison of cellulose microfibril orientation and plasma membrane-bound microtubules might help elucidate this difficult question. This technique might also be useful for providing further details for the role of the kinesin-like protein found to be necessary for the directed deposition of cellulose in *Arabidopsis* (Zhong *et al*., 2002).

Three-dimensional anaglyph analysis of plasma membrane sheet ultrastructure
As previously demonstrated by the fixative-lysis experiments, it is essential to understand the three-dimensional nature of TEM specimens. One way this is done is to use the goniometer stage of the TEM to capture tilted images of the specimen and create 3D anaglyphs using a computer to color and align the two images. In the 3D anaglyph shown in Figure 16A, a bundle of plasma membrane-bound cortical microtubules can be seen along with several membrane-bound clathrin-coated vesicles. On the left a piece of

rough endoplasmic reticulum can be seen lying atop a microtubule and spreading over an area of the plasma membrane. The surface of the membrane appears pebbled. In some places, many clathrin-coated vesicles appear to bud off from a small region (Figure 16C). Cellulose has a relatively high tensile strength – certainly much higher than plasma membrane lipids. When the cell body tears away, frequently the cellulose microfibrils which were wrapped around the cell tear through the delicate plasma membrane (Figure 16C). The area surrounding the plasma membrane containing bound ribosomes and polysomes can be seen in the bottom of Figure 16C. Many highly-oriented plasma membrane-bound microtubules exist in the cell cortex of BY-2 protoplasts. Just interior to this plasma membrane-bound microtubule system is a large network of rough endoplasmic reticulum (Figures 16 A, B, and D). These structures have a large number of ribosomes and polysomes bound to their surfaces and although they always pass over (from the view here) and occasionally interact with the plasma membrane-bound microtubule system, they also appear to be associated directly with the plasma membrane in places. For the specimen shown in Figure 16D, the degree of sonication to generate sheets was reduced, the fixation was increased (to include osmium tetroxide and uranyl acetate as well as the standard aldehyde combination fixative), and a very thin replica was produced. The structure of the membrane itself is markedly improved from that seen in the other images in this figure. The use of the anaglyph technique gives a clearer perspective on the three-dimensional nature of these specimens and may be useful for future analysis of terminal complex height.

The cytoplasmic domain of the terminal complex

Using a new technique developed to image the cytoplasmic domain of transmembrane proteins and correlate these domains with extracellular markers, terminal complexes have been imaged and positively identified by their association with the ends of cellulose microfibrils. As discussed in detail below, some enlargement of the apparent diameters of the terminal complexes is due to the presence of the metal coating itself and the accretion of a metal "cap" during shadowing. Also, the accuracy of measurements is limited due to the granularity of the metal grains comprising the replica itself. Despite these limitations, the diameter of the hexagonal terminal complexes has been measured. As stated above, the hexagonal terminal complexes measure 59 nm from side-to-side and 65 nm from point-to-point. The small standard deviations may indicate that these are intact terminal complexes. Based on the broadening of microtubule diameters (Figure 23), the thickness of the shadowing film is estimated to be 4-5 nm. This is in agreement with the thickness of the film calculated from the known mass of platinum evaporated at a given angle from a known distance (see below). Furthermore, according to Willison and Rowe (1982), the accretion of a metal cap by particulate specimens shadowed at high angles is usually less than 5 nm. Taken together, 5-10 nm should be subtracted from the values measured on the replica to estimate the "true" size of the terminal complex. Terminal complexes, therefore, measure approximately 50 nm from side-to-side and 55 nm from point-to-point. This is roughly twice the 25 nm diameter reported for rosette TCs seen by freeze-fracture.

Estimation of the height of shadowed molecules can be done in several ways. The estimation of the height of particles by measuring the shadow length in uni-directionally-shadowed samples is only possible on very flat surfaces (e.g. purified molecules on mica or glass). Because the surface of the plasma membrane is so rough following sonication, uni-directional shadowing for the estimation of particle height is of no use. It is theoretically possible to measure the height of shadowed particles by careful measurement of the height of particles at high tilt angles. Here again, the roughness of the plasma membrane makes this measurement difficult. The calculation of the three-dimensional volume of the terminal complexes prepared by this technique may further be made difficult due to the flattening effect of drying specimens for metal shadowing. However, some idea of the height of the rosette TCs can be obtained through comparison with other features of the membrane of known size such as microtubules and ribosomes (see below).

Comparison of cytoplasmic domains with terminal complexes seen by freeze-fracture and sectioning

Rosette terminal complexes from vascular plants are known to be comprised of six subunits. These rosettes are transmembrane proteins. Furthermore, the size and shape of the rosette TCs seen in vascular plants by freeze fracture is constant (Brown, 1996). Freeze-fracture micrographs show the presence of rosette structures on the P fracture face. Since the P fracture face is the cytoplasmic leaflet of the plasma membrane bilayer, there are no cellulose microfibrils present. The rosette terminal complexes are therefore

54

identified by their association with "microfibrils impressions". The hexagonally shaped terminal complexes seen in this study directly connected to cellulose microfibrils mirrors what has long been observed indirectly on freeze-fracture micrographs.

Terminal complexes have only rarely been seen in sectioned material. In one early study, particles suspected of having a role in cellulose biosynthesis were found just outside the plasma membrane in thin sections of Beech and Willow (Robards, 1969). In another study, linear terminal complexes were imaged in the alga *Boergesenia forbesii* (Kudlicka *et al*., 1987). In cross-section, these linear terminal complexes were measured to be 35 nm from exoplasmic face to endoplasmic face. In addition, cortical microtubules are present in these micrographs, allowing the terminal complexes to be directly compared to the diameter of microtubules. The terminal complexes appear to extend into the cytoplasm slightly more than the diameter of the nearby microtubules (Figure 23). Microtubules are known to be 24 nm in diameter by x-ray crystallography; however, the microtubules here are larger than this due to the presence of microtubule-associated proteins (MAPs). Therefore, the diameter of the rosette terminal complex is probably very similar to that seen in *Boergesenia* by Kudlicka *et al.* (1987).

Possible implications of the hexagonal morphology of the cytoplasmic domain of the terminal complex

An analysis of proteins of different cross-sectional areas has revealed that a linear relationship exists between the number of trans-membrane alpha-helices a protein has and the size of the cross-sectional area on freeze-fracture replicas (Eskandari *et al*.,

1998). The area contributed by an individual alpha-helical transmembrane domain is

1.40 nm^2. The diameter of the subunits of the rosette terminal complex determined by

UHV freeze-fracture is 8 nm (Reiss *et al*., 1984; Rudolph and Schnepf, 1988; Rudolph *et al*., 1989). The area of these subunits is therefore indicative of the presence of 36

transmembrane alpha-helices. Six transmembrane helices are predicted at the COOH

terminus of CesA proteins and two are predicted at the N-terminus (Pear *et al*., 1996;

Arioli *et al*., 1998; Doblin *et al*., 2002). Perhaps each subunit is indeed made up of six of

these CesA proteins with their six carboxy-terminal transmembrane helices and the

predicted N-terminal transmembrane helices have another function.

Based on these observations, a model for the organization of the terminal complex

has been proposed (Figure 24).   Thirty-six transmembrane alpha helices from six CesA

proteins associate into one subunit of the hexagonal rosettes seen by freeze-fracture. The

six cytoplasmic domains self-order into a hexagonal array due to the association of the

transmembrane regions within the hydrophobic interior of the plasma membrane. Glucan

chains are synthesized by catalytic sites located in the cytoplasm and are transported

through a pore formed by the thirty-six transmembrane helices. The subunits then self-

order into a complete rosette by a method not yet fully elucidated. The arrangement of

CesA proteins in this model would account for the ability of cellulose synthesis mutants

to make a cellulosic product with decreased crystallinity because each subunit would be

capable of making a six-glucan chain product and transporting it through its

transmembrane pore to the cell wall (Brown and Saxena, 2000). Now that an

approximate volume for a functional terminal complex has been established, perhaps

computer-aided modeling can be used to determine whether it there is room for 36 CesA proteins in the rosette terminal complex.

Non-hexagonal terminal complexes

The cytoplasmic regions of some of terminal complexes do not have any apparent hexagonal symmetry and are highly variable in structure (Figure 22). Perhaps the most likely explanation of these non-hexagonal terminal complexes is the presence of terminal complexes that are in the process of being broken down and/or inactivated. The fact that terminal complexes have a very short half-life has been proven (Rudolph *et al.*, 1989). The particles making up these terminal complexes could be proteolytic enzymes and cleaved portions of the terminal complex. These disrupted, partially degraded terminal complexes may aggregate but still retain some members that are still bound to the microfibril tip. A large percentage (20%) of rosette terminal complexes of the moss *Funaria hygrometrica* was seen to be in a non-rosette conformation (Reiss *et al.*, 1984). The authors' conclusion was that these terminal complexes may represent disintegrating or aggregating terminal complexes.

Alternatively, this variable morphology may be indicative of the presence of various adapter proteins on the cytoplasmic face of the terminal complexes (Delmer, 1999; Somerville *et al.*, 2005). These adapter proteins may attach to the cytoplasmic face of the terminal complex and modify its behavior. For example, a molecule specific for terminal complexes and microtubules could bind to the terminal complex and confer the ability to travel along microtubules. This would explain how terminal complexes

57

sometimes synthesize microfibrils which are perfectly aligned with cortical microtubules and sometimes the microfibrils they synthesize are randomly oriented. Plant cells would then need only to regulate the synthesis of this adapter protein to make the switch between random and microtubule-oriented cellulose biosynthesis. It might be possible to image terminal complexes attached to microtubule-aligned microfibrils and compare their structure with terminal complexes attached to microfibrils which can be seen to pass under cortical microtubules. A consistently altered morphology of microtubule-aligned terminal complexes would confirm the presence or absence of an adapter protein which confers microtubule-guiding properties to terminal complexes. This theory is made even more attractive by the discovery of a kinesin-like protein whose presence seems to influence the orientation of cellulose in the secondary walls *Arabidopsis* (Zhong *et al*., 2002).

Another candidate for binding to the cytoplasmic face of the terminal complex is sucrose synthase. At certain times, sucrose synthase may bind to the terminal complex, thereby increasing the local concentration of UDP-glucose and increasing the rate of cellulose synthesis. This might be especially important when secondary wall biosynthesis begins. A protein which could bind to the terminal complex and mask possible proteolytic-cleavage sites could extend the half-life of terminal complexes (Nakashima *et al*., 2003). If the rate of terminal complex insertion into the plasma membrane were kept constant, this would also result in an increase in the rate of cellulose deposition. These are only a few of the possibilities if these non-hexagonal terminal complexes are actually hexagonal terminal complexes with bound adapter proteins.

Finally, the non-uniform size and shape of the non-hexagonal terminal complexes may be an artifact of the specimen preparation technique. In particular, the sonication is obviously damaging to the plasma membrane. Sonication may also be removing non-covalently bound proteins. The cytoplasm of plant cells is full of proteins so it is possible that some of these particles are present simply due to random chance.

Can microtubules guide terminal complexes?

Although the exact height of the terminal complexes cannot be measured by this technique, they can be seen to protrude from the inner surface of the plasma membrane a non-trivial distance. Also, the tight association between cortical microtubules and the plasma membrane can be seen in Figure 23. These two facts taken together lend credence to the theory that terminal complexes may be passively guided by the physical presence of these tightly plasma membrane-associated cortical microtubule arrays. Thus terminal complexes would be bracketed between microtubule rails, as hypothesized by Giddings and Staehelin (1991). It is also possible that the pressure of terminal complexes on these plasma membrane-bound microtubules causes the re-orientation of microtubules themselves, as hypothesized by Fisher and Cyr (1998; Himmelspach *et al.*, 2003).

Limitations inherent in measuring specimen dimensions on metal replicas

There are two major sources of potential artifacts contributing to the images in this study. The first is the relatively rough method of preparation required to extract portions of the plasma membrane in order to track cellulose microfibrils back to terminal complexes.

The second is the inherent uncertainty of measurements made on metal replicas of biological specimens.

Replicas of biological specimens are used primarily to gather qualitative information about the specimen. When quantitative information, such as particle size, height, etc. is required, great care must be taken. Several types of artifacts make the interpretation of quantitative data obtained from metal replicas problematic. The first and most obvious is the presence of the metal film itself. The deposition of a 2-5 nm thick layer of platinum/carbon on the specimen broadens the features of the specimen. Less obvious is the contribution of specimen broadening by the accretion of a cap. The accretion of cap material must be taken into consideration when fine structure (e.g. <50 nm) in replicas is measured (Willison and Rowe, 1982). Furthermore, on specimens below approximately 100 nm in size, the granularity of the film will begin to limit resolution (Willison and Rowe, 1982). Replicas are also backed with pure carbon to stabilize the platinum grains and strengthen the replica so that it does not distort or fall apart during processing. The presence of the pure carbon backing may also contribute to the apparent broadening of the terminal complexes by deflecting a small amount of electrons in the beam. This will be most pronounced when the thickness of the carbon film is increased with respect to the beam, as occurs around particulate objects. However, despite these limiting factors, the cytoplasmic domain of the terminal complexes seen here are roughly twice the size of the rosette TCs seen in cross-section with freeze-fracture (50 nm vs. 25nm). It seems unlikely that the presence of the platinum-carbon shadow causes the doubling of the apparent size of the terminal

complexes. The thickness of the platinum/carbon films used in this report can be

estimated to be approximately 2.5 nm by the following equation:

$$M = \frac{t16\pi r^2 d}{(3\sin \alpha)10^7}$$

where,

      M = the mass of material to be evaporated (g)

      t = thickness of the evaporated film (nm)

      α = shadowing angle

      r = source to specimen distance (cm)

      d = density of material being evaporated (g x cm^{-3})

For the replicas produced for this study, M = 0.006g; α = 75 degrees; r = 8 cm; and d =

21.5 for platinum (Bradley, 1965; Willison and Rowe, 1980).

Future methods for further elucidating the structure of the terminal complex

The visualization of terminal complexes by metal shadowing has drawbacks because a

replica is imaged and not the actual specimen. A technique which does not rely on

shadowing would increase the resolution of the terminal complex. Also, because of the

infrequency of locating a terminal complex on isolated plasma membrane sheets, these

specimens would be most amenable to analysis by cyroelectron tomography. With this

type of analysis, the thinness of the plasma membrane sheets would allow for the

acquisition of images at high tilt angles. Recently, this technique has been used to

elucidate the formation of the somatic cell plate in meristematic cells of *Arabidopsis*

(Segui-Simarro *et al*., 2004). Perhaps, using electron tomography, the association of

cellulose microfibrils under the plasma membrane sheet with the exocytoplasmic face of the terminal complex could be visualized in three-dimensions. Ultimately, it may be possible to use computer algorithms to identify the linear cellulose microfibrils and capture a whole 3D tilt series of the particle associated with its end (Böhm *et al.*, 2000).

Now that the dimensions of the cytoplasmic domain of terminal complex have been visualized and measured, computer-aided modeling may be used to determine the number of possible CesA proteins in a single terminal complex. Also, immunocytochemical localization of proteins thought to be members of the terminal complex may also contribute to the elucidation of the structure of the terminal complex. Interactions detected between three different CesA proteins have given rise to the theory that three CesA proteins are present in the same rosette TC (Taylor *et al.*, 2003). In Chapter 5, the cytoplasmic domain of terminal complexes was labeled with anti-CesA antibodies. Perhaps, using antibodies specific for the different CesA proteins, the presence of three different CesA proteins in a single rosette terminal complex can be directly proven.

Conclusions

A new technique for imaging the cytoplasmic domains of transmembrane proteins and cortical structures, and correlating these structures with extracellular landmarks has been developed. This technique has been used to visualize the cytoplasmic domain of rosette terminal complexes in isolated plasma membrane sheets of Tobacco BY-2 cells. This is the first direct evidence which supports the hypothesis that rosette terminal complexes

have a fairly substantial cytoplasmic domain. Free ends of cellulose microfibrils were only rarely observed, suggesting a covalent link between microfibrils and terminal complexes. Plasma membrane sheets have been prepared on glass and mica surfaces coated with poly-L-lysine or silane (APTES) and also on positively-charged glass surfaces. Some terminal complexes have been shown to be hexagonal in shape while others seem to be composed of multiple subunits. The size of the hexagonal terminal complexes has been shown to be 45 x 50 nm in diameter and the height of the hexagonal particles has been estimated to be 35 nm. This new imaging technique will allow the further elucidation of the structure of the terminal complex and may also aid in mapping the association of terminal complexes with other cytoplasmic structures such as cortical microtubules and ribosomes.
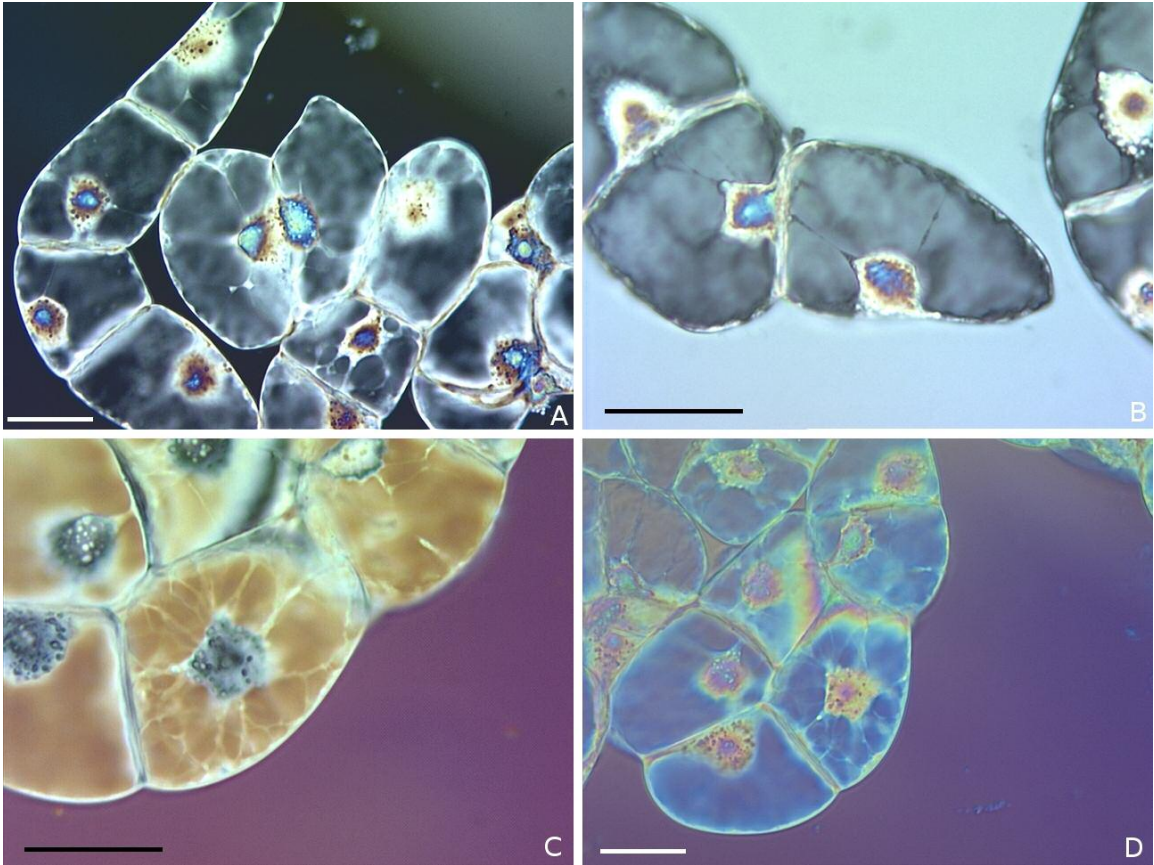
Figure 1. Jamin-Lebedeff interference contrast micrographs of Tobacco BY-2 suspension cultured cells. Scale bars = 50 µm.

An aliquot of the tobacco BY-2 cell cultures used in this study was "optically stained" by Jamin-Lebedeff interference contrast microscopy. The highly vacuolated nature of these cells can easily be seen along with the presence of cytoplasmic strands connecting the nucleus with the plasma membrane.
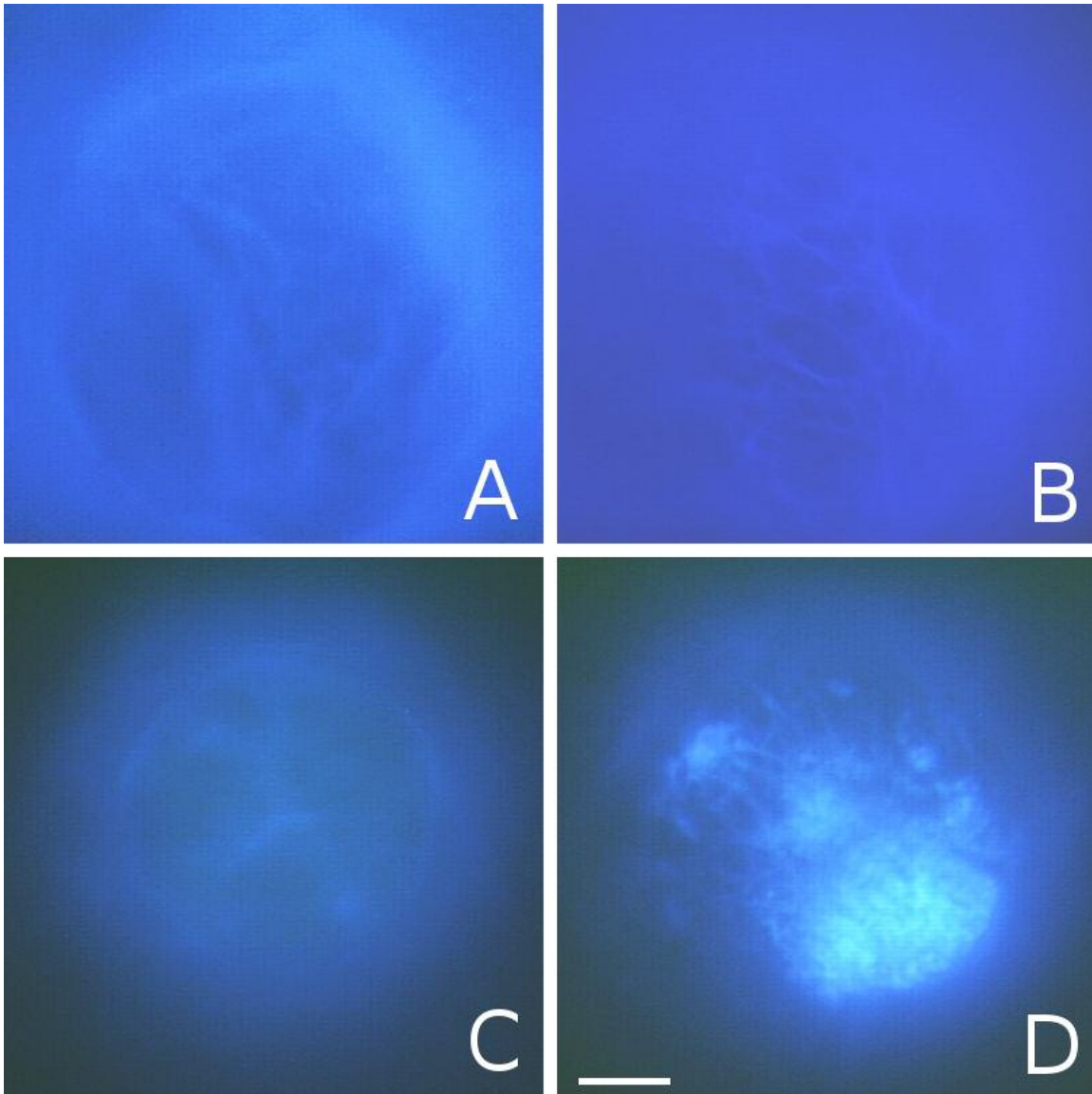
Figure 2. Cellulose microfibril synthesis is disrupted by binding protoplasts to poly-L-lysine coated surfaces. Scale bar in D (10 microns) is the same for all figures in the plate.

Protoplasts were isolated and either attached to poly-L-lysine coated coverslips or left free in solution (on a rotisserie) and allowed to regenerate a new cell wall for 1 hour in an osmotically adjusted culture medium.

(A) Upper surface of a protoplast allowed to regenerate free in the culture medium and showing microfibrils.

(B) Lower surface of the same protoplast as in (A). Many cellulose microfibrils can be seen here.

(C) Upper surface (away from the coverslip) of a protoplast regenerated on a poly-L-lysine coated coverslip. A few microfibrils can be faintly seen.

(D) Lower surface (attached to the coverslip) of the same protoplast from (C). A few microfibrils can be seen along with a large amount of amorphous, Tinopal-stained material.
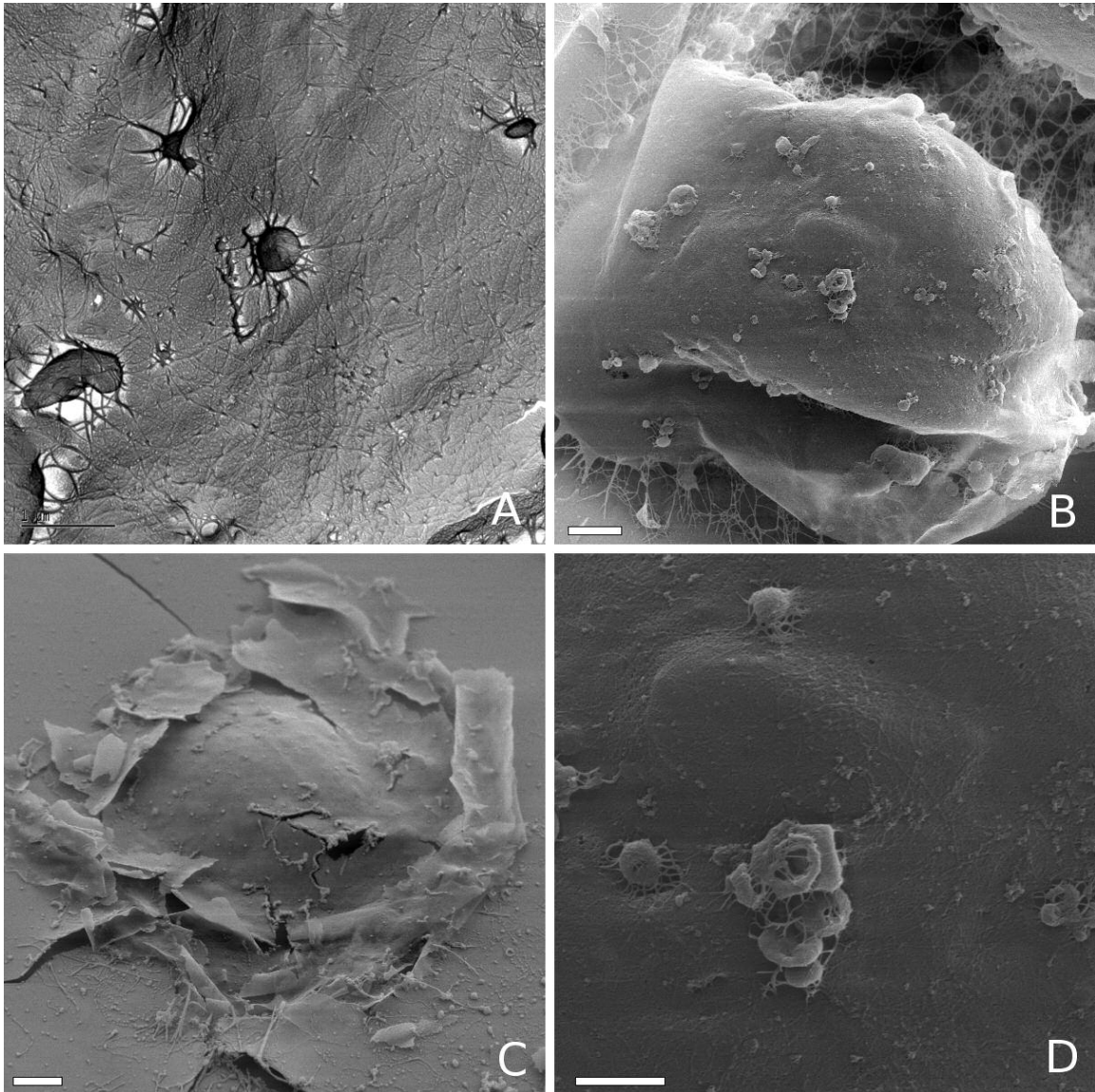
Figure 3. "Membrane sheets" prepared by the "fixative lysis" method viewed by TEM (A) and SEM (B-D).

Protoplasts adhered to poly-L-lysine coated coverslips were lysed with hypo-osmotic fixative solution. One mL of the fixative solution was allowed to run over the coverslips held at a 45 degree angle. Sheets were then dehydrated and coated with platinum-carbon and viewed by TEM and SEM.

(A) A replica of a "fixative-lysed membrane sheet" viewed by TEM. A large number of cellulose microfibrils can be seen on the surface of the membrane. The membrane itself is completely intact although several vesicle can be seen budding off of the membrane. Scale bar = 1 μm.

(B) A scanning electron micrograph of a "fixative-lysed membrane sheet". The three dimensional nature of the image clearly demonstrates the fact that this is an intact cell and not a true sheet. The cell is leaning to one side, probably due to the force of the fixative which was run over the sample while the coverslip was held at an angle. Many cellulose microfibrils can be seen spanning the gap between the cell and the glass substrate. Scale bar = 2 µm.

(C) Another example of "fixative-lysis". One can clearly see that this is not a true membrane sheet, but rather the cell surface was shadowed and then collapsed to a flat structure. When the replica is collected, the replica of the cell is filled with water. As the water evaporates, surface tension pulls the replica inwards until it shatters. Under the TEM, these shattered cell replicas are similar in appearance to plasma membrane sheets. Scale bar = 2 µm.

(D) A higher magnification image of the cell shown in (B). A fine network of cellulose microfibrils can just be detected covering the surface of the cell. This meshwork of microfibrils can be compared with that shown in (A). Scale bar = 1 µm.
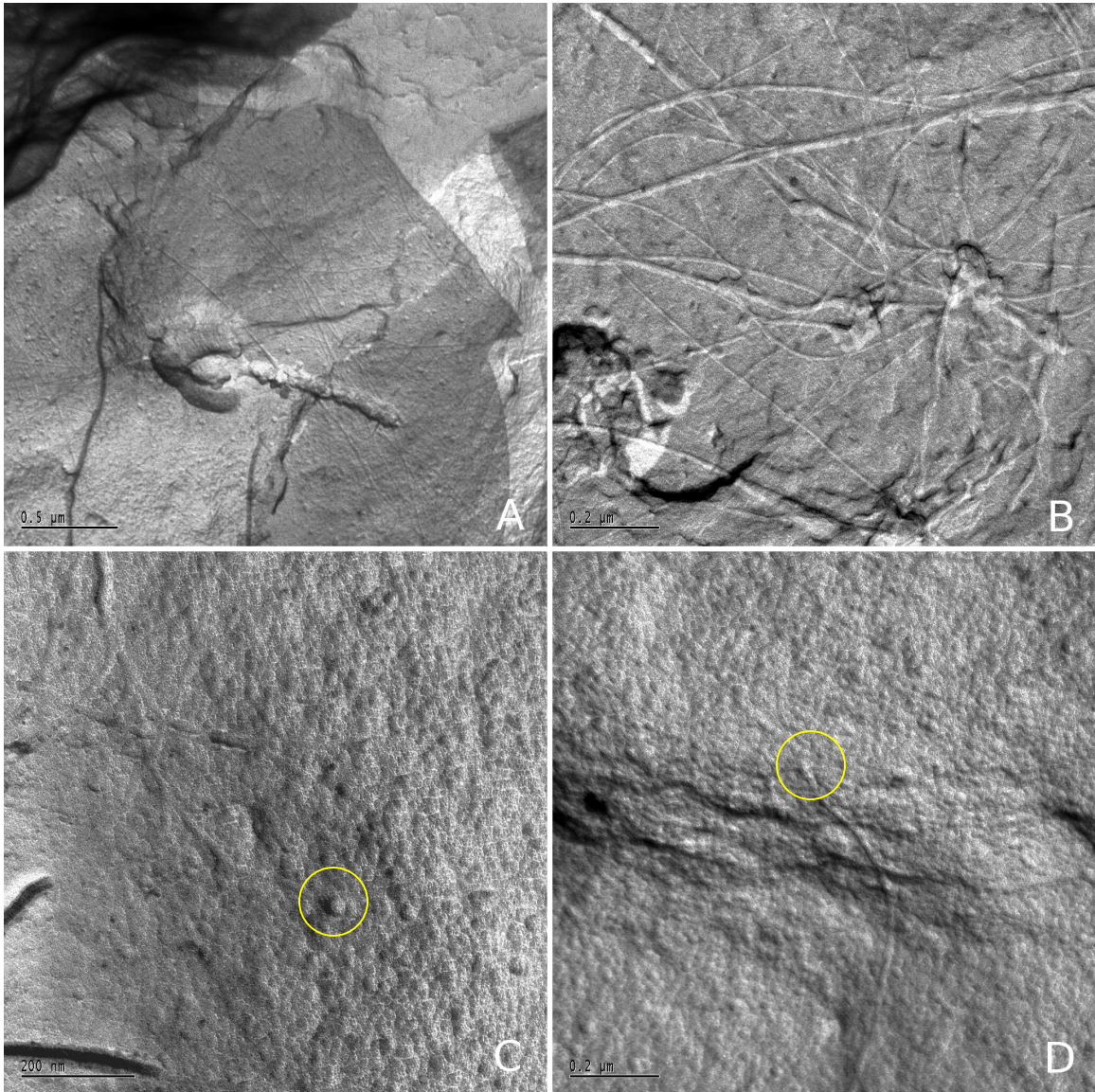
Figure 4. The surface of BY-2 protoplasts.
Protoplasts were produced from BY-2 protoplasts, allowed to regenerate some cellulose
microfibrils for 30 minutes, then fixed with glutaraldehyde and post-fixed with 1%
osmium tetroxide. These well-fixed cells were then attached to poly-L-lysine coated
coverslips and prepared for examination by TEM.
(A) A relatively low-magnification image showing a substantial number of cellulose
microfibrils present on the surface of the cell. Scale bar = 0.5 μm.
(B) A higher magnification image of a uni-directionally shadowed specimen. Scale bar
= 0.2 μm.
(C) and (D) Cellulose microfibrils appear to terminate in small, globular structures
(circled) on the surface of protoplasts. These structures are only slightly larger than the
microfibril itself. Scale bars = 0.2 μm.
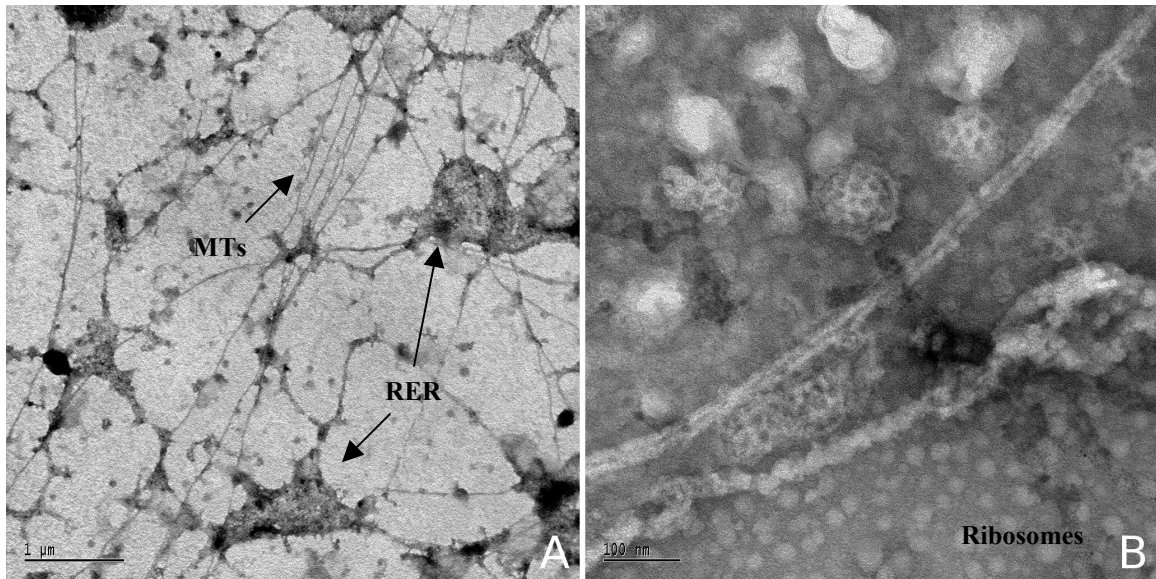
Figure 5. Negative stained plasma membrane sheets from tobacco BY-2 protoplasts.

Plasma membrane sheets were made from BY-2 cells by binding protoplasts to poly-L-lysine treated, carbon-coated grids, then rapidly plunging the grids into hypo-osmotic medium 200 times. Membrane sheets were immediately fixed. After fixation, grids were rinsed briefly with distilled water and then negatively stained with UA. Although microtubules, clathrin-coated pits and vesicles, and ribosomes are clearly identifiable, no cellulose microfibrils can be seen under membrane sheets prepared in this way.

(A) In this lower-magnification image, a network of microtubules can be seen. The majority of the microtubules appear to be oriented in the same direction; however, some microtubules are oriented in different directions. Several patches of rough ER can be seen associated with the microtubule system and the plasma membrane. Scale bar = 1 μm.

(B) The edge of a plasma membrane sheet is shown here. Several clathrin-coated pits/vesicles are apparent, along with a single microtubule. This microtubule appears to be a doublet. A large number of negatively-stained ribosomes can be seen bound to the PLL just outside the membrane sheet. Scale bar = 100 nm.
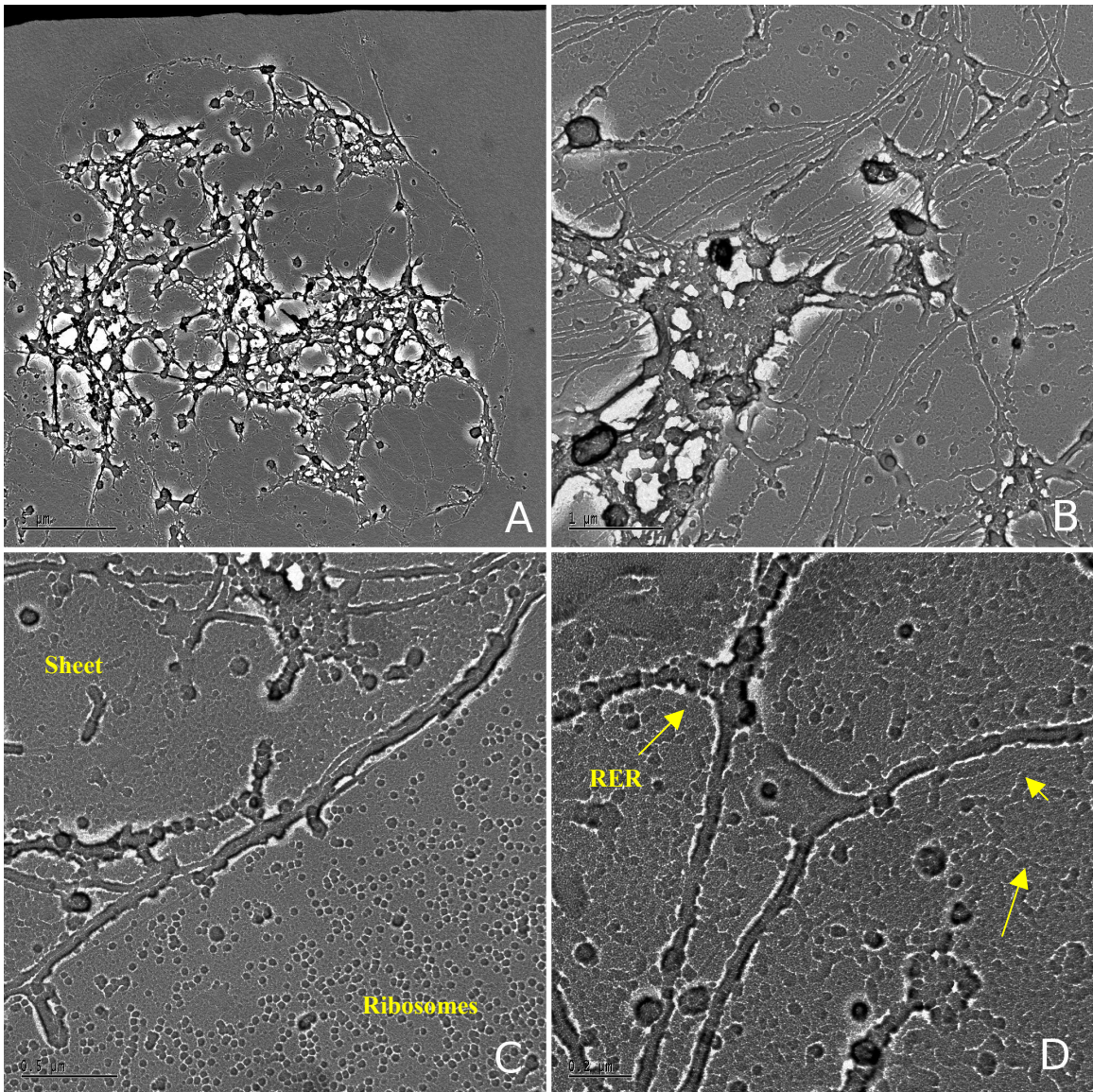
Figure 6. Ultrastructure of the cell cortex of BY-2 protoplasts made by the "Sonobe" method of lysis and shadowed with platinum/carbon

A) A low magnification view of a plasma membrane sheet. A relatively extensive network of what is most likely rough endoplasmic reticulum can be seen attached to the sheet. Scale bar = 5 μm.

B) A higher magnification image clearly showing parallel bundles of cortical microtubules attached to the membrane sheet under the rough ER network. Scale bar = 1 μm.

C) An edge of a membrane sheet is shown here. The membrane sheet is to the upper left and the surface of the coverslip is in the lower right. The membrane sheet appears to have torn along a microtubule. A cellulose microfibril can be seen running parallel to this microtubule. On the outside of the sheet, on the glass surface (lower right) a large number of ribosomes can be seen. Scale bar = 500 nm.

D) At higher magnification some cellulose microfibrils can be seen along with microtubules and a small piece of rough ER. The cellulose microfibrils are only apparent in rare areas such as the ones here (arrows). Scale bar = 200 nm.
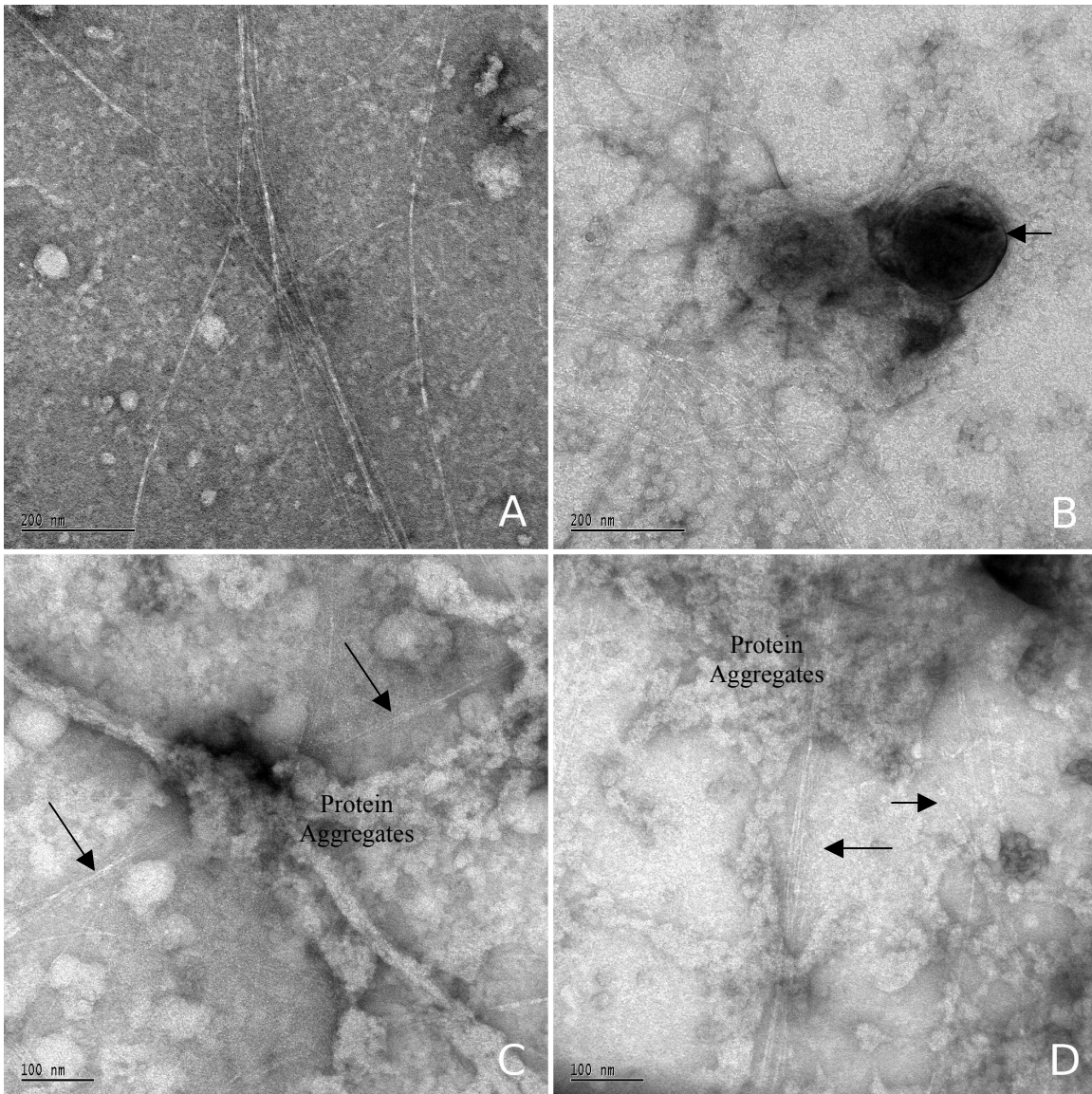
Figure 7. Removal of lipids with chloroform/methanol reveals cellulose microfibrils.

(A) Cellulose microfibrils are easily recognized with negative staining. Scale bar = 200 nm.

(B) Some vesicles (arrow) appeared to be somewhat resistant to the chloroform/methanol treatment. These vesicles may be coated with a layer of protein. Microfibrils can be seen in the background. Scale bar = 200 nm.

(C and D) Protein (and possible lipid remnants) aggregated into clumps or patches following the removal of the lipid bilayer with chloroform/methanol. Many cellulose microfibrils can be seen under the amorphous pools of protein aggregates (arrows).
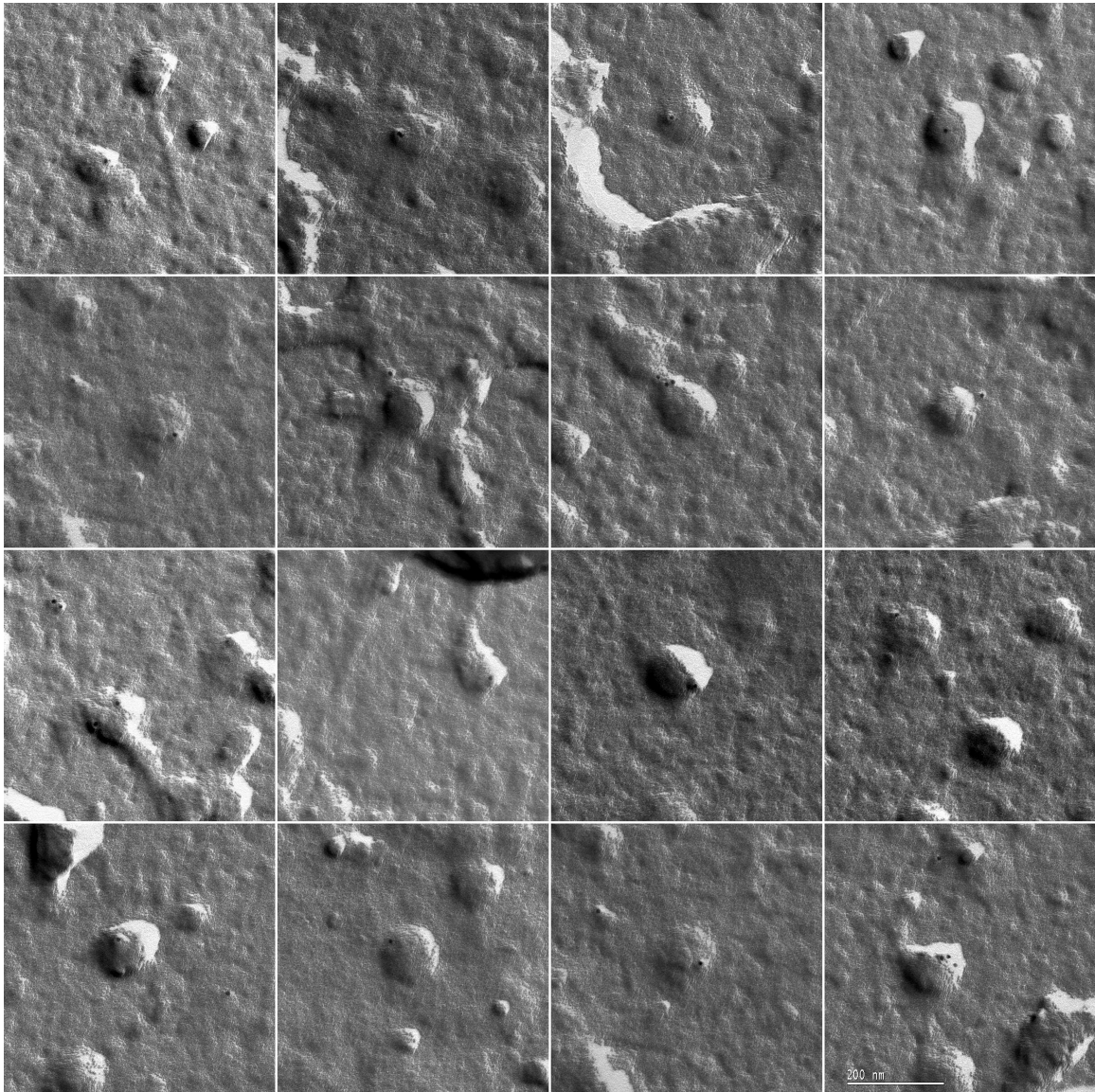
Figure 8. Plasma membrane sheets labeled with anti-CesA, detected by 10 nm gold

Plasma membrane sheets were produced by the Sonobe technique on grids, fixed, and labeled with anti-CesA antibodies. The CesA antibodies were then reacted with a goat anti-rabbit antibody conjugated to 10 nm gold nanoparticles. In this montage, gold particles can be seen to be associated with structures of a relatively constant diameter in the range of 90-100 nm. Gold particles can also be seen adhered to the surface of the plasma membrane sheets. Gold particles are not seen associated with structures of other sizes. Scale bar = 200 nm.
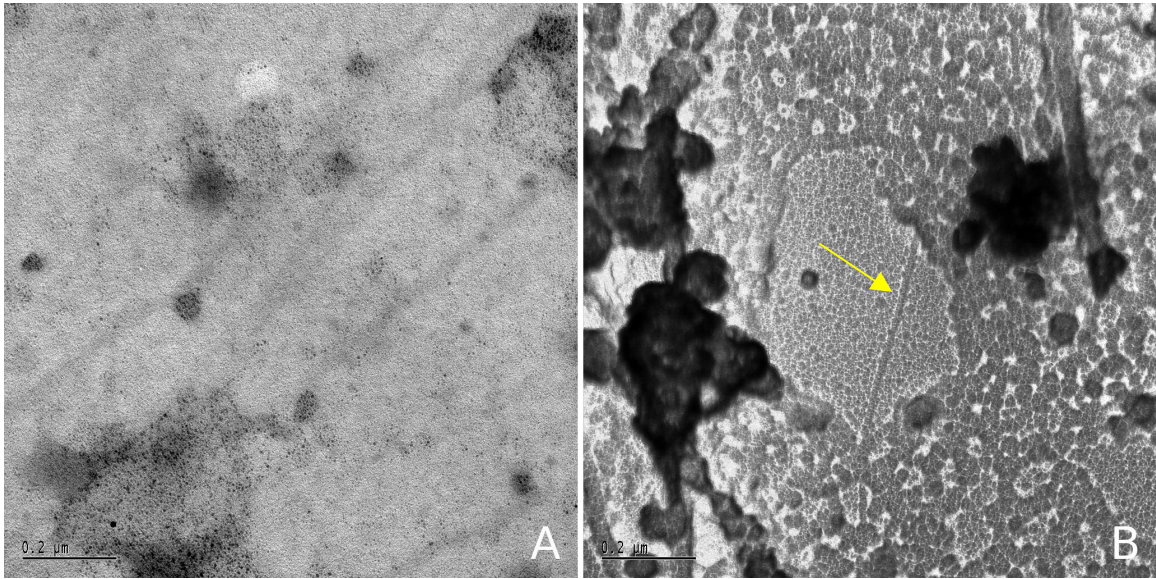
Figure 9. Periodic acid-thiocarbohydrazide-silver proteinate (PATAg) reagents used to localize cellulose microfibrils under plasma membrane sheets

Plasma membrane sheets were made either on glass coverslips or on carbon-coated grids. Plasma membrane sheets on grids were reacted with the PATAg reagents directly and imaged unstained to examine the pattern of silver deposition. Plasma membrane sheets made on glass coverslips were replicated (as usual) and the replicas were then treated with the PATAg reagents.

A) Small silver particles have been deposited over the entire surface of the membrane sheet. Scale bar = 0.2 μm.

B) Although silver appears to be present inside some of the dark vesicular structures here, the cellulose microfibril (arrow) revealed through a small tear in the plasma membrane does not show any silver binding. Scale bar = 0.2 μm.
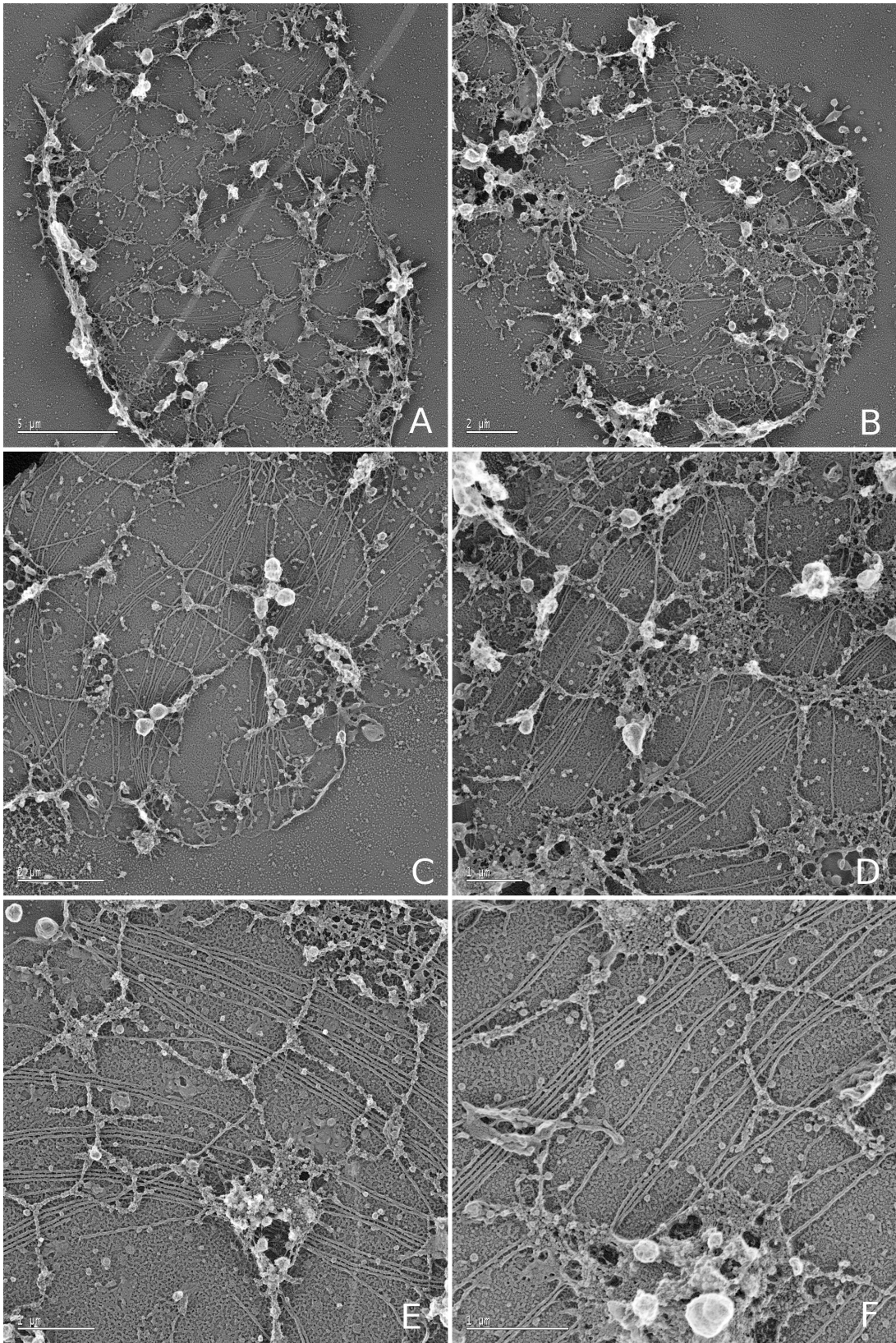
Figure 10. Ultrastructure of cell cortices prepared by sonication.

(A - C) Plasma membrane sheets at low magnification. Note the presence of parallel microtubules, extensive endoplasmic reticulum network, and ribosomes covering the area just outside the membrane sheet.

(D-F) Higher magnification images of membrane sheets prepared by sonication. The surface of the membrane is visibly altered from that of plasma membrane sheets prepared by the Sonobe technique. Also seen here are parallel microtubules and rough endoplasmic reticulum networks. Clathrin-coated vesicles can be just discerned budding off the membrane between the microtubules.
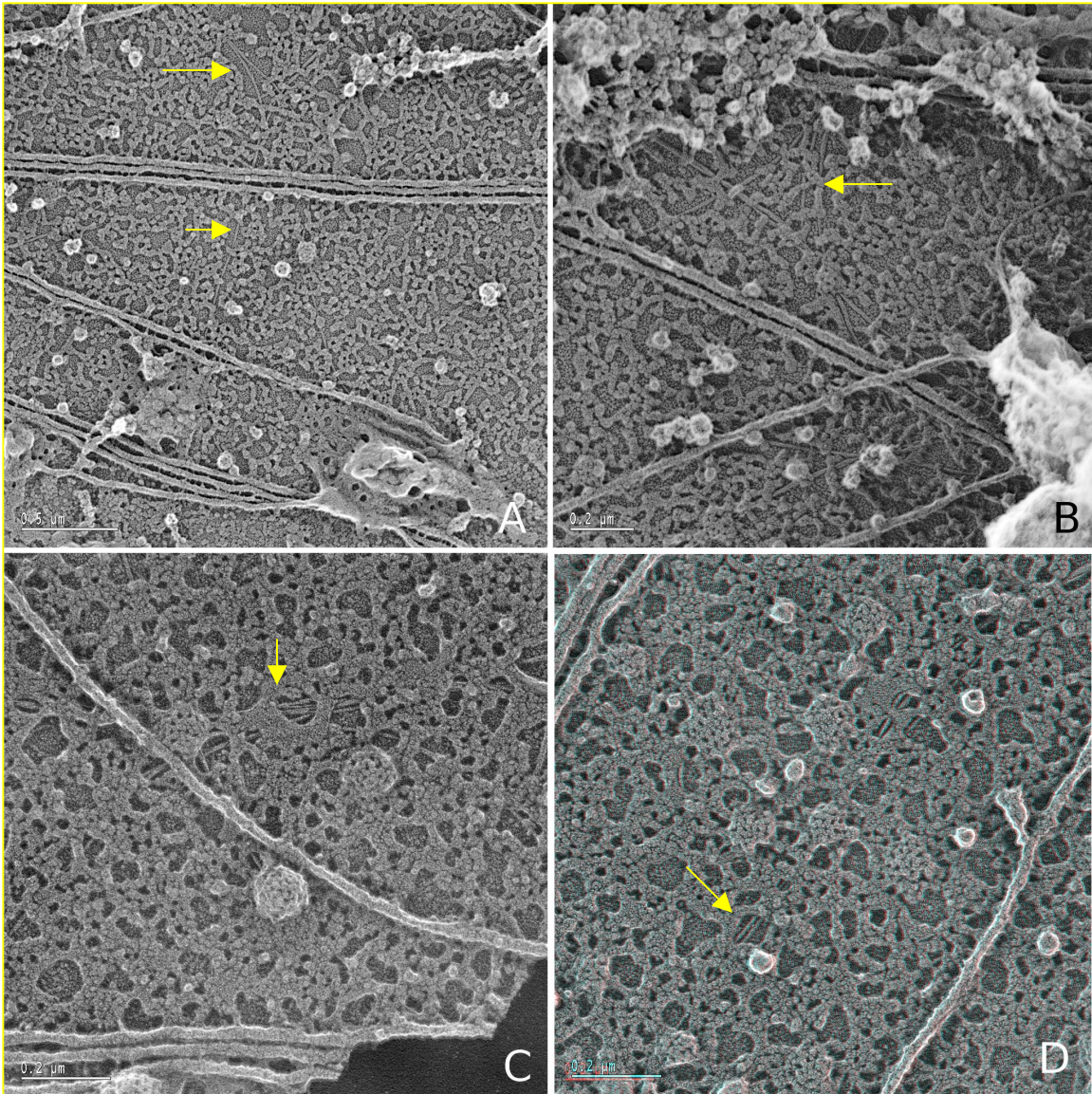
Figure 11. Cleaning of sheets by sonication allows the imaging of cellulose microfibrils through holes in the plasma membrane sheets.

(A – C) Higher magnification images of plasma membrane sheets prepared as in Figure 10. At this magnification, the presence of cellulose microfibrils (arrows) can be discerned under the remnants of the plasma membrane.

(D) A 3D anaglyph of the plasma membrane sheet in a region containing many clathrin-coated pits and a few cellulose microfibrils (arrow).
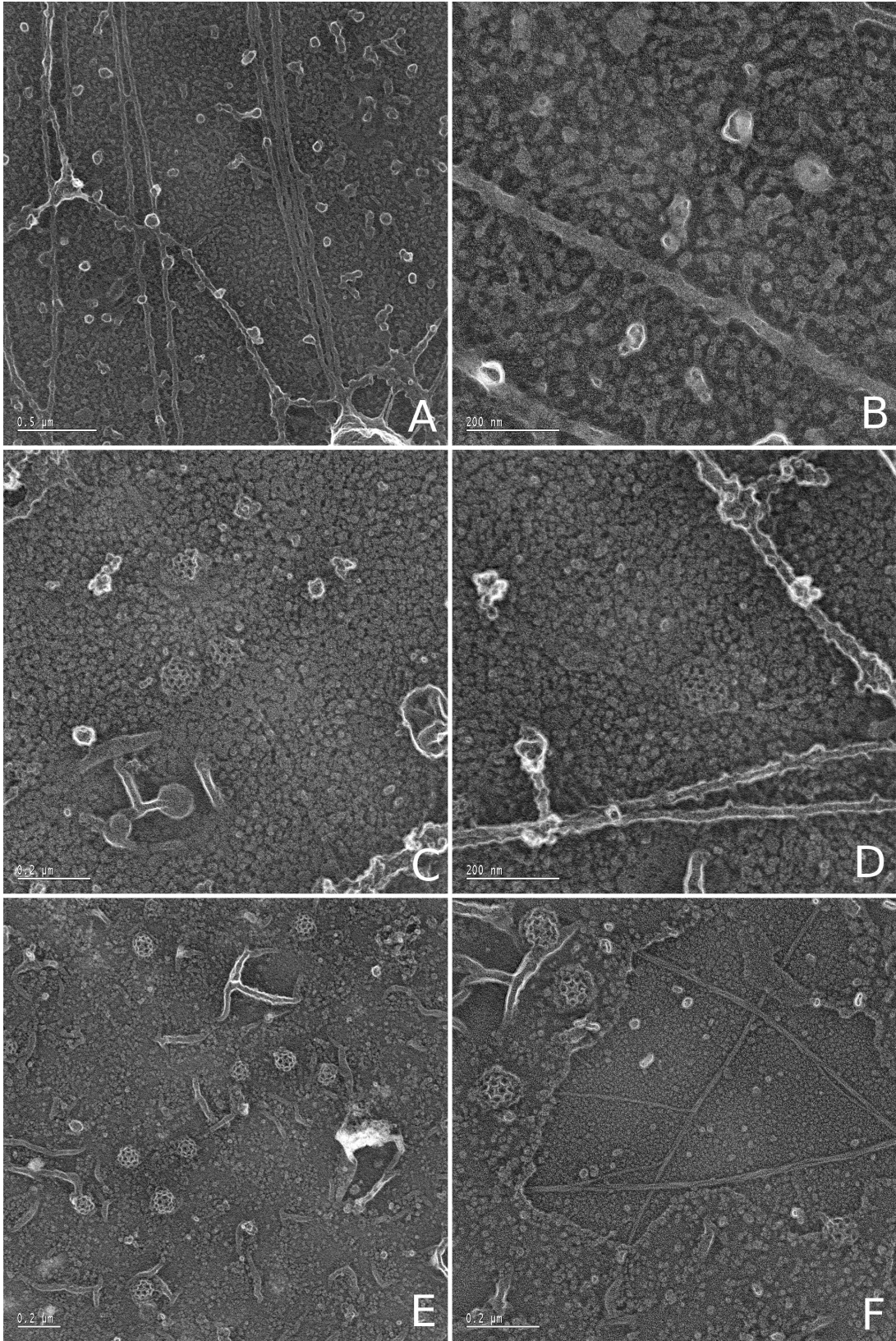
Figure 12. The effect of various fixatives on membrane sheet ultrastructure.

Plasma membrane sheets were prepared by sonication for 5 seconds and fixed in 4% formaldehyde, 1% glutaraldehyde for 1 hour. Some specimens were then post-fixed for 1 hour in 1% osmium tetroxide. Some of these specimens were then tertiary-fixed in 1% uranyl acetate for 3 hours. All specimens were then rinsed in glass-distilled water, dehydrated in graded ethanol followed by HMDS and air-dried.

(A and B) Membrane sheets fixed in combination aldehyde fixative only.

(C and D) Membrane sheets fixed in combination aldehyde fixative and post-fixed in osmium tetroxide.

(E and F) Membrane sheets fixed in aldehyde, osmium tetroxide, and tertiary-fixed with uranyl acetate.
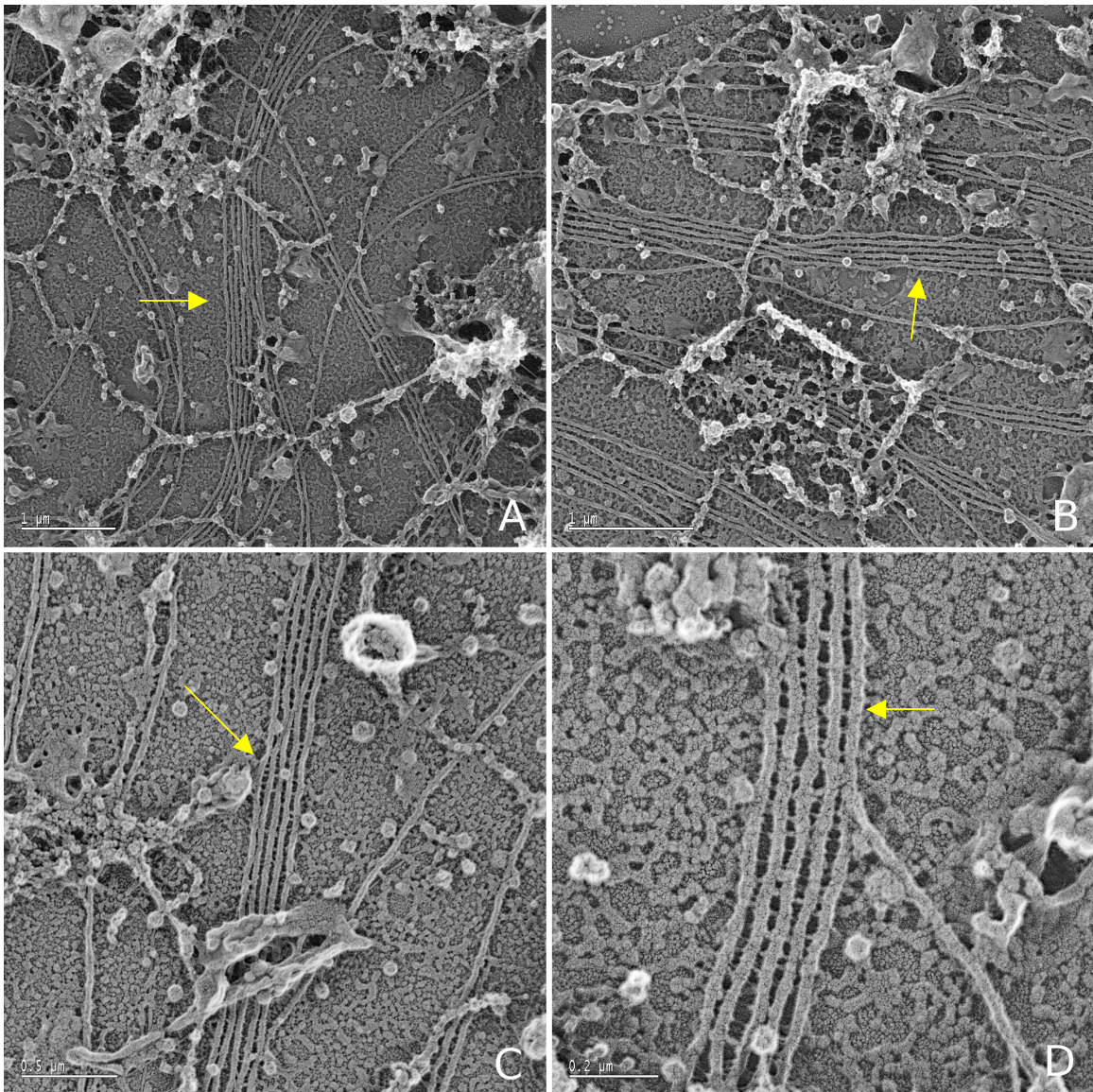
Figure 13. Microtubule bundles

(A and B) Plasma membrane-bound cortical microtubules frequently bundle, as seen in these images (arrows). Scale bar = 1 µm.

(C and D) Cross-bridges can be seen between members of the bundle (arrows).
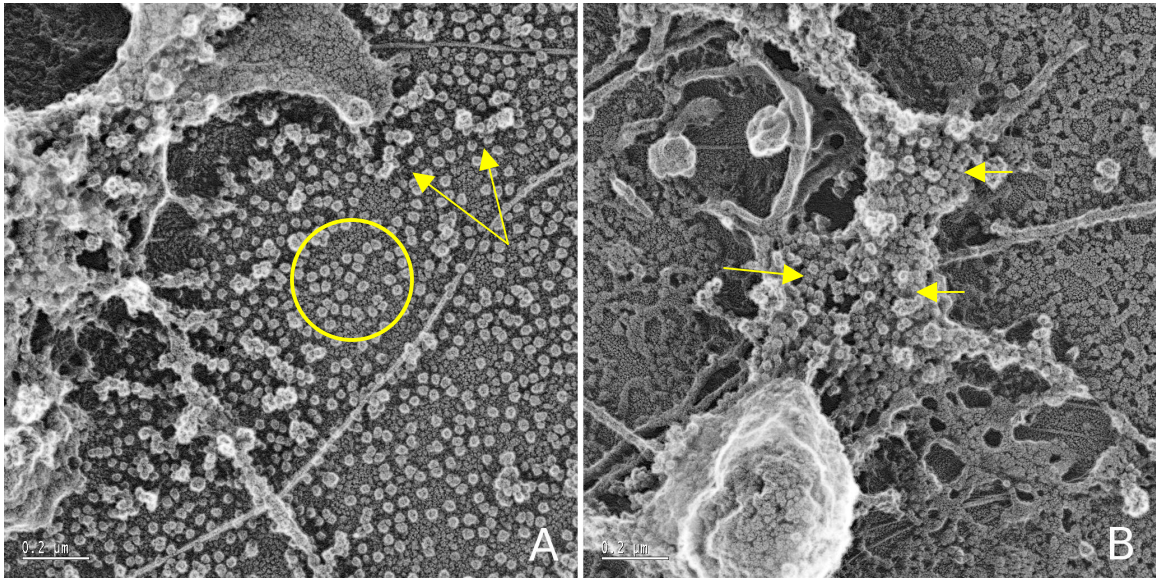
Figure 14. Ribosomes and rough ER

(A) A large number of ribosomes (encircled) can be seen bound to the glass in the area surrounding the membrane sheets. Aggregates of ribosomes may be polysomes (arrows).

(B) This cytoplasmic structure is covered in particles (arrows) the same size as the ribosomes seen in (A), marking this structure as rough endoplasmic reticulum.
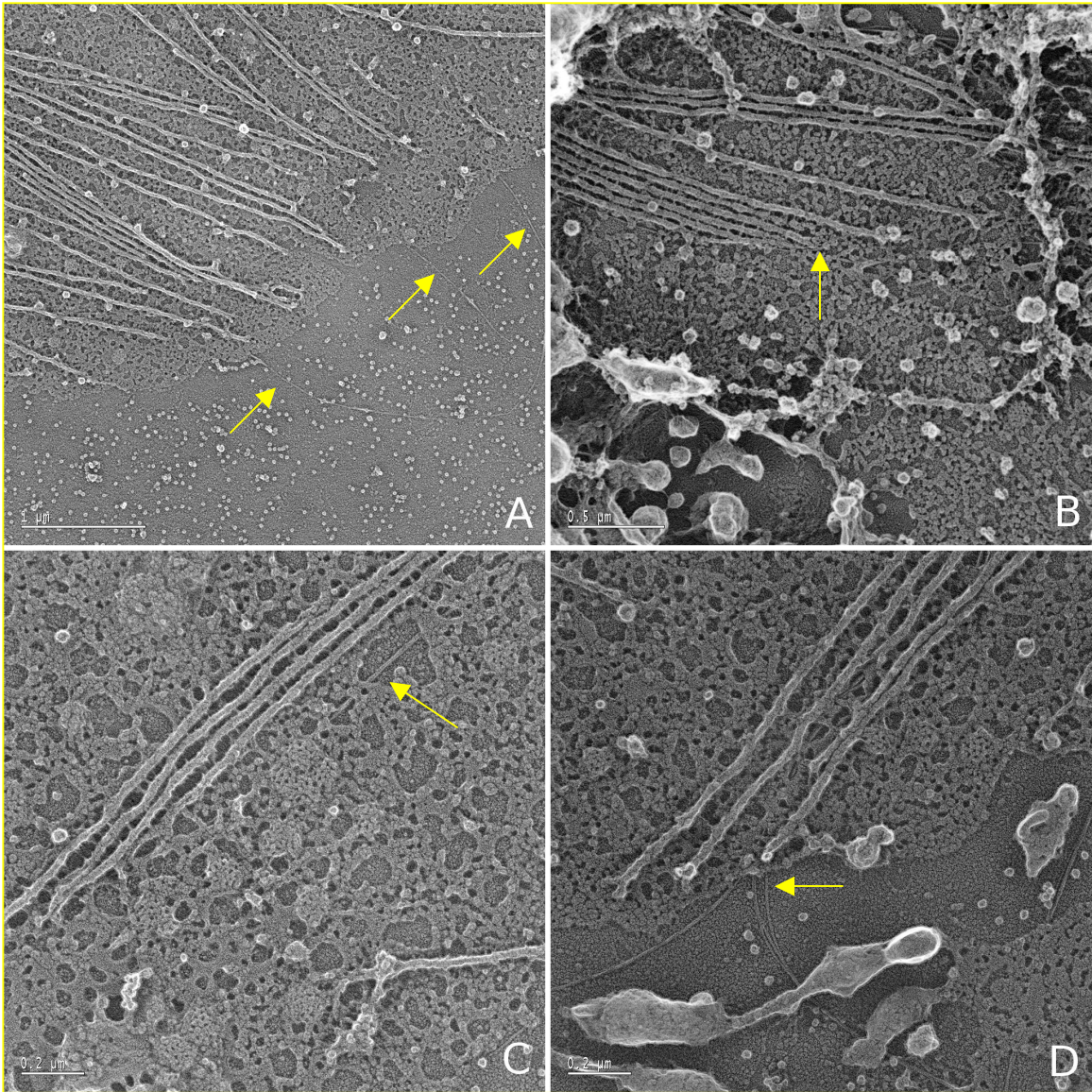
Figure 15. Microtubule oriented cellulose deposition

(A) In this image of the edge of a plasma membrane sheet, parallel plasma membrane-bound microtubules have broken off where the cell body was sheared away. Three cellulose microfibrils (arrows) can be seen extending past the edge of the membrane sheet in a direction parallel to that of the microtubules.

(B) A bundle of plasma membrane-bound microtubule can be seen in the center of this image. Just below the microtubule bundle, a cellulose microfibril can be seen to closely follow the microtubules, even changing direction slightly to follow the curving edge of microtubule ends.

(C) A cellulose microfibril running parallel to a microtubule bundle. Numerous clathrin-coated pits can be seen on the surface of the membrane sheet.

(D) Several cellulose microfibrils can be seen as they pass out from under this bundle of microtubules. On closer inspection, the cellulose microfibrils can be seen between the microtubules all the way out of the image.
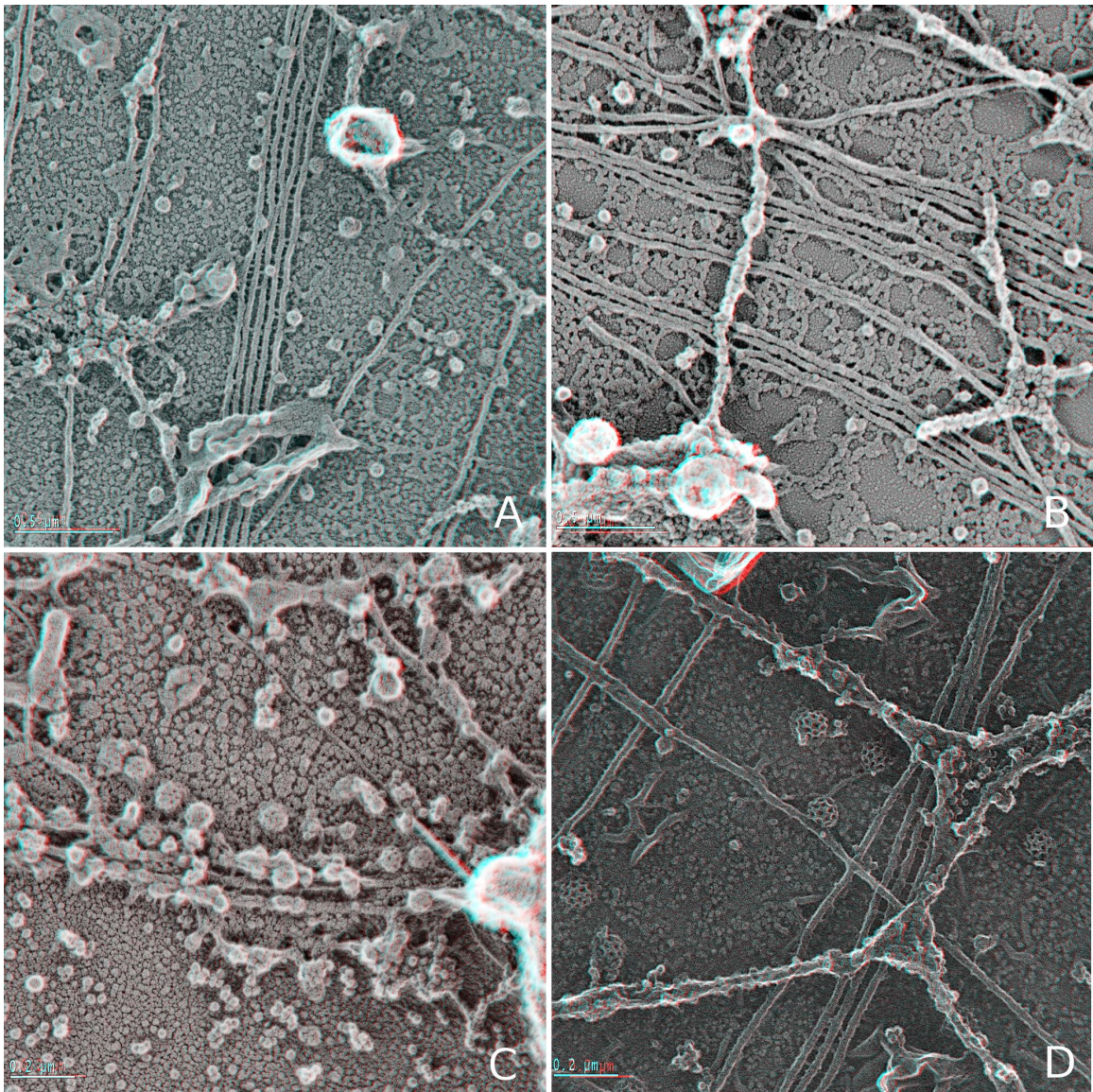
Figure 16. Three-dimensional anaglyphs of BY-2 membrane sheets

For each anaglyph, two images were collect by tilting the stage of the TEM +/- 5 degrees. These stereo images allow a better understanding of the Z vector of membrane sheets.

(A.) A relatively low-magnification image showing a bundle of five plasma membrane-bound cortical microtubules. Clathrin-coated vesicles can be seen bound to the membrane surface.

(B.) Many highly-oriented, plasma membrane-bound cortical microtubules can be seen here. Just above the plasma membrane-bound microtubules is a network of rough

endoplasmic reticulum and its system of associated microtubules. These structures can be easily distinguished by the large number of ribosomes bound all over their exterior.

(C.) A row of clathrin-coated vesicles appears ready to bud off of the membrane in this image of the edge of a membrane sheet. A cellulose microfibril can be seen on the lower right side of the image. It has torn through the soft sheet.

(D.) Plasma membrane-bound microtubules can be seen under the rough ER network. Several clathrin-coated pits/vesicles are apparent attached to the membrane surface between the microtubule systems. Also, the preservation of the structure of the surface of the membrane has been dramatically improved here due to a different fixation schedule (see Materials and Methods 5).
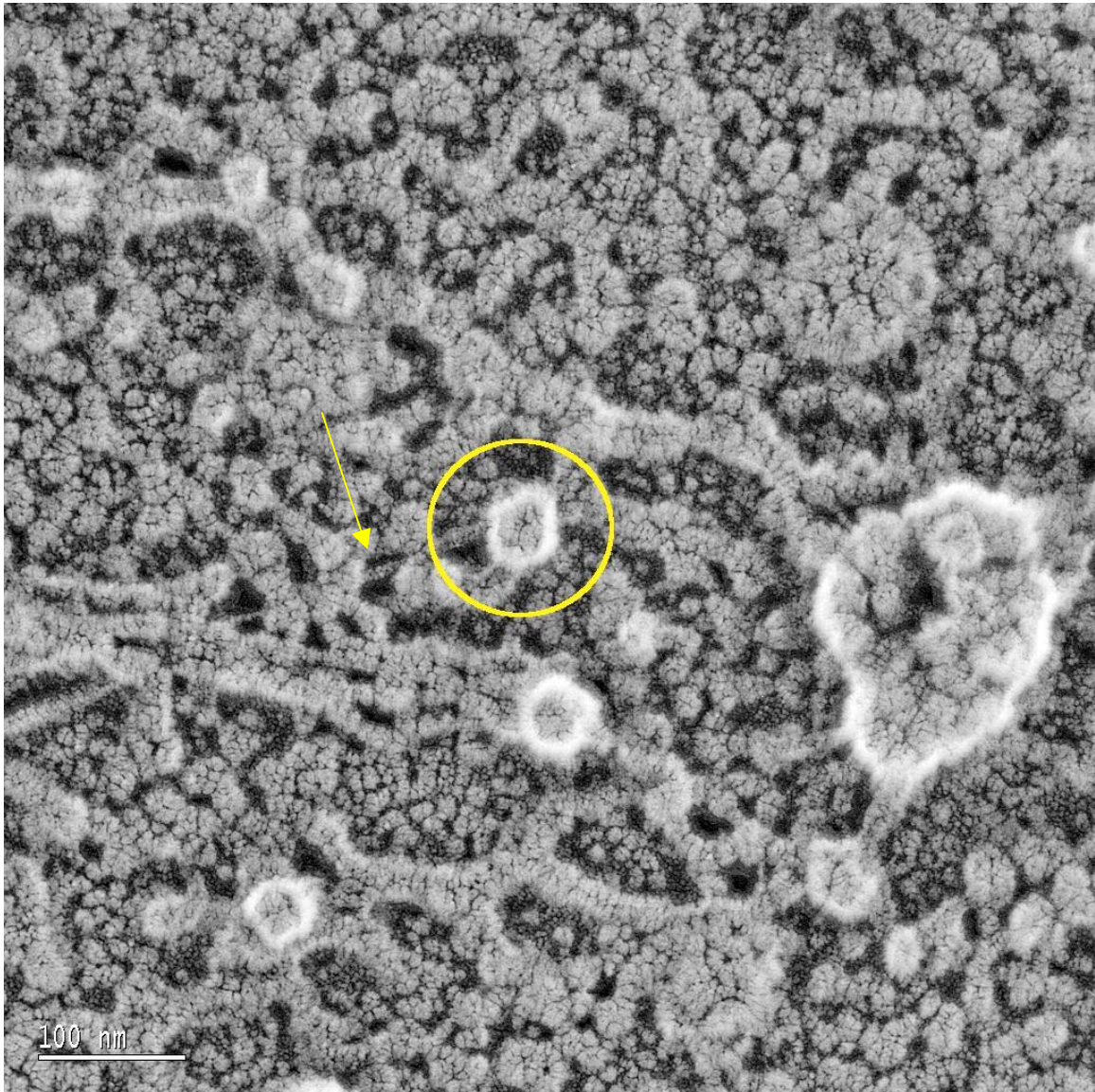
Figure 17. The cytoplasmic domain of a rosette terminal complex (circled) attached to the end of a cellulose microfibril (arrow).

This terminal complex replica measures approximately 50-55 nm in diameter. The cellulose microfibril to which it is attached measures ~7.5-8.5 nm in diameter.
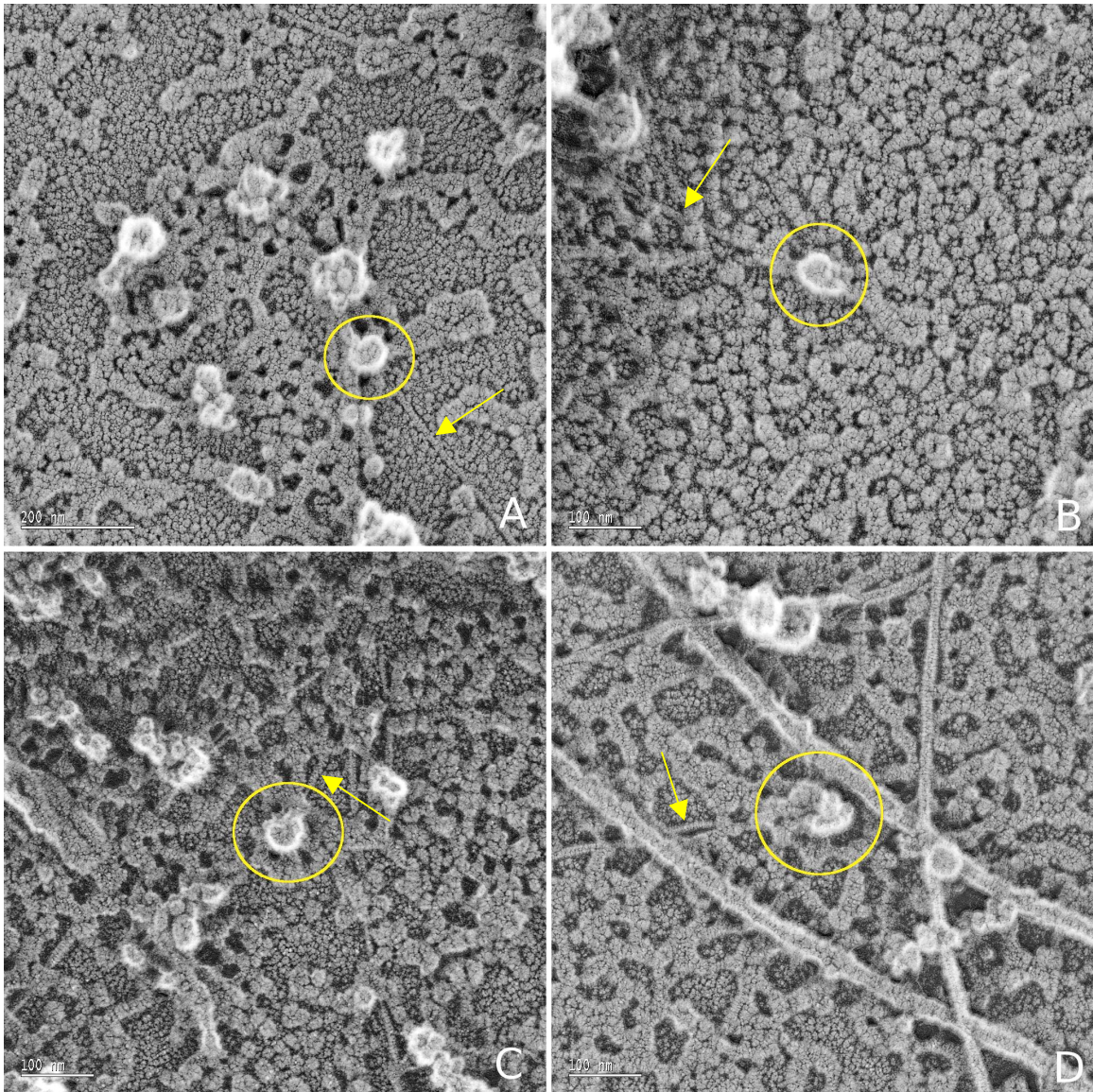
Figure 18. The cytoplasmic domain of rosette terminal complexes (circled) identified by their association with the termini of cellulose microfibrils (arrows).
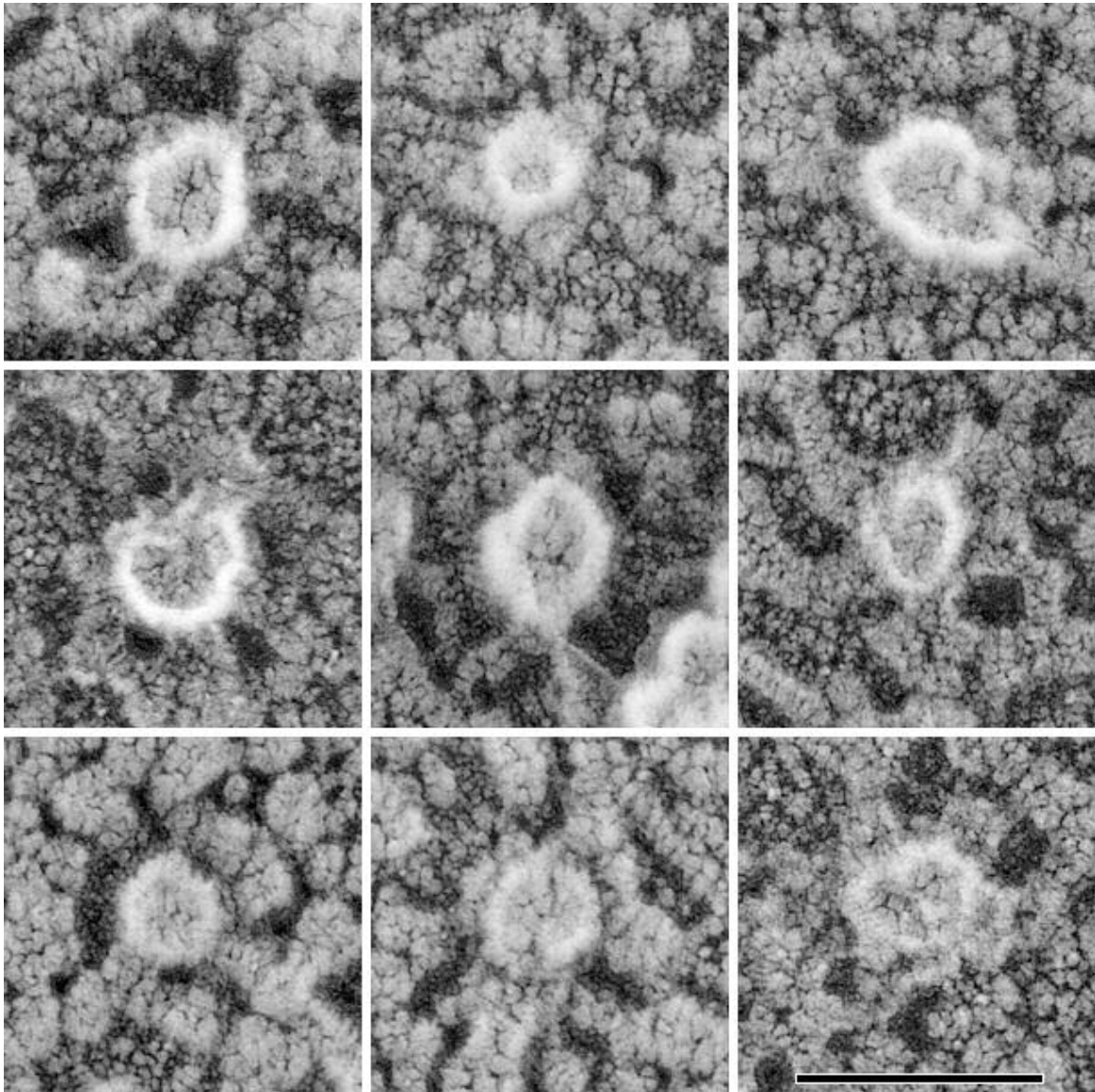
Figure 19. A montage of globular terminal complex cytoplasmic domains at the same magnification.

All of these terminal complexes appear to be composed of a single, globular structure 40-60 nm in diameter. The smaller terminal complexes on the bottom row appear to be not as tall as the larger terminal complexes in the top two rows, perhaps indicating that they are degraded terminal complexes. Scale bar = 100 nm
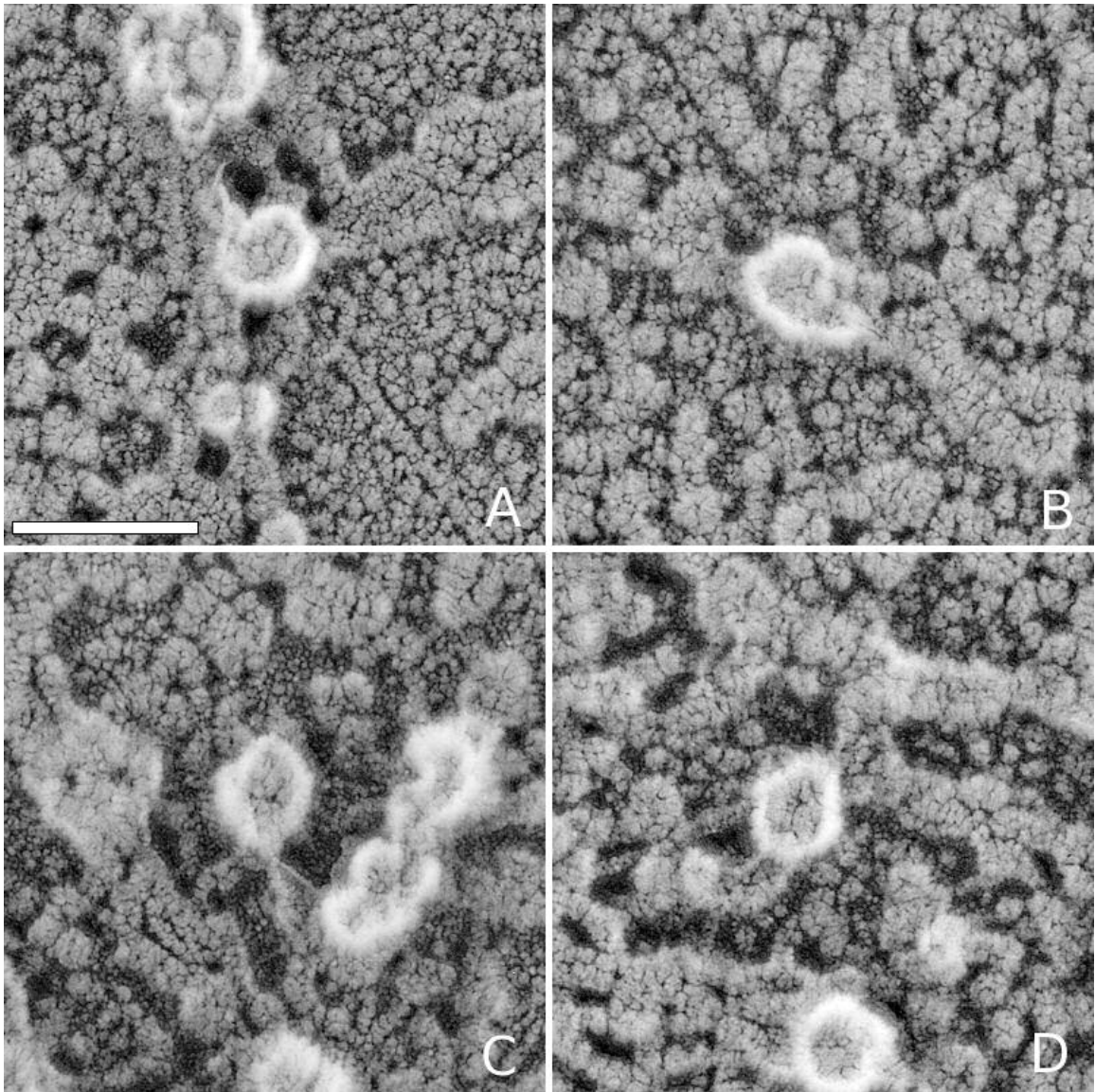
Figure 20. Some of the most clearly hexagonal terminal complex cytoplasmic domains are presented in this figure. Scale bar = 100 nm.
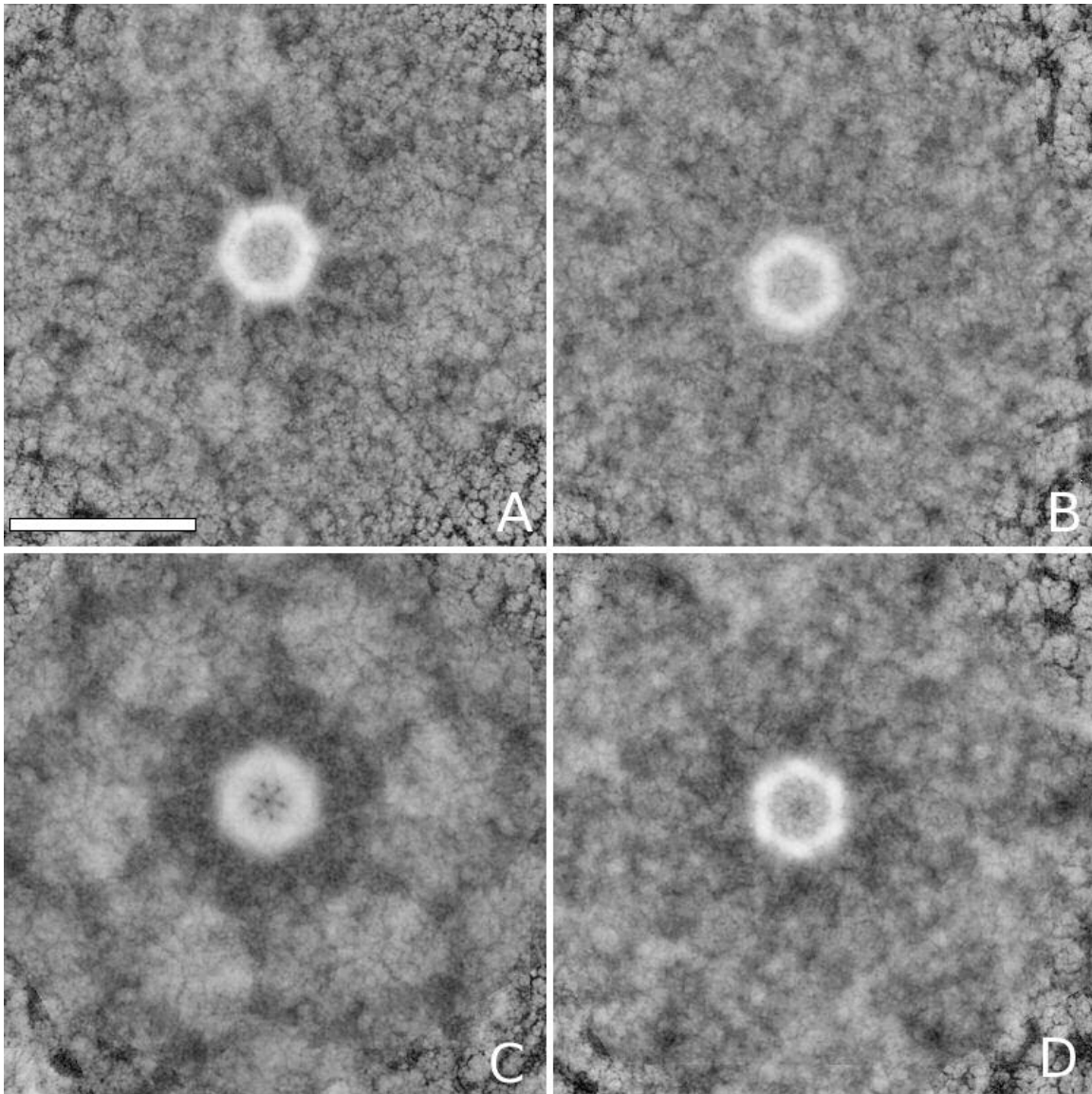
Figure 21. Rotational analysis of the hexagonal particles shown in Figure 20. Images were rotated in 60 degree increments and added back to the original image. Rotation of images by anything other than 60 degrees cause smearing out of the hexagonal shape into a circular shape. Scale bar = 100 nm.
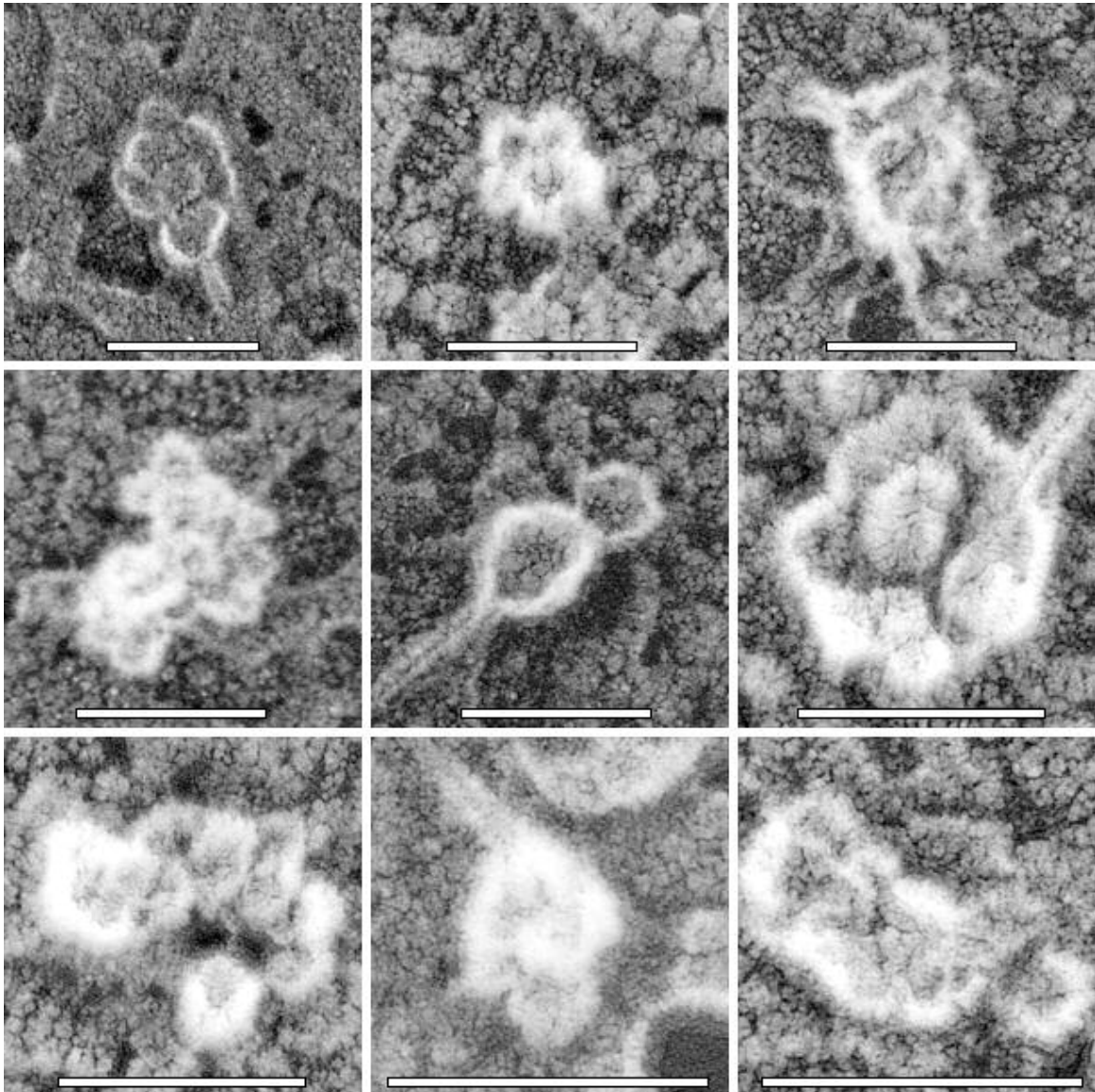
Figure 22. Occasionally, the cytoplasmic domain of rosette terminal complexes are observed to have visible substructure. Some of these terminal complexes are composed of multiple globular subunits, but others appear to be falling apart. Scale bars = 100 nm.
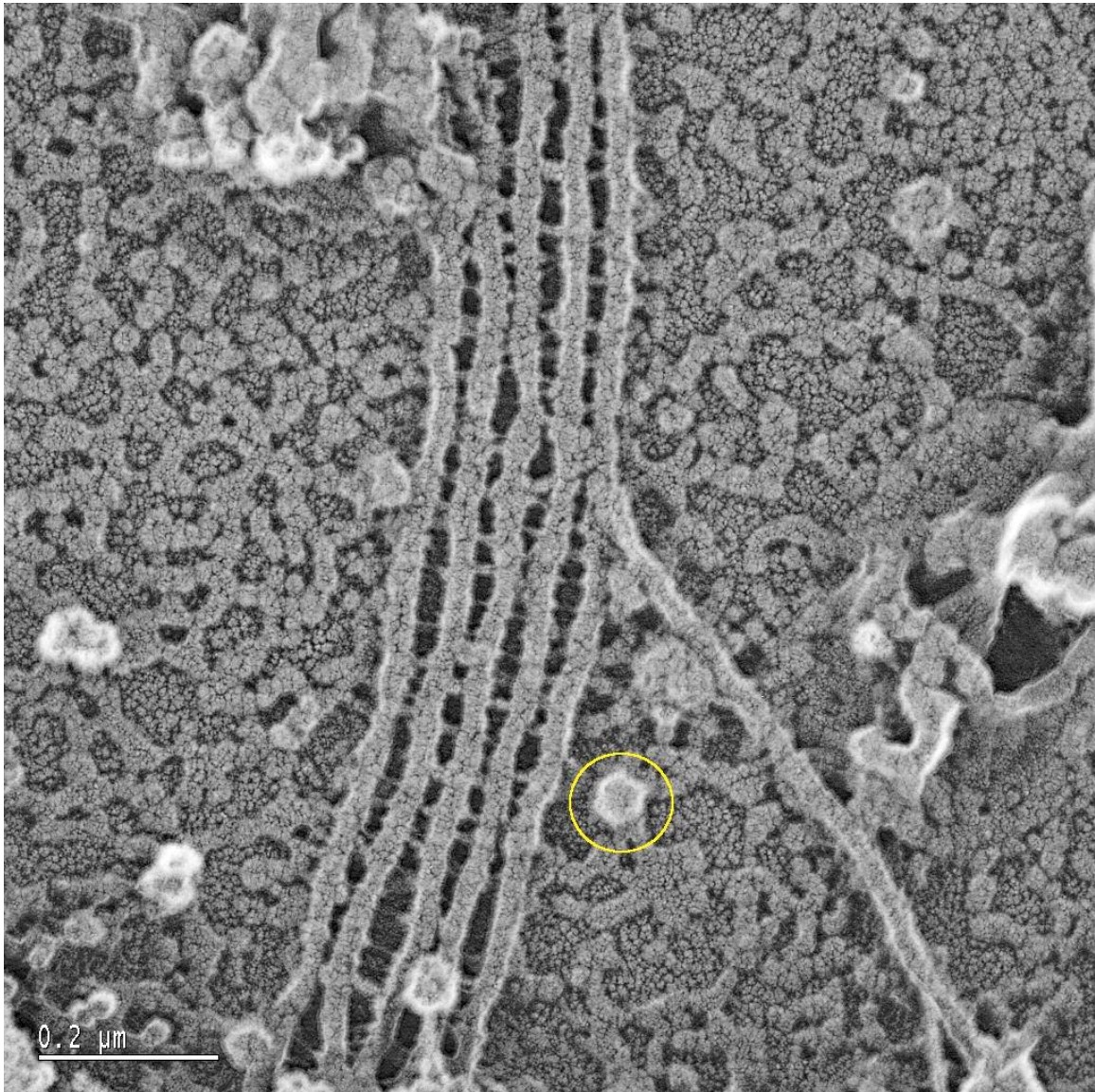
Figure 23. The height of the hexagonal cytoplasmic domain can be estimated to be 35 nm based on a comparison with nearby cortical microtubules. Scale bar = 0.2 μm.

(A) Two CesA proteins with six C-terminal transmembrane alpha-helices. Transmembrane regions are cyan, catalytic regions are yellow.

(B) The transmembrane helices (cyan) from six CesA proteins associate to form one subunit of a rosette TC. A central exit pore may be present (Rudolph *et al.*, 1989).

(C) A rosette TC from the outside the cell. Six transmembrane domains (cyan) associate into one 8nm subunit.

(D) Rosette TC from side view. Large cytoplasmic domains (yellow) are visible with smaller transmembrane domains (cyan) above.

Figure 24. A model of the association of individual CesA proteins into subunits and then into a rosette terminal complex with a hexagonal cytoplasmic domain.

(A) The cross-sectional area of the subunits of the rosette terminal complex are 8 nm, indicative of the presence of 36 transmembrane alpha helices.

(B) Six CesA proteins, each having 6 C-terminal transmembrane alpha helices (cyan), associate to form one subunit of the rosette terminal complex. These 36 transmembrane regions have a hollow core (black) allowing the export of a six glucan chain product.

(C and D) The diameter of the cytoplasmic domain of the rosette terminal complex has been found to be about twice the diameter of the rosette terminal complex seen in freeze-fracture images. Thus, these larger cytoplasmic domains (yellow) probably control the association of the individual CesA proteins into a functional terminal complex.

Appendix 1 - Bowling AJ, Amano Y, Lindstrom R, Brown Jr RM. (2001). Rotation of cellulose ribbons during degradation with fungal cellulase. *Cellulose* 8: 91-97

Degradation of bacterial cellulose ribbons with a commercial cellulase Celluclast 1.5L (Novo Nordisk), from the fungus *Trichoderma reesei,* causes a rotational movement of the cellulose. Purified cellulases (CBH I, CBH II, and EG II) do not induce rotation of bacterial cellulose; however, ratios of CBH I and EG II, in the range of 1.75:1 to 10:1, (CBH I / EG II) do induce motion of bacterial cellulose. Equimolar amounts of CBH I or CBH II and EG II do not result in motion during degradation. Based on these observations, we provide further evidence that cellulose chains may have intrinsic chirality: as the cellulase enzymes degrade the fibrils, the crystalline structure of the cellulose is altered, allowing the linear cellulose polymers to relax into a lower energy state, thus relieving the strain induced by crystallization of the nascent beta-glucan chains during the biogenesis of the microfibril. This conversion of linear, crystalline polymers into more relaxed conformations produces the torsional motion observed during treatment of bacterial cellulose with fungal cellulase.

Introduction

Cellulose

Cellulose, the most abundant macromolecule, is a homopolymer of β-1,4-linked glucose molecules. High resolution electron microscopy of negatively stained cellulose in the model system, *Acetobacter xylinum* (White and Brown, 1981) has revealed a hierarchical association of 50-80 microfibrils (3.0- to 3.5-nm) that associate into flat structures 40 – 60 nm wide known as ribbons. The ribbons are highly twisted, with one complete turn every ~700nm (White and Brown, 1981; Hanley *et al.*, 1997; Hirai *et al.*, 1998). The bacteria rotate during synthesis.

Careful analysis of shadowed cellulose microfibrils synthesized by *Acetobacter xylinum* have shown them to be right-handed helices (Hirai *et al.*, 2000); however, previous reports show just the opposite, namely a left-handed twist of the cellulose ribbons and microfibrils synthesized by *Acetobacter xylinum* (Ruben and Bokelman, 1987; Ruben *et al.*, 1989). Cellulose microfibrils of *Micrasterias denticulata* have also been shown to be right-handed by AFM, TM-AFM, and TEM (Hanley *et al.*, 1997). Also, the induced circular dichroism of methylcellulose chains and cellulose oligomers indicates a helical conformation for β-1,4 glucans (Ritcey and Gray, 1988). Furthermore, ^{13}C NMR spectroscopy has revealed that the β-1,4 linkages between glucose subunits in cellulose derivatives adopt a 35° conformation when in free solution (Buchanan *et al.*, 1989). This suggests that the glucan chains appear to be most relaxed as a 5/4 helix. Thus, in native crystalline cellulose, the van der Waals and hydrogen bonding forces between the glucan chains are holding the crystal together despite conformational

hindrances. Hence, the crystalline native cellulose I allomorph can be thought of as being under constant internal stress.

Use of Tinopal can cause the formation of a mini-sheet in the form of a closed tube-like structure (Cousins and Brown, 1997; Haigler and Chanzy, 1988). When the dye molecules are subsequently photoisomerized by intense UV illumination, they lose their affinity for the cellulose, causing the single glucan chain sheets to collapse into microfibrils (Cousins and Brown, 1997). During this process, the cellulose undergoes a massive torsional motion. It is believed that this motion is the result of the final crystallization of the mini-sheets into microfibrils. The removal of the dye either by washing or photoisomerization allows the crystallization of the cellulose, while the addition of cellulases destroys the crystallinity of the cellulose. Both of these processes cause rotation of cellulose.

Cellulase

The class of enzymes known as cellulases are responsible for the reduction of cellulose microfibrils into their constituent glucose subunits (Tomme *et al.*, 1995). One of the most studied organisms is the fungus, *Trichoderma reesei* (Teeri *et al.*, 1998). Cellulase reactions occur as a group effort of several enzymes which work synergistically to degrade cellulose for consumption by *Trichoderma*.

The binding of cellulase to its substrate is a complex process involving the interaction of the cellulose binding domain (CBD) and the catalytic core of the enzyme with the substrate (Gilkes *et al.*, 1992; Linder *et al.*, 1996; Srisodsuk *et al.*, 1997). The

first stage of action involves binding of the CBD of the cellulase protein to the surface of the cellulose. Once bound, these enzymes initiate catalytic activity. For EG, the function is to cleave the β-1,4 glycosidic bond internally, yielding a reducing end and a non-reducing end. CBH, on the other hand, may bind anywhere along the crystalline surface but initiates its catalytic activity only at a reducing chain end (CBH I) (Divne *et al.*, 1995) or a non-reducing chain end (CBH II) (Divne *et al.*, 1994). Once catalysis is initiated, the enzymes are believed to physically move along the microfibril as they progressively clip cellobiose from the reducing or non-reducing ends. This processivity has been indirectly measured through FRAP analysis (Jervis *et al.*, 1997).

Using time-lapse microscopy, and speculating that cellulose is produced under strain, we investigated the motions of the bacterial cellulose substrate during interaction with cellulase. If, as this report suggests, β-1,4 glucan polymers produced by *Acetobacter xylinum* have internal stress built into the nascent crystalline microfibrils. The results will provide a better understanding of the dynamic interactions of cellulosic materials at both macro- and microscopic levels.

Materials and Methods

Cellulose

Cellulose used in this experiment was synthesized by *Acetobacter xylinum* strain AY201 (ATCC 23769). Pellicles of cellulose were removed from culture tubes, washed in 0.5 M NaOH, and then frozen with liquid nitrogen and ground with a mortar and pestle. Another strain of *Acetobacter*, NQ5 (ATCC 53582), was also tested. This strain of *Acetobacter* undergoes periodic reversals of ribbon synthesis and produces a thicker bundle of cellulose ribbons than AY201 strains. "Pre-treated" cellulose was made by incubation of AY201 cellulose with 16.9 µM EG II.

Cellulase

The cellulase mixture denoted "Complete Cellulase" in this work is a dilution of the commercial product Celluclast 1.5L^{TM}, which is an extract of *Trichoderma reeseii* (courtesy of Dr. Martin Scheulin, Novo Nordisk Bioindustrials, Inc., Danbury, CT; ID# 101187). A stock solution was made by diluting 1 volume of Celluclast^{TM} into 4 volumes of 50 mM acetate buffer (pH 5.0). The total enzyme concentration of this diluted Celluclast™ was 4.2 % protein (w/v), as determined by the Bradford method (Bradford, 1976) using bovine serum albumin as a standard. Purification of CBH I, CBH II, and Endoglucanase II (EG II) was achieved by a combination of column chromatography as previously reported (Amano *et al.*, 1996; Shiroishi *et al.*, 1997).

Treatment of Cellulose with Cellulase

1 mg of cellulose prepared as above, suspended in pH 5.0 acetate buffer, was placed onto a microscope slide. Varying quantities and types of cellulases were added to the cellulose, and a coverslip was placed over the reaction vessel. The reaction was performed at 23°C on the stage of a Zeiss videomicroscope.

Light Microscopy

A Zeiss Universal Microscope operating with phase contrast optics was used to image reactions. Time-lapse images of the reactions were captured with an Optronics CCD camera, and recorded onto a Panasonic optical disk recorder (ODR) at 4 frames per minute (15 sec. intervals). After capture, selected sequences from the ODR were digitized and stored on a computer using a Matrox Meteor PCI frame grabber and Image Pro Plus software. Images were saved in JPEG format, and Adobe Premiere was used to combine the JPEG images into an AVI movie. For web presentation, the AVI was converted into Mpeg format.

Results

Rotation of cellulose ribbons was induced by the addition of the diluted Celluclast
solution (1.0% and 4.2% total protein), and various ratios of purified CBH I and EG II
(Table A1). Figure A1 shows the rotation of bacterial cellulose fibrils after treatment
with diluted Celluclast. Images were collected at 15 second intervals using phase
contrast optics. Every 10th image is shown in Figure A1. The entire set of figures spans
about 20 minutes (the time-lapse movie of this sequence is on the Internet and can be
found at: http://www.botany.utexas.edu/facstaff/facpages/mbrown/movies/movies.htm).
This sequence shows a right-handed 360° rotation of a bacterial cellulose ribbon. In the
field of view, some cellulose appears to dissolve and not undergo any rotation.

Table A1 provides data on the various enzymes added to bacterial cellulose and
the effects on rotation. Two concentrations of diluted Celluclast (1% and 4.2% total
protein) both induce rotation. It appears that the lower concentration of Celluclast
enzyme induces a more intense rotation. Rotation of the cellulose ribbons was
completely abolished after treatment with diluted Celluclast in the presence of 1% methyl
cellulose.

Purified CBH I, CBH II, or EG II used alone did not induce rotation of bacterial
cellulose. Even a combination of all three purified enzymes, when applied in equal μg
amounts, did not produce rotation. Only when the amount of EG II was reduced would
mixtures of purified EG II and CBH I cause rotation. An upper and a lower limit of EG
in the mixture was established (Table A1). Addition of CBH I to cellulose which had
been pre-treated with EG II did not induce rotation (Table A1). Because relatively large

heterogeneous particles were used for light microscopic observations, the quantity of

cellulose present in each sample was impossible to determine. Therefore, we cannot

determine whether the cellulases present in each sample were completely coating the

surface of each cellulose microfibril.

Discussion

Cellulose ribbons produced by *Acetobacter xylinum* in liquid culture are twisted in a right-handed manner (Hanley *et al.*, 1997; Hirai *et al.*, 1998). The alga *Micrasterias denticulata* also produces right-handed helical cellulose microfibrils (Hanley *et al.*, 1997). In both organisms, the spacing between twists is approx. 700 nm. It is fairly obvious that the twist of the bacterial ribbon provides a plausible explanation for the rotation of the bacteria observed during time lapse video of cellulose ribbon assembly (Colpitts, 1977; Brown, personal observations), as well as rotation of bacterial ribbons observed during degradation with cellulase.

It is important to understand the mechanism/s leading to twisting either during biosynthesis or degradation. Two opposing views have been elaborated with respect to the twisting of cellulose during synthesis: (a) the twisting is caused somehow by the bacteria themselves during synthesis (Hirai *et al.*, 1998); or (b) the intrinsic chirality of cellulose is responsible for the twisting (Gray, 1996).

To believe that the bacteria have some torque-generating system which would be completely independent of cellulose crystallization would require a substantial quantity of supporting data. Unfortunately, this does not exist, and the studies supporting this mechanism have scant solid evidence supporting this idea. To provide support for their model, Harai, *et al.* (1998) state that when Acetobacter cells are treated with carboxylmethylcellulose (CMC) during the synthesis of cellulose, they produce twisted, and splayed microfibrils. They further state that this "twisting should be produced simply by the rotation of the bacterial cell itself around its longitudinal axis". They go on to state

that by analogy, the intact ribbon twisting is also a result of the action of the bacterial cells themselves (Hirai *et al.*, 1998). However, these authors have some interesting results and explanations of polymeric additives on the biosynthesis of cellulose under specified experimental conditions; however, these results cannot easily be interpreted to explain an independent motility factor controlling rotation of the bacteria which in turn, regulates the twist of microfibrils and ribbons.

On the other hand, Haigler and Chanzy (1988) make the following statement about the rotation of *Acetobacter* cells during synthesis: "It should be emphasized that since the bacterium has no flagella or other mechanisms of locomotion, the twist of the cellulose and the rotation of the bacterial cell about its axis must be attributed to the cellulose molecules themselves or to their interaction at the cell surface". This second concept also is supported by Gray (1996) and Hanley, *et al.* (1997). To quote the latter, "The chiral nature of the cellulose molecular chain is thus reflected in the physical and mechanical properties of cellulose materials (Gray, 1996), but the relationships between expressions of chirality at different morphological levels (molecule, microfibril, cell wall, etc.) remain unclear".

Furthermore, when *Acetobacter* cells grown on agar generate cellulose, they do not move in a straight line (Brown, personal observations). Instead, they move in an a spiral path and generate cellulose ribbons which are not twisted. Theoretically, this spiral ribbon could be converted into a twisted ribbon by extending the ends of the ribbon away from each other into a linear arrangement. Possible charge interactions between the agar, the cellulose, and the bacterial cells initiate the spiral synthesis pathway, and the

chirality of the cellulose molecules forces the bacterium to curve into a spiral as it extrudes cellulose. This indicates that it is not the rotation of the bacterial cell itself which produces twist in the cellulose ribbon. It is the chirality of cellulose which causes bacteria to rotate.

The current study has shown that bacterial cellulose rotates as it is degraded by *Trichoderma* cellulases. This is the reverse of the process observed by Cousins and Brown (1997). Rotation of cellulose can be thought of as a visual indication of the helix to crystal (photoisomerization) and crystal to helix (cellulase degradation) transitions. It should be emphasized that, in our case, the rotational motions of cellulose ribbons are associated with the degradation process of cellulose. On the other hand, Cousins and Brown (1997) demonstrated the collapse of a tube with a helical seam into a helical arrangement of splayed microfibrils. Rotation by this strain-relief model is possible only if there is internal stress present within the dye-coated cellulose tube. Furthermore, the rotation of cellulose aggregates observed during photoisomerization suggests that the force of crystallization is itself enough to straighten (at least partially) some of the bacterial cellulose.

In the biosynthesis of native cellulose I, the structure of the terminal complex facilitates the crystallization of glucan chains in a parallel fashion. It is possible that the nascent glucan chains co-crystallize before they can relax into their preferred conformations, thus locking stress within the crystal. This is supported by evidence which shows that helical cellulose mini-sheets straighten as they begin to form hydrogen

bonds with each other following photoisomerization of cellulose-bound Tinopal dye molecules (Cousins and Brown, 1997).

How can stress/strain relationships be involved when bacterial cellulose is treated with cellulases? We hypothesize that internal stress is being released during degradation of the crystalline cellulose by cellulase. This might occur if CBH I molecules are interdigitating into the cellulose and releasing strain to cause the rotation. It has been shown that treatment of cotton fibers with chemically inactivated CBH I leaves holes or depressions following removal of the cellulase molecules (Lee *et al.*, 2000). This suggests that the CBD and some of the linker could be interdigitating into the cellulose; however, the structure of CBH I is highly suggestive of a surface mode of action for these enzymes (Divne *et al.*, 1998). In addition, biochemical studies (Valjamai *et al.*, 1998) and computer simulations (Sild, 1999) suggest that CBH I and CBH II act predominantly on the surface of cellulose. We suggest as one possible explanation for surface vs penetration site of action is that the CBD and the linker region may interdigitate between the microfibrils, but leave the catalytic core on the surface to carry out the degradation of glucan chain ends. In order for interdigitation to occur, hydrogen bonds and/or van der Waals interactions between glucan chains would have to be broken. While this model suggests that CBH I itself theoretically should induce rotation, we find that EG II is still required to allow CBH I access to the core of a microfibril.

There are several possible reasons why a combination of EG II and CBH I (not CBH II) could induce rotation. Differences between CBH I and CBH II which may be responsible for rotation include the different degrees of processivity of the two exo-

enzymes, and their opposite affinities for the two ends of a polysaccharide chain. Although it is difficult to see how the preference of the cellobiohydrolases for opposite ends of cellulose might be responsible for CBH II's inability to induce rotation of cellulose, it is plausible to consider the differences in their processivity. CBH I has a much longer tunnel (50 Å) than CBH II (20 Å) (Henriksson *et al.*, 1995) which may translate directly into the increased processivity of CBH I. In addition, because CBH II also possesses some endo-activity (Ståhlburg, 1993), it is possible that CBH II makes too many nicks in the cellulose, thus eliminating the integrity of the backbone of the cellulose which is necessary for rotation to occur.

While both CBH I and CBH II hydrolyze cellulose from the chain ends, only CBH I appears to effectively degrade the crystalline core of a microfibril (which would be the region where the most energy for rotation is stored). On the other hand, CHB II appears to prefer amorphous regions (Chanzy *et al.*, 1983; Irwin *et al.*, 1993; Divne *et al.*, 1998). This model accounts for the difference between CBH I and CBH II; however, it does not explain the requirement of EG II for rotation. In our opinion, EG II is required to be present along with CBH I to allow access to the crystalline core of the ribbon. If the cellulose is pre-treated with EG II followed by treatment with CBH I, rotation does not occur (Table A1), suggesting that the synergy between both enzymes is required for the dynamic release of strain leading to rotation.

There are several lines of evidence to indicate that cellulose molecules are indeed right-handed helices. Individual glucan chains recently have been imaged in a novel form, called nematic ordered cellulose (Kondo *et al.*, 2001), in which single polymer

chains have been observed to be twisted. Because this cellulose does not crystallize into ordered allomorphs, the glucan chains exist in their most native and relaxed form. Also, induced circular dichroism of Congo Red dye by methylcellulose and cellulose oligomers suggest a helical conformation for these polymers (Ritcey and Gray, 1988). Furthermore, ^{13}C NMR relaxation studies and two-dimensional nuclear Overhauser exchange spectroscopy (NOESY) have shown that the lowest energy state of a substituted glucan chain is a 5/4 helix. This shows that the cellulose chain undergoes a 360° rotation for every 5 glucose residues, or approximately 38 turns per micrometer (Buchanan *et al.*, 1989). Since it is known that this is not the conformation of glucan chains within native crystalline cellulose I, either the helical nature of the specimen in the Buchanan study was due solely to the substituted nature of the glucan chain, or some forces are causing the glucan chains in native crystalline cellulose to deviate from their preferred helical conformations.

In conclusion, the results of the current study provide further evidence supporting, at least on theoretical grounds, that cellulose chains may have intrinsic chirality. Alteration in this chirality could occur when glucan chains associate during biosynthesis. The number of chains, their position at biosynthesis, and factors controlling crystallization, all might contribute to the twisting of the glucan chain aggregate, microfibril, or ribbon.

In thinking to the future, the dynamic properties of cellulose observed during both synthesis and degradation may lead to the development of a very inexpensive nano-motor, which could be activated by the crystallization/decrystallization cycle. Given that

cellulose has piezoelectric properties, it is not unreasonable to consider the development of such a device. A future study might be aimed at determining the torque force generated during the degradation of cellulose.

Conclusion

Time-lapse video microscopy has revealed that cellulose microfibrils rotate as they are degraded by cellulase. This is indirect evidence that cellulose I microfibrils are under internal torsional stress. Analysis of the time-lapse images has revealed that the rotation occurs in a right-handed manner. Since cellulose is a right-handed molecule, this means that as cellulose microfibrils are degraded and their diameters decrease, they become more twisted. Furthermore, the difference in ability of CBH I and CBH II to induce rotation is probably due to the fact that CBH I has a higher activity on crystalline cellulose than CBH II. This also explains the requirement of endoglucanase, which greatly enhances CBH I's ability to degrade crystalline cellulose.

Enzyme(s) + AY201 Cellulose	Rotation
5 µl 1.0% Celluclast	++
5 µl 4.2% Celluclast	+
5 µl 4.2% Celluclast + 10 µl Methyl Cellulose	-
10 µl Heat denatured 4.2% Celluclast	-
10 µl 1% CBH I	-
10 µl 1% CBH II	-
10 µl 1% EG II	-
EG Pre-treated Cellulose + 5 µl CBH I	-
EG Pre-treated Cellulose + 10 µl CBH II	-
5 µl 1% CBH I + 5 µl 1% CBH II	-
5 µl 1% CBH II + 5 µl 1% EG II	-
5 µl 1% CBH I + 5 µl 1% EG II	-
8 µl 1% CBH I + 8 µl 1% EG II	-
8 µl 1% CBH I + 4.8 µl 1% EG II	(+)
8 µl 1% CBH I + 4.0 µl 1% EG II	+
8 µl 1% CBH I + 1.6 µl 1% EG II	++
8 µl 1% CBH I + 0.8 µl 1% EG II	+

- No rotation
(+) slow rotation
+ rotation
++ intense rotation

Table A1.1. Assay of cellulose rotation during enzyme treatment
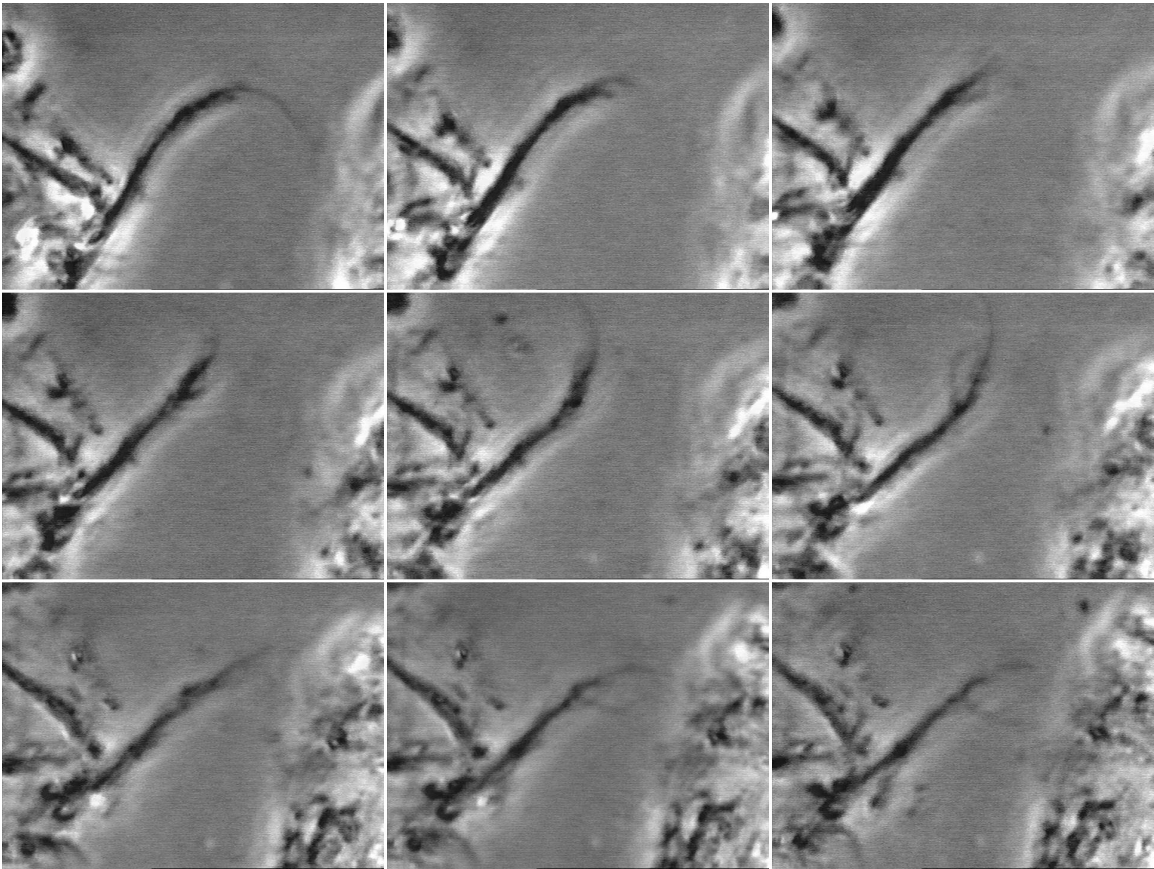
Figure A1.1. A time-lapse sequence showing the rotation of bacterial cellulose during degradation by complete cellulase. The central aggregation of microfibril ribbons is undergoing rotational motion as the time course progresses. Approximately 150 second intervals are represented between each image.

Appendix 2 – The evaluation of the marine alga *Boergesenia forbesii* for use as an experimental system for imaging linear terminal complexes in isolated plasma membrane sheets

The formation of protoplasts and the synthesis of cellulose by these protoplasts were recorded by time-lapse videomicroscopy. The rate of synthesis of cellulose by the protoplasts was graphed and analyzed. An unknown material was found coating protoplasts at a very early stage of regeneration. This substance prevents the isolation of plasma membrane sheets from protoplasts of *Boergesenia*. This compound is speculated to act as a glue to prevent aplanospores from being washed out of the optimal growth zone. Walls of adult *Boergesenia* were isolated, shadowed, and analyzed by TEM. A possible terminal complex was imaged by this technique. Cell walls of *Boergesenia* were isolated and cellulose microfibrils were imaged by AFM. Cell walls of *Valonia* were isolated with intact plasma membranes and imaged by AFM. Putative terminal complexes in the plasma membrane of *Valonia* were imaged.

Introduction

Cellulose is synthesized by transmembrane protein complexes in the plasma membrane of plant cells. These transmembrane proteins are highly labile and have only been successfully imaged by quick-freezing plant tissues and freeze-fracturing the plasma membranes. Although the freeze-fracture technique yields valid and informative information about transmembrane proteins in general, and the terminal complex in particular, it is somewhat limited by the fact that only a cross-section of transmembrane proteins can be imaged. Our goal in this study was to develop a new technique which would allow the imaging of the intact cytoplasmic domain of the terminal complex. This new information would expand what we currently know about terminal complexes through cross-sectional analysis from freeze-fracture studies.

Terminal complexes from vascular plants are hexameric structures 24-25 nm in diameter and they synthesize cellulose microfibrils 3-3.5 nm in diameter (Herth, 1983; Jarvis, 2003; Somerville *et al*., 2004). Bacteria and algae, on the other hand, have linear terminal complexes. *Boergesenia* and *Valonia* have large linear terminal complexes which synthesize correspondingly large cellulose microfibrils (Itoh, 1989). The terminal complexes of *Boergesenia* have an average length of 665 nm and are composed of 3 rows of subunits, each of which are 8 nm in diameter. These massive terminal complexes assemble microfibrils up to 29 nm thick (Itoh, 1989; Itoh *et al*., 1983).

Our idea was to apply an established technique for the isolation of patches of plasma membrane on PLL-coated surfaces (Heuser, 2000; Hirai *et al*., 1998; Van der Valk, 1980; Marchant, 1977; Clark *et al*., 1975) to image the cytoplasmic domain of

terminal complexes. This technique works very well for animal cells in particular, due to the fact that animal cells do not have a cell wall to interfere with the binding of the plasma membrane to the PLL and to confer structural stability to the cells during the bursting process. Cellulose molecules have no charge and as such will not bind to the positively-charged PLL coating. Also, the cellulose microfibrils of the wall do not shear cleanly at the glass/specimen interface when the cells are torn away from the glass. The cellulose microfibrils then tear up through the plasma membrane sheet or lay on top of it, obscuring the inner surface of the plasma membrane. For these reasons, in order to isolate patches of plasma membrane from plant cell, protoplasts must be produced.

Usually, protoplasts are prepared by incubation of plant cells or small pieces of tissue in solutions of fungal or bacterial enzymes which dissolve cellulose (cellulases) and pectins (pectinases). These cells are then glued to a solid surface by electrostatic interactions between the negatively-charged lipids on the outer surface of the cell and the positively-charged PLL coating on the substrate (coverslip) surface. Plant protoplasts are easily burst by washing the cells with a hypo-osmotic solution. Without their protective cell walls, these cells swell rapidly and burst.

Adult thalli of *Boergesenia* undergo a massive redistribution of cytoplasm and organelles upon wounding (Ishizawa *et al.*, 1979). The cytoplasm and organelles are partitioned into many small spherical protoplasts within 90 minutes of wounding (unpublished data; available on the web at the following URL: http://www.botany.utexas.edu/facstaff/facpages/mbrown/movies/movies.htm). Over the next few hours, these protoplasts synthesize a new cellulosic wall (Figure A2.1 and also

114

at the URL listed above). The easy production of many naturally occurring protoplasts as well as having huge terminal complexes and microfibrils led us to believe that *Boergesenia* would be an ideal specimen for the imaging of the cytoplasmic domain of terminal complexes in isolated patches of plasma membrane.

First, the synthesis of cellulose around a nascent protoplast was followed by time-lapse polarization microscopy. An isotropic substance was found coating the protoplasts and preventing the formation of plasma membrane sheets so adult thalli were used in subsequent experiments. Adult thalli of *Boergesenia* were frozen in liquid nitrogen and cut into pieces. These pieces of cell wall with adherent plasma membrane were shadowed and imaged by TEM. Also, pieces of the related alga, *Valonia*, were prepared for analysis by atomic force microscopy (AFM).

Materials and Methods

Culturing and Wounding

Boergesenia were cultured in artificial seawater at 28 degrees C and 14 hour days. Large clumps of cells were transferred to fresh artificial seawater monthly. For wounding experiments, large *Boergesenia forbesii* thalli (~1 cm) were carefully teased apart from clumps with forceps, and wounded by cutting off the holdfast region and cutting a hole in the rounded end of the cells. Cells were allowed to form protoplasts for 90 min in artificial seawater. Protoplasts were manually extruded from the mother wall and collected.

Light microscopy

Protoplasts were placed either into a Sikes-Moore chamber or within a wax ring on a glass slide and covered with a coverslip. All specimens were imaged using a Zeiss Universal microscope, using either a long working distance objective (Leitz) for the Sikes-Moore chamber, or a Zeiss neofluor objective. Cell wall regeneration was followed using polarized optics from 3 hours post-wounding to 8 hrs post-wounding, with images taken at 40 sec intervals.

Electron microscopy

Large thalli were frozen, unwounded, in LN2. Both ends of the cell were cut off to yield a roughly cylindrical specimen. This cylinder was cleaved lengthwise using a LN2-cooled razor blade. These two halves were thawed in 0.5% glutaraldehyde, 8 mM

HEPES and fixed overnight at RT. These fixed pieces were cut into small (<3mm) pieces and collected on Formvar-covered grids. These grids were unidirectionally shadowed with Pt/C and imaged in a Philips EM420 TEM.

Atomic force microscopy

Large thalli were wounded and the protoplasts extruded after 3 hrs. These protoplasts were placed onto poly-L-lysine coated round glass coverslips and imaged under fluid with in contact mode with a Digital Instruments Nanoscope IIIa. The old "mother cell" walls were opened with dissecting scissors, laid cytoplasmic face up, and dried onto a round glass coverslip and imaged in contact mode.

Results

Light and Electron microscopic analysis of *Boergesenia* cell walls

Protoplasts of *Boergesenia* which had been removed from within the mother cell wall and placed inside a wax ring slide were monitored from 3 hours post-wounding to just over 8 hours post-wounding, with images collected every 40 seconds. By polarization microscopy, the formation of cellulose around a protoplast over a 5 hour period can be followed. The bright white appearance of the cellulose layer is due to the highly birefringent nature of the crystalline cellulose microfibrils being made by this *Boergesenia* protoplast.

The images from the time-lapse series were converted to grayscale and the histogram values were read out into a spreadsheet. For each image, the number of pixels of grey values 245-255 were summed and the results were graphed (Figure A2.2). Because the white areas in the images correspond to the highest gray values, this graph should correspond to the newly deposited cellulose. A movie of this can be found at: http://www.botany.utexas.edu/facstaff/facpages/mbrown/movies/movies.htm

Protoplasts of *Boergesenia* were allowed to wound for 3 hrs, and then transferred to a solution containing cellulase and pectolyase for 1 hour to remove nascent cell walls. These protoplasts were washed and glued to poly-L-lysine coated coverglasses and subjected to hypo-osmotic lysis. The resulting specimens were mounted on slides to assess the formation of membrane sheets. Figure A2.3 depicts the results of this process. Hypo-osmotic bursting seems to have been unsuccessful; however, the force of the coverglass in contact with the slide burst several of these "protoplasts", leaving behind

118

empty bags. The exact composition of these early wall-like structures is unknown; however, these empty walls are totally isotropic by polarization microscopy, indicating that they are not composed of crystalline cellulose microfibrils.

Large adult thalli of *Boergesenia* were frozen in liquid nitrogen and cleaved in half lengthwise with a cold razor blade. The cell fragments were thawed in a fixative solution, collected on Formvar-covered grids, rinsed, and shadowed uni-directionally with Pt/C at a 45 degree angle. The presence of many large cellulose microfibrils in the cell wall of *Boergesenia* is apparent (Figure A2.4A). These large microfibrils are synthesized by linear terminal complexes. One possible linear terminal complex can be seen in Figure A2.4B.

Analysis of cell wall fragments from *Boergesenia* and *Valonia* by AFM

Adult thalli of *Boergesenia* were wounded and aplanospores were allowed to form. The aplanospores were removed and an atomic force microscope was used to image these empty "mother cell" walls. The walls were not treated in any other way except a brief rinse in distilled water to prevent the formation of salt crystals upon drying. Cellulose microfibrils can be clearly seen in both the height and deflection images (Figure A2.5). The microfibrils appear very clear and sharp with only one small region of distortion.

Cells of *Valonia ventricosa* were frozen in LN2 and cleaved, just as was done for *Boergesenia*. These cell fragments were thawed in fixative, rinsed, and mounted on round glass coverslips for AFM. The inner surface of a *Valonia* cell is shown in Figure A2.7. At least two distinct classes of particles can be seen associated with the plasma

membranes of these cells. In the upper right corner, a patch of plasma membrane has been removed, allowing the visualization of cell wall microfibrils. One particle was located at the tip of a microfibril (Figure A2.8). The particle is round instead of the linear morphology expected. Two other particles of similar diameter can be observed in this image. In the height image, the particles appear to be at the maximum of the z range. These particles are between 100-200 nm taller than the surface of the plasma membrane.

Discussion

Time-lapse video-microscopy of *Boergesenia* aplanospore cell wall regeneration

Boergesenia forbesii exist as large, multinucleate, uni-cellular thalli. Upon wounding, cells of this organism undergo a rapid and dramatic partitioning of the cytoplasm and cellular organelles into many spherical cells. At first, these spherical cells resulting from the wound-response have no cellulosic cell wall (i.e. they are protoplasts) but over the next few hours they synthesize many large cellulose microfibrils. The rapid and copious production of cellulose by *Boergesenia* protoplasts was documented (Figure A2.1) and graphed (Figure A2.2). This high rate of cellulose deposition, coupled with the fact that this organism has very large linear terminal complexes, seemed to indicate that this alga would be an excellent specimen for the in situ imaging of terminal complexes.

Naturally-formed protoplasts of *Boergesenia* were isolated from within mother walls. These protoplasts were bound to PLL-coated coverslips and subjected to hypo-osmotic stress to make plasma membrane sheets. No plasma membrane sheets were able to be isolated by this process. This inability to isolate plasma membrane sheets is most likely due to the presence of a non-cellulosic material which was found to be coating these protoplasts from a very early stage of recovery (Figure A2.3). Althought the composition of this material remains unknown, due to its lack of birefringence we can be reasonably sure that it is not composed of crystalline cellulose microfibrils.

Based on what is known about the life cycle of this alga in its native environment, we speculate that this compound probably serves not only as a temporary cell covering, but also functions as a glue to insure that the nascent aplanospores remain in a favorable

location for germination. *Boergesenia* in the wild are usually found in intertidal zones adhering to rocks and other immovable objects through their holdfast region. As the *Boergesenia* thalli grow and their surface area increases, eventually the force of the waves becomes sufficient to burst the cells. When this happens, a rapid wound-response takes place, culminating in the creation of many aplanospores inside of each wounded thallus. Often the aplanospores do not escape the mother cell wall and germinate inside the remnants of the old wall. However, if the aplanospores are released from the mother wall they are subject to being washed either too far inland where they may dry out at low tide, or they may be washed out to sea where they may not receive enough sunlight to germinate and grow optimally. In either case, their survival and/or reproduction would be impaired. The presence of a sticky coating around the aplanospores would help them adhere to substrates in the immediate vicinity, thereby increasing the likelihood that they will be in an environment well-suited for growth and reproduction.

TEM imaging of shadowed wall fragments of *Boergesenia*

Large adult thalli of *Boergesenia* were frozen in LN2, cut into pieces, and thawed in fixative. These pieces were oriented plasma membrane-side up on Formvar-covered EM grids, rinsed in glass-distilled water, and shadowed. In some areas, the plasma membrane had torn away from the cell wall, revealing the cellulose microfibrils comprising the cell wall of these adult cells. The microfibrils which are shown in Figure A2.4 can be seen to be in direct contact with the plasma membrane in many places on the grid. Because terminal complexes deposit cellulose into the innermost wall layer, the microfibrils

nearest the plasma membrane are those most recently deposited. The microfibrils in Figure A2.4A appear to be oriented randomly. This wall fragment is from the cylindrical region of a baseball bat-shaped thallus. Perhaps more highly-oriented microfibrils would be present at other locations around the cell. Although the plasma membrane appears to have pulled away from the wall in the region shown in Figure A2.4B, a structure resembling a linear terminal complex can be seen associated with the end of a cellulose microfibril. This structure looks very similar to those seen by Mizuta and Harada (1991) on intact sheets of *Boergesenia* plasma membranes.

AFM analysis of inner plasma membrane surface of *Valonia* macrophysa

Empty walls of cells which had formed aplanospores were carefully cut open, rinsed in distilled water, laid interior-side up on a round glass coverslip, air-dried, and imaged by contact-mode AFM. The clarity of the images in Figure A2.6 and the lack of any distortion of the image due to stickiness of the specimen indicates that there is no coating on these microfibrils. The walls of Boergesenia at this stage of life are then composed of pure cellulose. In particular, this means that *Boergesenia* cells do not produce the glue-like substance secreted by aplanospores constitutively. Further proof that this substance is indeed acting as a glue could be obtained by isolating some of these aplanospore walls and measuring it's stickiness by AFM.

Valonia cells were prepared for AFM by freezing, cleaving, rinsing, and drying them in the same way that *Boergesenia* was prepared for TEM (except for the shadowing). At low magnification, many particles can be seen adhering to the inner

surface of the plasma membrane. Some cellulose microfibril impressions can be seen, especially in the height image. The size of the terminal complex that generated these huge microfibrils should be correspondingly large, facilitating their location by AFM. Unfortunately, only limited clear areas could be found between regions where chloroplasts remained bound to the plasma membrane. One particle was found at the end of a cellulose microfibril (Figure A2.8). This particle appeared spherical in shape instead of the expected elongated ovals seen in *Boergesenia* (Figure A2.3; see also Mizuta and Harada, 1991). The particle is also very tall, perhaps 100-200 nm. The height of terminal complexes from *Boergesenia* has been reported through thin-sectioning studies to be approximately 35 nm (Kudlicka *et al*., 1987). The terminal complexes of *Boergesenia* and *Valonia* are identical by freeze-fracture electron microscopy, therefore we would expect the terminal complexes to look very similar by other forms of imaging. For these reasons, the particle in Figure A2.8 is most likely not a terminal complex.

Conclusions

The naturally-forming protoplasts of *Boergesenia* are not an ideal source for the isolation of plasma membrane sheets due to the presence of an unidentified material found coating the aplanospores at a very early stage of protoplast recovery. It may be possible, however, to isolate membrane sheets from these protoplasts by utilizing more vigorous isolation techniques than those used in the present study (see Chapter 5). Alternatively, if chloroplasts could be removed, perhaps by the technique described in Chapter 5, large areas of plasma membrane would be exposed for analysis, increasing the odds of

successfully imaging the cytoplasmic domain of an intact linear terminal complex.

Hopefully the height information would provide further information about the volume of

terminal complexes as well as strengthen the evidence provided by thin-sectioning

(Kudlicka *et al*., 1987).
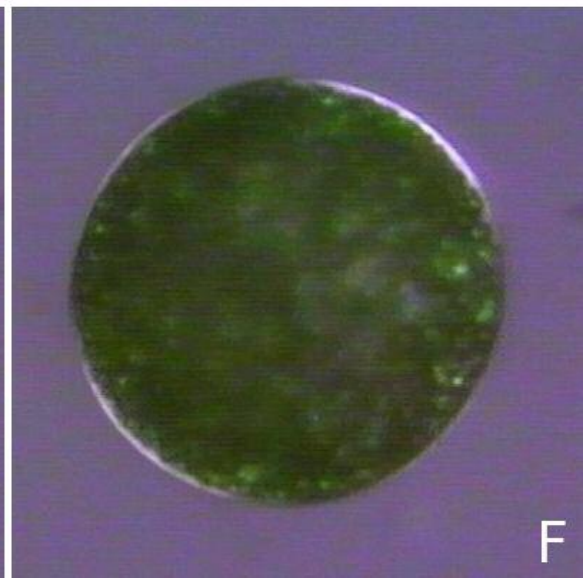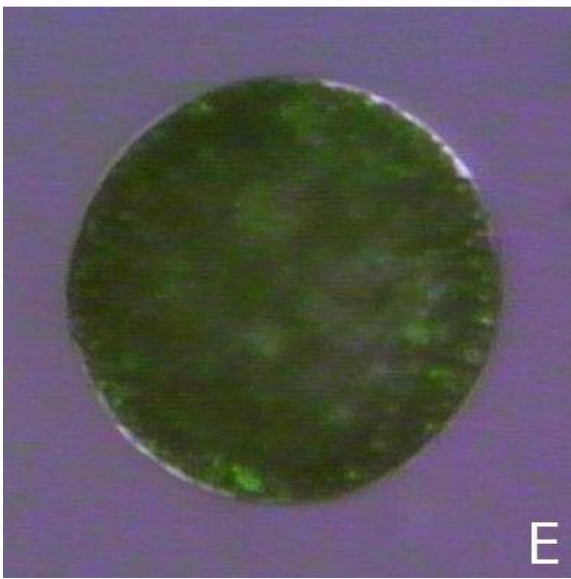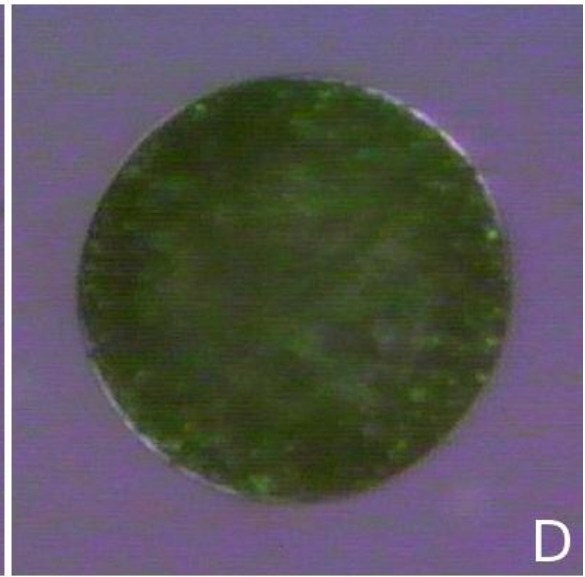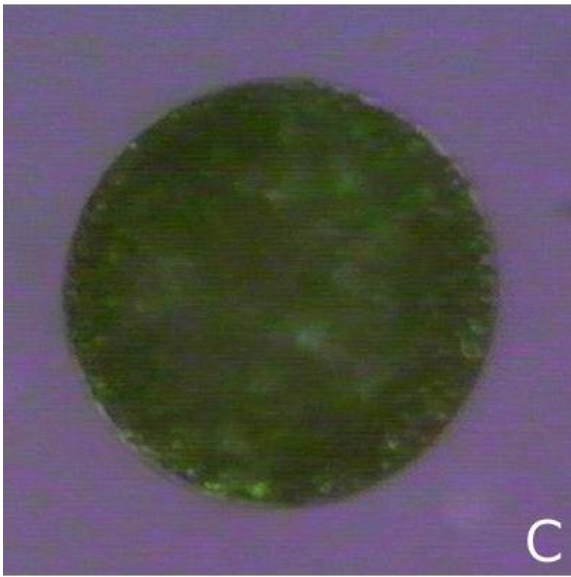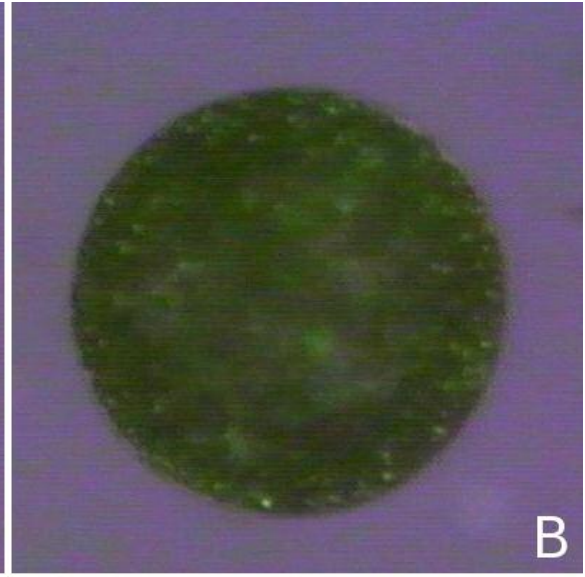
Figure A2.1. *Boergesenia forbesii* protoplasts regenerating a cellulosic wall.

An adult thallus of *Boergesenia* was wounded and allowed to form protoplasts. The protoplasts were released from the mother wall and collected. The protoplasts were allowed to regenerate for 3 hours. The images shown here are of a single protoplast, from 3 hours to 8 hours post-wounding (60 minutes between images). The newly deposited cellulose appears by polarization microscopy as a bright "corona" around the protoplasts.

A) 3 hours post-wounding

B) 4 hours post-wounding

C) 5 hours post-wounding

D) 6 hours post-wounding

E) 7 hours post-wounding

F) 8 hours post-wounding
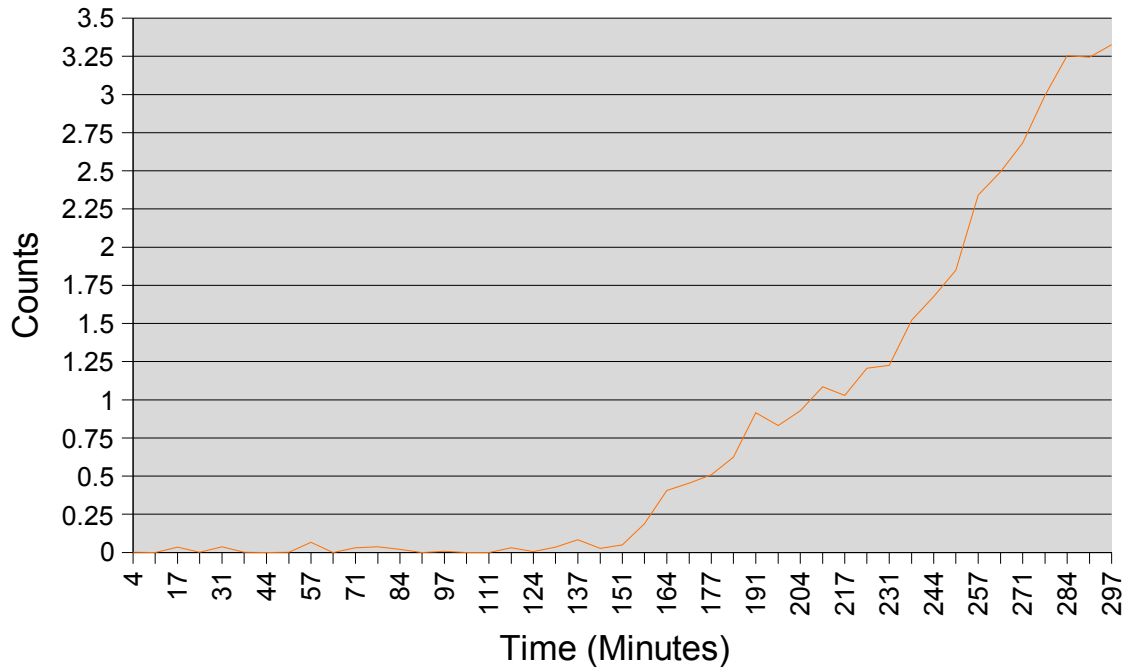
Figure A2.2. The quantity of cellulose increases over five hours as protoplasts synthesize cellulose. The number of white pixels for each image in the time-course have been summed and graphed here. The increase in the number of white pixels corresponds to the deposition of highly birefringent cellulose microfibrils into the cell wall of the aplanospore.
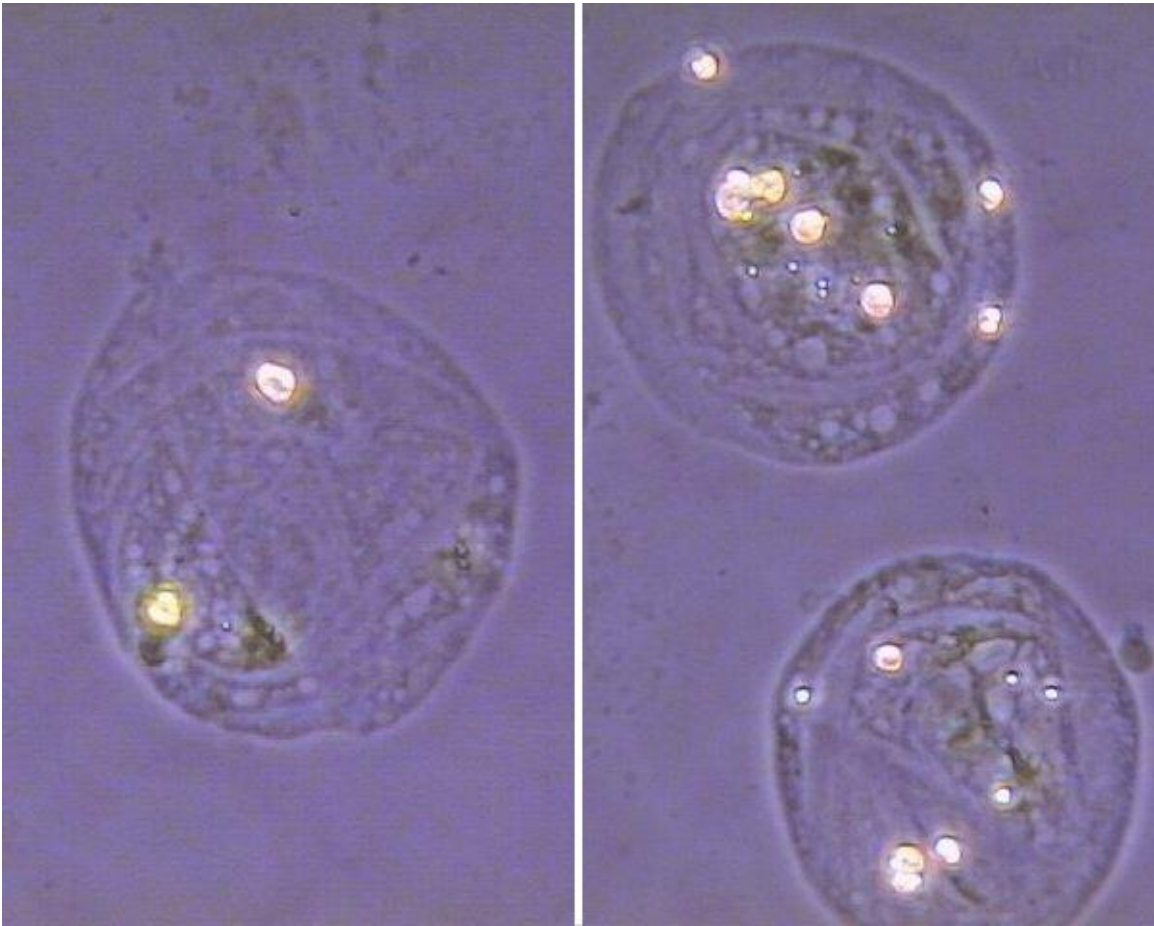
Figure A2.3. Non-birefringent wall material from nascent Boergesenia aplanospores.

Boergesenia aplanospores were allowed to form for 90 minutes within the mother cell wall. They were then removed into artificial seawater, collected, placed onto a slide, and coverslipped. Some aplanospores were crushed between slide and coverslip, releasing the cell contents and allowing the visualization of the coating material left behind.
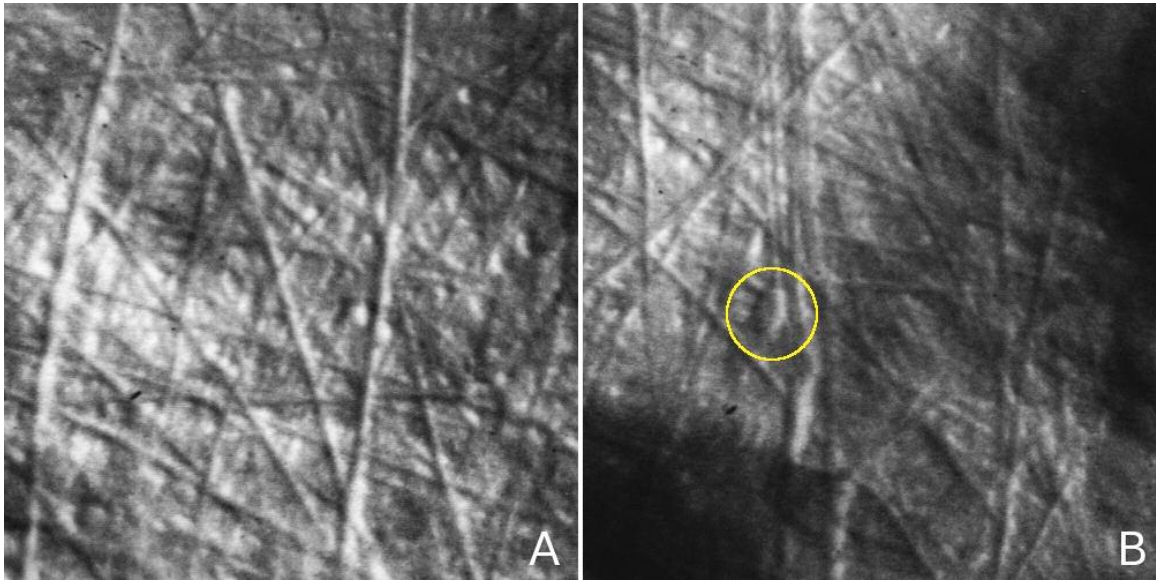
Figure A2.4. The inner surface of the plasma membrane of Boergesenia.

(A) Many cellulose microfibrils of the cell wall can be seen.

(B) A possible linear terminal complex can be seen associated with the end of a cellulose microfibril (yellow circle).
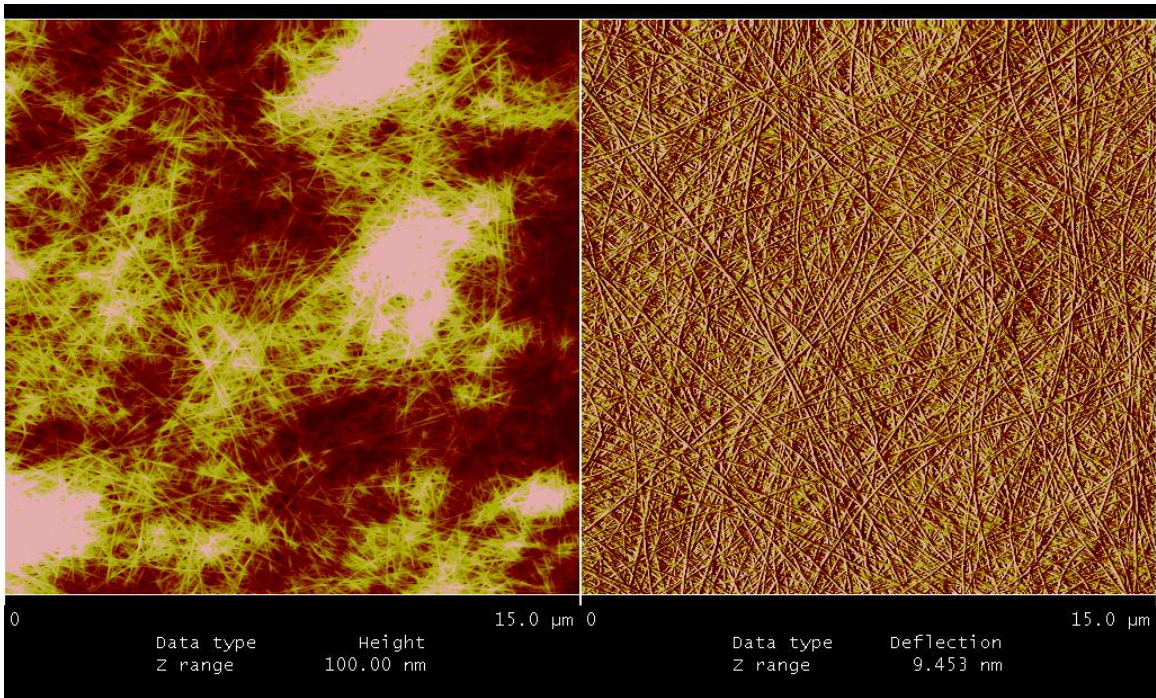
Figure A2.5. The inner surface of the cell wall of an isolated Boergesenia cell wall. Imaged by contact-mode AFM.
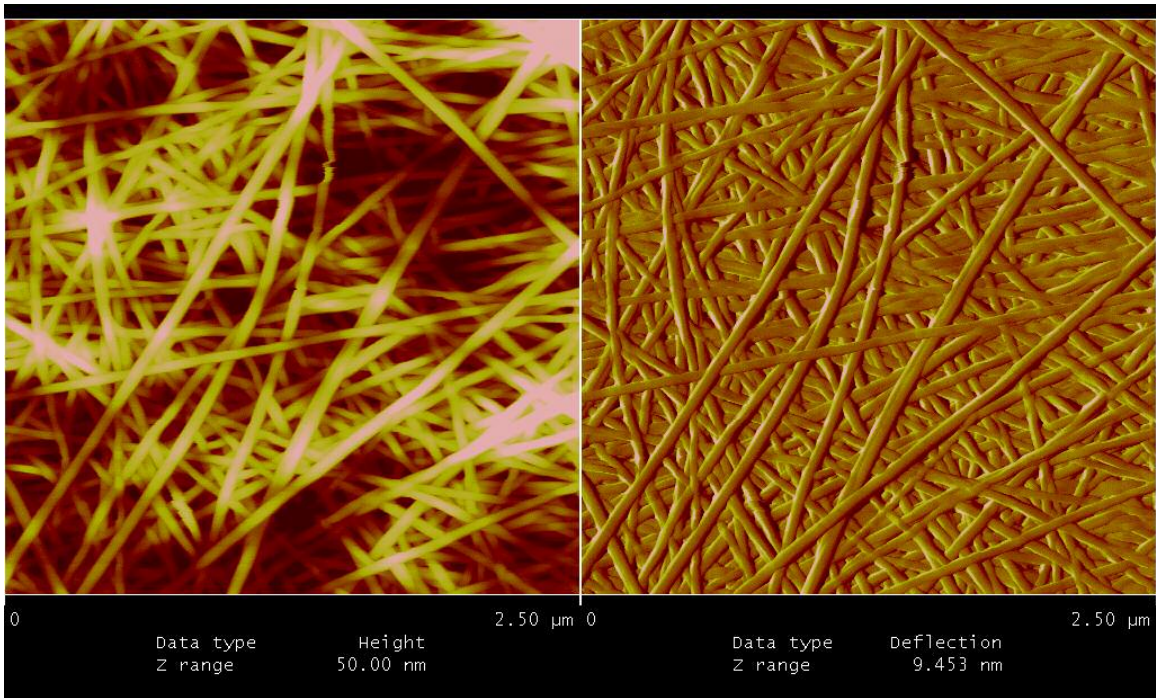
Figure A2.6. A higher magnification view of the interior region of the *Boergesenia* cell wall seen in Figure A2.5.
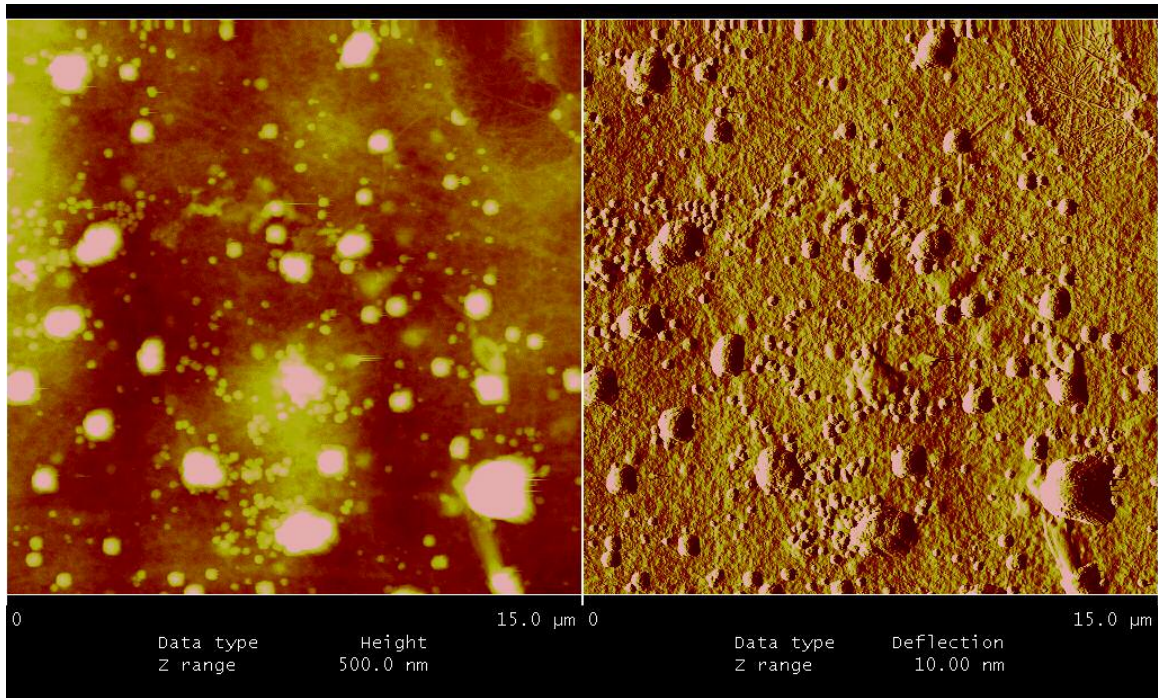
Figure A2.7. A low-magnification image of the inner surface of the plasma membrane of a *Valonia* cell. Many particles of approximately 100 nm in diameter can be seen, however, no particles which correspond to linear terminal complexes can be detected.
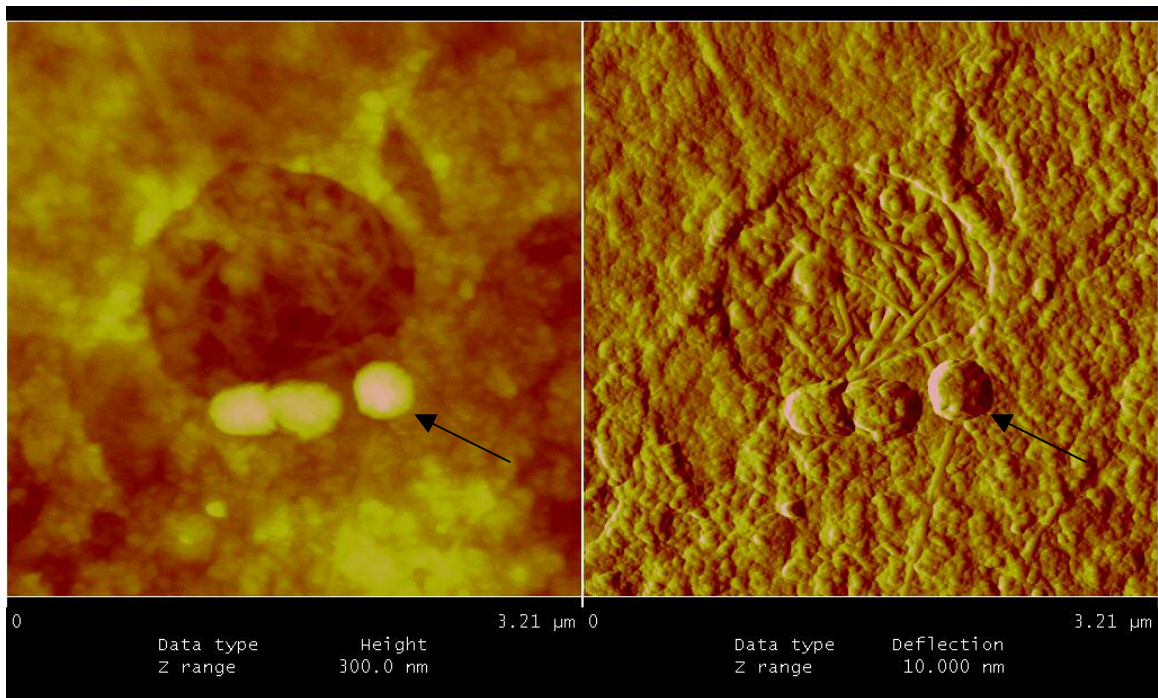
Figure A2.8. An AFM image of the inner surface of the plasma membrane of a *Valonia* cell.

A single cell of *Valonia* was frozen in liquid nitrogen, cut into pieces, and thawed in 1% glutaraldehyde. The pieces were spread on glass coverslips, rinsed with PBS and glass-distilled water, and air-dried. Specimens were imaged in contact mode. In this deflection image, the inner surface of the plasma membrane can be seen. There is a small hole in the membrane near the center of the image. The cellulose microfibrils comprising the cell wall can be seen in this "window". A cellulose microfibril appears to end in a large particle on the edge of this hole (arrows). This particle may be a terminal complex. In the height image, this putative terminal complex appears relatively tall, being one of the highest structures in the image.

Appendix 3 – The evaluation of plasma membrane sheets isolated from cotton fiber cytoplasts for use as an experimental system for imaging rosette terminal complexes

Cytoplasts of cotton fibers were produced and isolated from submerged fibers of *in vitro*-cultured cotton ovules. Plasma membrane sheets were isolated from these cytoplasts. Parallel bundles of cortical microtubules were found to be associated with these isolated plasma membrane sheets by scanning electron microscopy. Despite the presence of microtubules, no fibrillar cellulose could be found associated with these cytoplasts. Due to the difficulty involved in isolating plasma membrane sheets from cotton fibers and the inability of these cytoplast membranes to synthesize cellulose, the cytoplasmic domain of the rosette terminal complex could not be imaged using this system.

Introduction

Cotton Fibers

Cotton (*Gossypium hirsutum*) fibers actively synthesizing secondary cells walls represent one of the most active cellulose-synthesizing systems known. On the day of anthesis, cotton fiber cells begin to elongate and continue to do so for the next 16-20 days. During this time, *in vitro*-grown cotton fiber cells synthesize a thin primary wall and reach a length of ca. 2 cm (Gould *et al*., 1986). Synthesis of the secondary wall begins at approximately 14 days post-anthesis (d.p.a.) and continues for 30-40 days. During this period, a 0.2-0.4 micrometer-thick primary wall containing <30% cellulose turns into a layer of almost pure (~94%) cellulose 8-10 micrometers thick (Seagull, 1990). Cotton fibers at 14 d.p.a. still only have a primary wall, are very delicate, and are easily damaged by mechanical pulling or handling (Andersland, 1998). For this reason, the use of an *in vitro* ovule culture is the most efficient way of collecting young cotton fibers as they begin to synthesize secondary walls.

In vitro submerged fiber culture

An *in vitro* technique for the culture of isolated cotton ovules was first published in 1974 (Beasley and Ting). By this technique, fertilized cotton ovules were taken from their bolls just after the day of anthesis and floated on the surface of culture medium containing specific plant hormones. This technique resulted in fibers growing only on the upper surface of the ovules. No fibers grew down into the culture medium. These air-grown fibers are difficult to wet, making the removal of the cell wall more difficult and

lowering the final yield of cytoplasts thus obtained. Air-grown cotton fibers require the use of vacuum to allow digestive enzymes to wet the hydrophobic cotton fiber walls (Andersland *et al*., 1998). More recently, an improvement on the Beasley and Ting technique which results in the production of submerged fibers from *in vitro*-cultured cotton ovules has been reported (Feng and Brown, 2000). The submerged fibers grown by this technique are never-dried and are therefore more amenable to being digested by wall-degrading enzymes.

Cotton fiber cytoplasts

Cotton fibers can achieve a length/width ratio of up to 4000:1 (Seagull, 1990). For this reason, when cotton fibers have their cell walls removed, they become very fragile and break into many small vesicles. Furthermore, because each cotton fiber cell has only one nucleus and that nucleus resides in the base of the fiber where it connects to the boll, each fiber generates only one true protoplast, but many anucleate protoplasts (cytoplasts). One fiber cell can generate approximately 100 cytoplasts (Gould *et al*., 1986). A procedure for the production of cytoplasts from *in vitro*-grown cotton fibers has previously been published by Gould *et al.* (1986) and was used here with a few modifications: because our fibers were submerged-grown, there was no need to use vacuum infiltration to get the wall-digesting enzymes onto the fibers; also, a slightly different cocktail of digestive enzymes was used to degrade the fiber cell walls.

Plasma membrane sheets

The cytoplasmic face of the plasma membrane was exposed for imaging by binding cytoplasts to polylysine-coated coverslips, osmotically bursting them, and washing away the cytoplasm, leaving a patch of plasma membrane still glued to the substrate. This technique was first used to produce membrane sheets from *Dictyostelium* for the visualization of cortical actin arrays (Mazia *et al*., 1974; Mazia, 1975; Clarke *et al*., 1975) and cortical granules of sea urchin eggs (Vacquier, 1975). A detailed review of the production and study of plasma membrane sheets and cell cortices was published by John Heuser (2000). The synthesis of beta-glucan microfibrils on isolated patches of plasma membrane isolated from tobacco suspension culture cells has been reported (Hirai *et al*., 1998). In order to determine whether cortical microtubules guided the formation of nascent cellulose microfibrils, these researchers incubated plasma membrane sheets having Taxol-stabilized microtubules with the cellulose precursor UDP-glucose. They were able to visualize the synthesis of microfibrils starting at only 2 minutes after the addition of UDPG.

Our goal is to develop a new technique which will allow the visualization of the cytoplasmic domain of the terminal complex. In order to optimize our chances of visualizing terminal complexes, an experimental system with a very high rate of cellulose synthesis, the cotton fiber secondary wall, was chosen. Because the cotton fiber wall is very difficult to degrade, submerged fibers from *in vitro* culture were utilized. Plasma membrane sheets were isolated from cytoplasts generated from submerged fibers, however, no cellulose was found associated with these membranes.

Materials and Methods

In vitro ovule culture

Cotton ovules were grown *in vitro* according to Feng and Brown (2000). Cotton flowers were collected on the day of anthesis. Sepals and petals were removed with a razor blade, and the flowers were submersed in 70% EtOH for 5 minutes. Each flower was washed with sterile H_2O, and the ovary was peeled with flame sterilized forceps. Ovules were carefully removed and floated on MS medium in a deep Petri dish. Ovules were incubated for 15-18 days in a dark room at 28 degrees C.

Preparation of cotton cytoplasts

Cotton cytoplasts were isolated using a modified version of the Gould *et al*. (1986) technique. A 15 day old ovule was selected from *in vitro* culture. Excess MS medium was blotted onto a sterile Kimwipe. The ovule was floated onto 0.5 mL of digestion medium containing 2% Celluclast, 0.1% pectolyase, 0.45 M mannitol, and 5 mM MES, pH 5.5 in an Eppendorf tube. The tube was placed onto a rocker at 28 degrees C. After 3 hours, the ovule was removed, and the digestion was continued for an additional 2 hours. After the digestion, the cytoplasts in digestion medium were transferred to a 15 mL screw top centrifuge tube and 120 microliters of 40% Ficoll in overlay buffer ("overlay buffer" = 500 mM sorbitol, 5 mM PIPES, 10 mM EGTA, 5 mM $MgCl_2$, pH 6.8) was added and gently mixed by inverting the tube. One mL of 5% Ficoll in overlay buffer was gently layered on top of the digestion medium containing cytoplasts. One mL of overlay buffer was carefully layered on top of the 5% Ficoll and the tube was centrifuged at 1000g for 8

minutes in a clinical centrifuge. Cytoplasts floated into the upper layer and were

collected with a glass Pasteur pipette.

Preparation of membrane sheets from anucleate cotton cytoplasts

Membrane sheets were prepared from cotton cytoplasts using a protocol very similar to

that used by Hirai *et al*., (1997). Isolated cotton cytoplasts were placed onto poly-L-

lysine coated coverglasses and allowed to settle onto the PLL layer for 5 minutes.

Cytoplasts were burst by addition of 20 microliters of 50 mM PIPES, pH 7.0, 2 mM

$MgCl_2$, and 5 mM EGTA. Coverslips with sheets attached were washed with 5 drops of

10 mM HEPES, pH 7.0. Specimens were then stained with Tinopal for fluorescence

microscopy.

Preparation of cotton membrane sheets for TEM

Plasma membrane sheets were prepared from cotton cytoplasts for TEM. Ten microliters

of isolated cotton cytoplasts were placed onto a poly-L-lysine-treated, carbon/Formvar-

coated 300 mesh copper grid for 5 minutes. The grids were inverted onto a 50 microliter

droplet of 50 mM PIPES, pH 7.0, 2 mM $MgCl_2$, 5 mM EGTA on Parafilm for 5 min.

The grid was washed with three drops of 10 mM HEPES, pH 7.0, then inverted onto a

droplet of 1% glutaraldehyde in 10 mM HEPES, pH 7.0 for 2 minutes. The grid was then

rinsed briefly on glass distilled H_2O, stained with phosphotunstic acid or silicotunstic

acid and air-dried. Other grids were prepared where the specimens were dehydrated with

95% EtOH (5 minutes) and HMDS (5 minutes), and then air-dried. These grids were

stored overnight in a desiccator, then rotary shadowed at 45 degrees with Pt/C in an

Edwards 360 high-vacuum evaporator.

Preparation of cotton membrane sheets for SEM

Isolated cotton cytoplasts in overlay buffer were placed on poly-L-lysine coated

coverglasses and allowed to settle onto the PLL for 5 minutes. Cytoplasts were burst by

addition of 20 microliters of 50 mM PIPES, pH 7.0, 2 mM $MgCl_2$, 5 mM EGTA, and

washed with 5 drops of 10 mM HEPES, pH 7.0. Coverslips with attached membrane

sheets were dehydrated in 95% EtOH (5 min), absolute EtOH (5 min), and HMDS (5

min), and then air-dried.

Results

Cytoplasts from *in vitro*-grown cotton fibers were prepared and used to make membrane sheets (Figure A3.1). These cytoplasts, shown here by phase contrast, appear very similar to those reported by Gould *et al*. (1986). In Figure A3.2 plasma membrane sheets made from cotton cytoplasts can be seen. These plasma membrane sheets look indistinguishable from membrane sheets made from other species (*Arabidopsis* and *Nicotiana* suspension cultures).

Membrane sheets from cotton were imaged using SEM (Figure A3.3). Membrane sheets displayed varying amounts of cytoplasmic remnants associated with the sheets. On some sheets, the debris seemed to be lacy or reticulate. Some membrane sheets had prominent microtubules associated with them. In some regions, the microtubules displayed a large degree of co-alignment (Figure A3.4).

Membrane sheets from cotton were observed on the TEM. Cytoplasmic remnants stained very dark with uranyl acetate (UA) (Figure A3.5). In Figure A3.6, rotary shadowing has revealed an extensive network of microtubules associated with a plasma membrane sheet. Vesicles can be seen attached to the microtubules at various places. Regions of considerable co-alignment can be seen as well as regions where the microtubules appear more net-like. No cellulose microfibrils were observed on any cotton cytoplast or membrane sheet.

Discussion

Plasma membrane sheets have been produced from cytoplasts isolated from submerged-culture cotton fibers. These membrane sheets were imaged by light microscopy, scanning electron microscopy, and transmission electron microscopy. Membrane sheets prepared from cotton were comparable with the results of membrane sheets obtained from tobacco and *Arabidopsis*.

Cotton cytoplasts isolated from submerged-culture cotton fibers (Figure A3.1) looked very similar to the cytoplasts obtained by Gould *et al.* (1986) from air-grown fibers. Because these cytoplasts were isolated from fibers that were just initiating secondary wall synthesis, it was hoped that these sheets would be very active in cellulose biosynthesis and posses a correspondingly high number of terminal complexes in their plasma membranes.

The mesh-like network of debris attached to the membrane sheet in Figure A3.3 is probably an intact piece of the cotton fiber cytoskeleton. Actin and tubulin were found to be the major cytoskeletal component of cotton fibers and the major protein component of detergent extracted cotton cytoplasts (Andersland *et al.*, 1998). Parallel arrays of cortical microtubules, such as those seen in Figure A3.4, have been imaged within intact cotton fiber cytoplasts (Andersland *et al.*, 1998) and on plasma membrane sheets isolated from tobacco (Van Der Valk, 1980; Sonobe and Takahashi, 1994). These structures are also similar to those reported by Westafer and Brown (1976).

Cytoplasmic remnants stain very darkly when stained with UA for TEM. Membrane sheets (Figure A3.5) isolated from cotton cytoplasts look very similar to the

membrane sheets made from *Mougeotia* (Marchant, 1978) and tobacco (Van Der Valk *et al.*, 1980; Van Der Valk and Fowke, 1981). The presence of microtubules is an indicator of the active state of the cytoplast at the time the membrane sheet was made (Van Der Valk and Fowke, 1981); however, no cellulose microfibrils could be found associated with plasma membrane sheets isolated from cotton fiber cytoplasts.

One possible reason that cotton cytoplast membranes were not successful for the imaging of terminal complexes in situ may be due to the fact that only 10% of cytoplasts show fluorescence after 24 hours in culture when stained with Calcofluor (Gould, *et al.*, 1986). After one week in culture, the percentage of cytoplasts showing fluorescence increased to 90%, however, linkage analysis performed on this nascent cell wall material indicated that the large majority of this material was beta-1,3-linked glucans and that only a small amount was composed of beta-1,4-linked glucans (Gould, *et al.*, 1986). Although immunocytochemical labeling of terminal complexes on freeze-fracture replicas has been successful (Kimura *et al.*, 1999), one of the strongest indicators of the presence of terminal complexes is their association with the termini of cellulose microfibrils. If cytoplasts are not making cellulose, this method of identification would not be feasible and this would reduce the confidence level of subsequent terminal complex identifications.

The fact that cellulose microfibrils cannot be found attached to cotton plasma membrane sheets is consistent with previous findings in *Funaria* where the osmolarity of the medium was shown to dramatically and rapidly decrease the number of rosette particles seen in freeze-fracture preparations of the plasma membranes (Rudolph *et al.*,

144

1989). Furthermore, this group also showed that rosette terminal complexes in *Funaria* have a half-life of only 20-30 minutes (Rudolph and Schnepf, 1988). Cotton cytoplasts are subjected to rather intense osmotic shock during their separation from fiber wall debris and they are anucleate, so they have no means of generating new mRNA for cellulose synthase enzymes which may have been deactivated during the isolation procedure. These facts seem to indicate that cotton fiber plasma membranes are not well-suited for the imaging of terminal complexes *in situ*.

Figure A3.1. A cytoplast isolated from submerged fiber culture. This cytoplast looks very similar to the cytoplasts reported by Gould *et al*. (1986). Scale bar = 50 microns
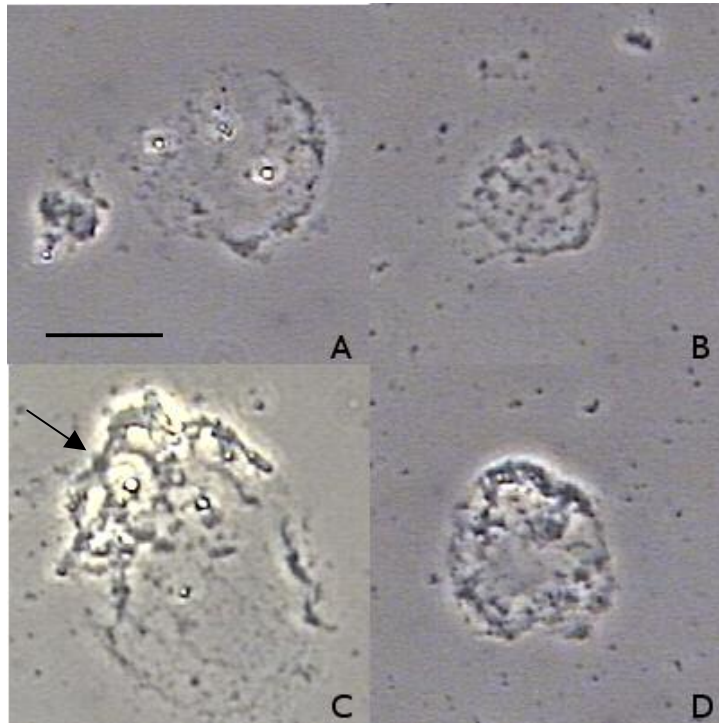
Figure A3.2. Representative plasma membrane sheets isolated from cotton cytoplasts. Some cytoplasmic remnants can be seen clinging to the sheets, especially in C (arrow). Scale bar = 20 μm

| Mag = 3.82 K X | 3μm ⊢——⊣ | EHT = 0.50 kV
WD = 2 mm | Signal A = InLens
Photo No. = 523 | Date :2 May 2002
Time :14:30 |
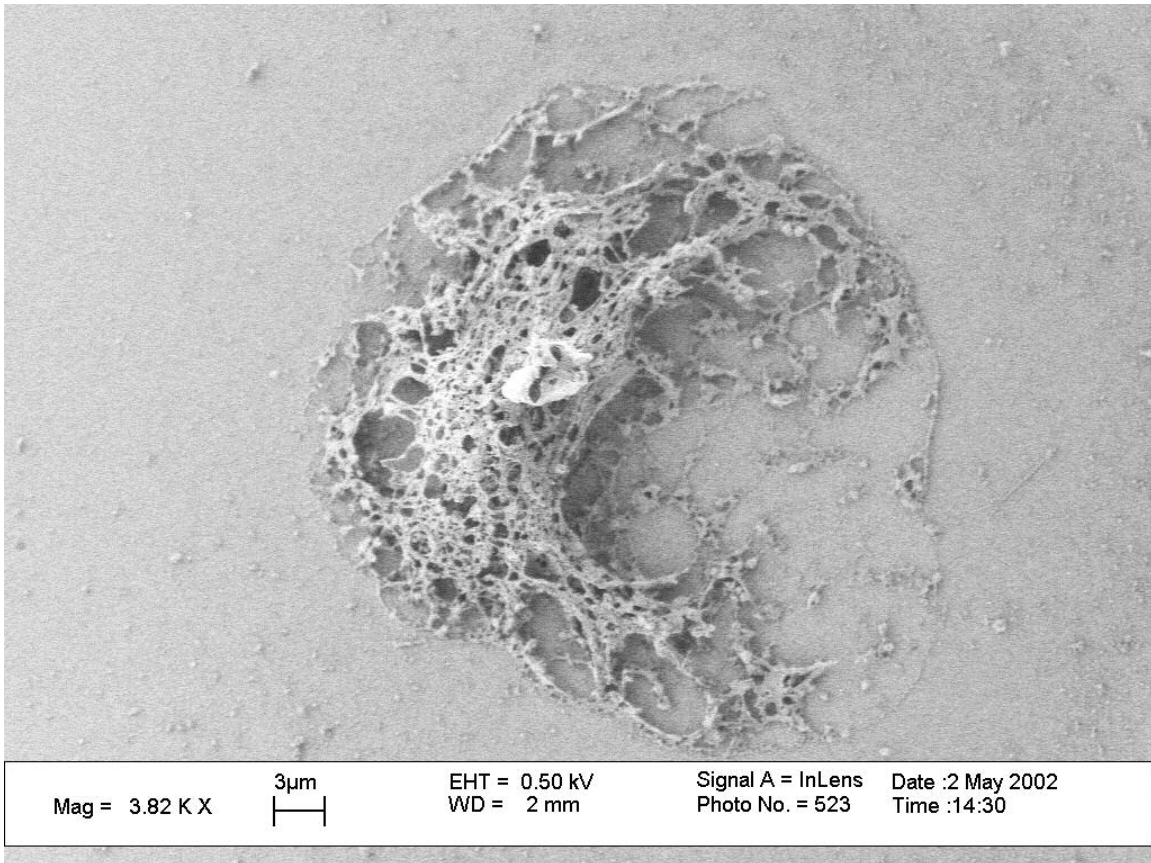
Figure A3.3. Scanning electron micrograph of a plasma membrane sheet from a cotton fiber cytoplast. Note the extensive 3D mesh which remains attached to the membrane sheet. This is possibly composed of cytoplasmic debris suspended in a framework of microtubules.
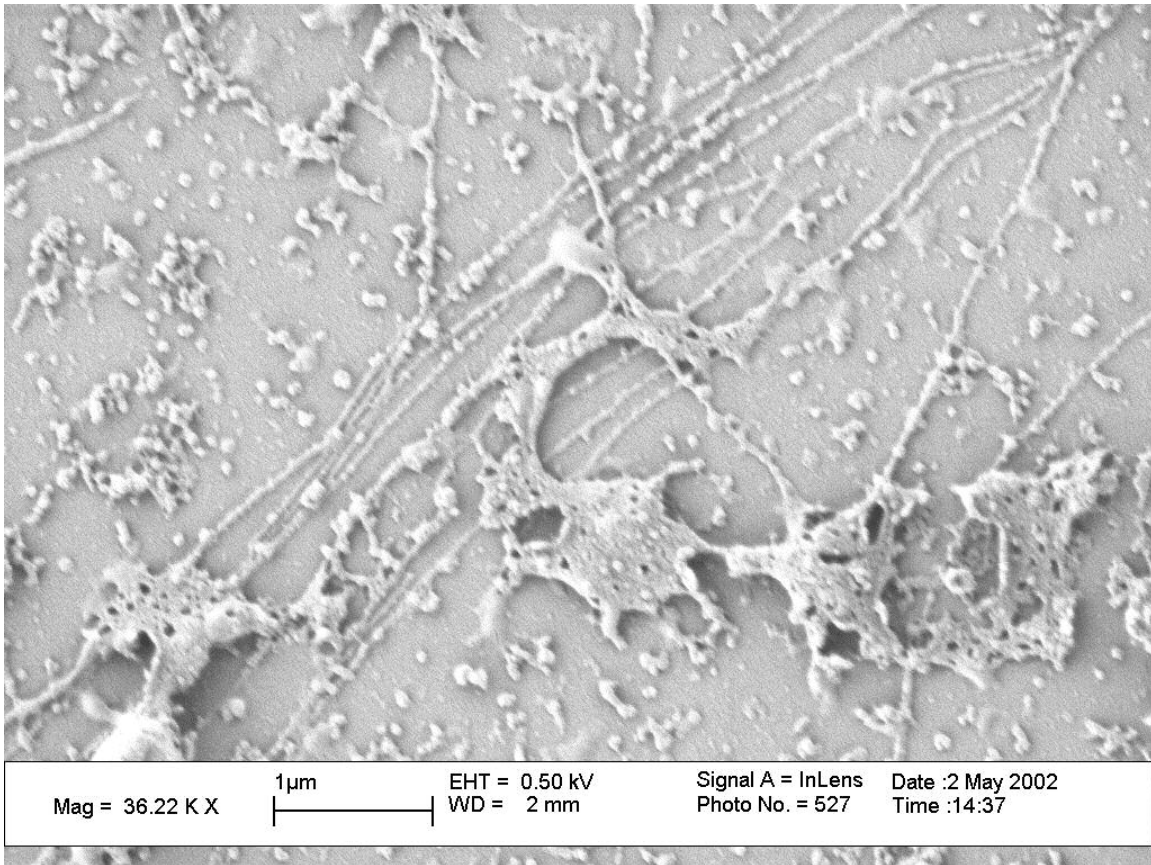
Figure A3.4. Scanning electron micrograph of a parallel array of cortical microtubules still attached to a plasma membrane sheet. This image was taken of the clear area to the lower right of Figure A3.3. Some cytoplasmic remnants can be seen obscuring parts of the underlying membrane.
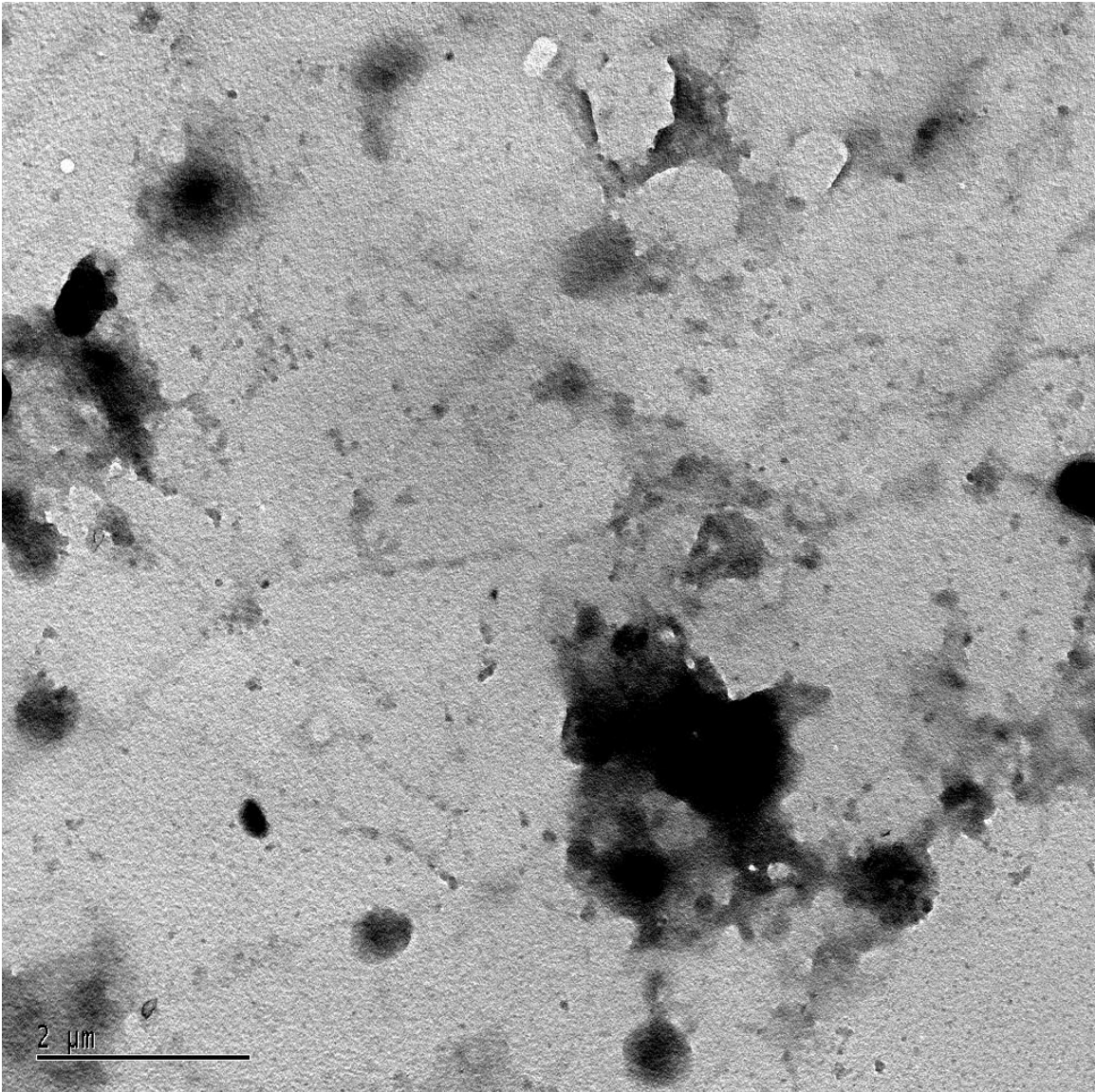
Figure A3.5. Plasma membrane sheets from cotton negatively stained with UA. This sheet has some darkly-stained cytoplasmic remnants. This membrane sheet looks very similar to those reported by Van der Valk (1980) made from tobacco membrane sheets.
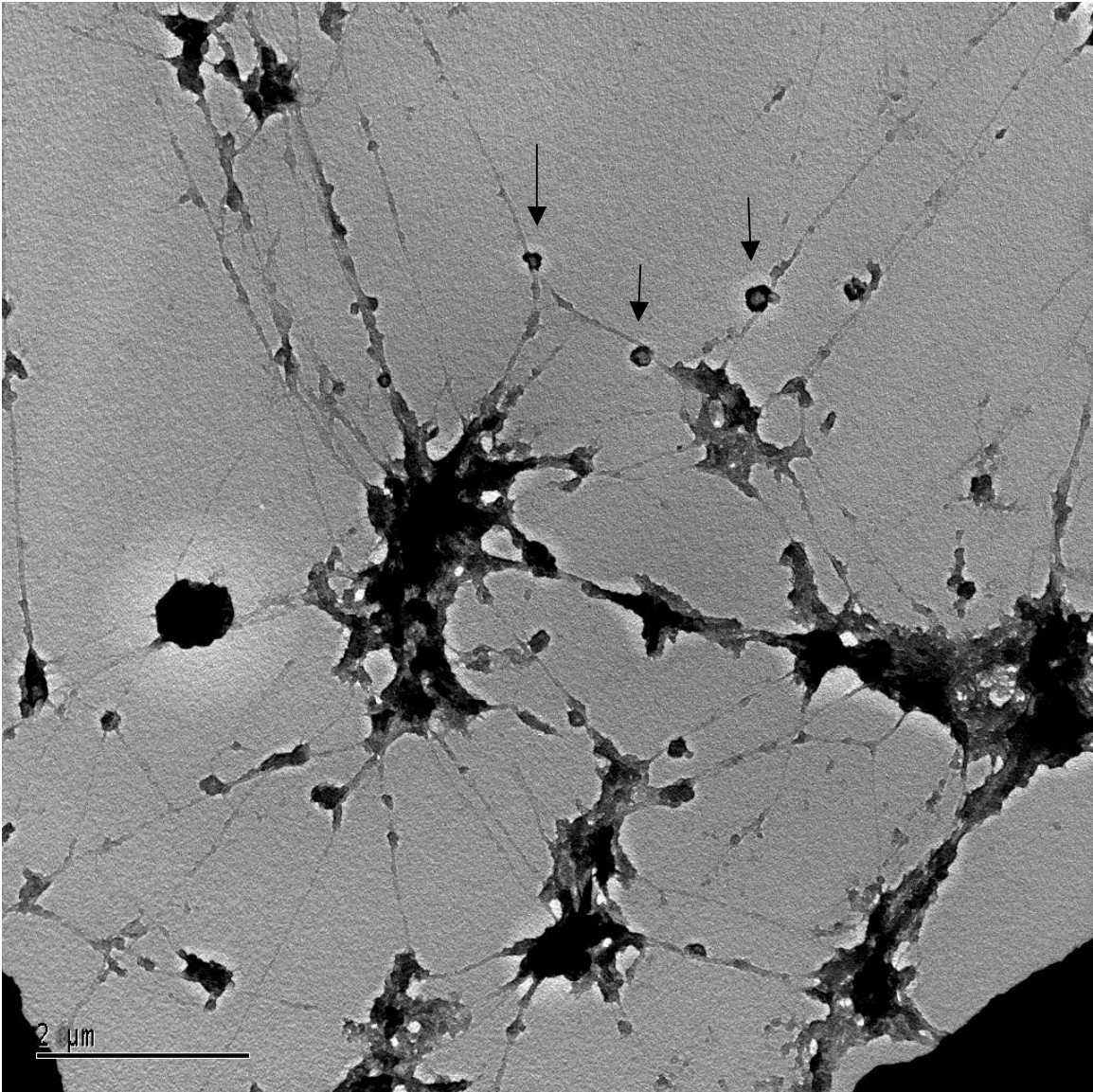
Figure A3.6. A cotton cytoplast membrane sheet with many adhering cortical microtubules. Some microtubules appear to have vesicles attached to them (arrows).

Appendix 4 - The evaluation of plasma membrane sheets isolated from *Arabidopsis* suspension culture cells as platforms for the *in situ* imaging of rosette cellulose-synthesizing terminal complexes

Protoplasts produced from *Arabidopsis* suspension culture cells produce cellulose microfibrils rapidly upon removal from digestive medium. Plasma membrane sheets isolated from *Arabidopsis* protoplasts are incapable of producing cellulose microfibrils *in vitro*. Although plasma membrane sheets isolated from *Arabidopsis* have been imaged by transmission electron microscopy, cellulose microfibrils could not be detected under intact plasma membrane sheets. Cellulose microfibrils could be imaged, however, after the lipids of the plasma membrane were removed, indicating that cellulose microfibrils are present but undetected under intact plasma membrane sheets. A method for partially extracting the plasma membrane during the isolation of plasma membrane sheets on poly-L-lysine coated substrates has been developed using Tobacco BY-2 cells (see Chapter 5) and used to image the cytoplasmic domain of rosette terminal complexes (see Chapter 6). Because cellulose microfibrils are present under plasma membrane sheets isolated from *Arabidopsis*, the procedures described in Chapters 5 and 6 should be applicable to *Arabidopsis* cells in the future.

Introduction

Cellulose Biosynthesis and Terminal Complex Ultrastructure

Cellulose is the main structural component of plant cell walls. It is synthesized by large multi-protein transmembrane protein complexes. In vascular plants, these protein complexes have been visualized by freeze-fracture electron microscopy as hexagonal rosettes (Mueller and Brown, 1980; Brown, 1996; Delmer, 1999). Attempts to isolate the proteins responsible for cellulose synthesis have met with very little success due to the lack of the ability to assay for cellulose synthase enzyme activity (Doblin *et al*., 2002; Somerville *et al*., 2004). There are several theories as to why cellulose cannot be synthesized in large quantities or purities *in vitro* such as the short lifetime of rosette TCs (Rudolph and Schnepf, 1988) or the depletion of various accessory proteins and/or essential boundary-layer lipids from the functional complexes in detergent-solubilized membrane fractions (Kudlicka and Brown, 1997). More recently, genetic approaches have been used to gain a great deal of information about the genes involved in cellulose biosynthesis.

Recent Advances in Cellulose Synthesis: The Genetic Approach

Although much work has been done to identify the genes involved in cellulose synthesis, the structure and composition of the rosette TC has yet to be fully elucidated. Many of the genes involved in cellulose biosynthesis have been identified by screening cellulose-deficient mutants of *Arabidopsis* (Doblin *et al*., 2002). Furthermore, two recent analyses of publicly available microarray data have revealed the co-expression of a number of

153

genes with several different CesA genes in *Arabidopsis* (Persson *et al.*, 2005; Brown *et al.*, 2005).

One question regarding the structure of the terminal complex is the number of cellulose synthase enzymes present in a given terminal complex and how many glucan chains a single terminal complex synthesizes. The number of glucan chains produced by a single terminal complex has long been thought to be between 30 and 36 (Herth, 1983; Reiss *et al.*, 1984; Delmer, 1999; Kimura *et al.*, 1999; Perrin 2001; Doblin *et al.*, 2002). This number of glucan chains, together with the hexameric structure of the rosette TC in freeze-fracture replicas, has given rise to the hypothesis that each subunit in the rosette must be composed of six catalytic sites (Brown and Saxena, 2000). If an intact terminal complex could be successfully imaged, the volume of the intact complex could be calculated and compared with the computed volumes of the three CesA proteins known to be required for the formation of cellulose in primary walls. Most of the current information about the genes of cellulose synthase enzymes active during primary and secondary wall synthesis has come from studying mutants of *Arabidopsis*.

Another question facing cellulose researchers today is what proteins are associated with the cellulose synthase enzymes in the rosette TC. This question can be addressed in part by the freeze-fracture replica-labeling technique (FFRL) (Fujimoto, 1995). This technique has been used to prove that cellulose synthase is definitely a member of the rosette TC (Kimura *et al.*, 1999). One drawback of this technique is that the replicas must be cleaned by incubation in SDS in order to remove the bulk of the specimen (so the electron beam can pass through it) and to expose the fractured surface to

antibodies. This cleaning of the replicas in SDS not only denatures the proteins which are bound to the replica but also may remove any proteins which were not directly incorporated in the replica during evaporation of the metal film. This includes any proteins which are associated with the (transmembrane) cellulose synthase enzymes but are not themselves transmembrane proteins and so are not cleaved during the freeze-fracture process. Thus, in order to determine whether a given protein is a member of the rosette terminal complex, an intact terminal complex would be required for the labeling reaction. Many of the proteins suspected as being associated with the terminal complex have been identified in *Arabidopsis*.

Isolation of Plasma Membrane Sheets

In order to answer these questions, a new technique which would allow the visualization of the cytoplasmic domain of intact terminal complexes was developed. The isolation of plasma membrane sheets on poly-L-lysine coated surfaces is an established technique for visualization of the cortex of both plant and animal cells. The isolation of patches of plasma membrane by binding cells to surfaces coated with the poly-cationic molecule poly-L-lysine was first reported 25 years ago (Mazia *et al*., 1975; Clarke, 1975; Vacquier, 1975). Although first used for the analysis of the cell cortex of sea urchin eggs and *Dictyostelium*, this technique was quickly adapted for use on plant protoplasts (Marchant and Hines, 1979). Microtubules and clathrin-coated vesicles/pits were imaged on plasma membrane sheets isolated from tobacco (Van der Valk and Fowke, 1981; Van der Valk *et al*., 1980). More recently, the formation of beta-glucans *in vitro* on plasma membrane

sheets isolated from tobacco BY-2 suspension culture cells has been demonstrated (Hirai *et al.*, 1998). A recent review of the plasma membrane sheet isolation technique has been published (Heuser, 2000).

The goal of this study was to use adapt the technique of Hirai *et al.* (1998) to synthesize in vitro cellulose on isolated *Arabidopsis* plasma membrane sheets and to use these sheets to image the cytoplasmic domain of intact and functional terminal complexes. Because most of the current work on the genetics of cellulose biosynthesis is being done in *Arabidopsis*, our first choice of plant material to use for the development of this new imaging technique was *Arabidopsis* suspension culture cells. In order to insure that any terminal complexes visualized were active terminal complexes, plasma membrane sheets isolated from *Arabidopsis* suspension culture cells which were capable of synthesizing cellulose *in vitro* were required. For this reason, plasma membrane sheets isolated from *Arabidopsis* were incubated with various combinations of UDPG plus compounds which have been found to facilitate cellulose synthesis *in vitro* (Hirai *et al.*, 1998; Kudlicka and Brown, 1997; Lai-Kee-Him *et al.*, 2002). Plasma membrane sheets with cellulose microfibrils were found and imaged on the transmission electron microscope. The presence of microtubules associated with the plasma membrane sheets was demonstrated as well as the presence of cellulose microfibrils under the plasma membrane sheets. Although terminal complexes were not found on plasma membrane sheets isolated from *Arabidopsis* suspension culture cells, this system was shown to be a viable option for future studies of terminal complex composition using the technique described in Chapter 5.

Materials and Methods

Culture conditions and protoplast isolation.

 Arabidopsis suspension cultures were grown in Murashige and Skoog (MS) medium on a gyratory shaker at 60 rpm in the dark at 28 degrees C. Protoplasts of *Arabidopsis* cells were made by digesting suspension-cultured cells in a medium containing 0.5% Celluclast, 0.1% pectolyase, 0.45 M mannitol, and 10 mM MES, pH 5.5. Protoplasts were gently pelleted and the digestion medium was poured off. The protoplasts were resuspended in 1 mL of a heavy solution (solution C) containing 500 mM sucrose, 1 mM $CaCl_2$, and 5 mM MES-KOH, pH 6.0. This solution was transferred to a glass centrifuge tube and 1 mL of a lighter solution, solution D, containing 400 mM sucrose, 100 mM D-sorbitol, 1 mM $CaCl_2$, and 5 mM MES-KOH, pH 6.0 was carefully layered on top of the protoplasts. A light solution, solution B, consisting of 500 mM D-sorbitol, 1 mM $CaCl_2$, and 5 mM MES-KOH, pH 6.0, was layered on top of the solution D and the tube was centrifuged for 5 minutes at 1000g in a clinical centrifuge. The interface between the top two layers was collected and diluted in additional solution B, and centrifuged again in a microfuge at ~500g.

Production of plasma membrane sheets.

Plasma membrane sheets were made by several methods for the purpose of comparison. The first method used was very gentle. Protoplasts were allowed to settle onto poly-L-lysine coated coverglasses for 1-2 minutes. An equal volume of a hypo-osmotic bursting medium consisting of 50 mM PIPES (pH 7.0), 2 mM $MgCl_2$, and 5 mM EGTA was

added to the protoplasts and they were allowed to swell and burst for 5 minutes. The coverslip was washed by holding it at a ~45 degree angle and dripping 10-15 drops of 10 mM HEPES (pH 7.0) over the area where the specimen was bound.

A second method used to generate plasma membrane sheets was dripping the bursting solution "uphill" of or directly onto the protoplasts while holding the coverglass at an angle. The drops of bursting solution would land uphill of the protoplasts and run downhill over them. The protoplasts would swell and burst in the hypo-osmotic medium. Cytoplasm and cellular organelles and debris would be swept away as the washing continued. This technique yielded some very good sheets and some that were not very good. The reason that the results were so variable is that there are several factors relating to the height that the drop falls before it hits the coverglass, how many drops fall directly onto the specimen, how rapidly the solution runs across the coverglass (how tilted the coverglass is), etc. Also, within the same coverglass, some sheets may have more drops fall closer to them and be cleaner than their neighbors, while some drops may have too many drops fall right onto them and be torn or removed from the coverglass completely.

And finally, plasma membrane sheets were also made by the method of Sonobe (1990). The coverslips with bound protoplasts were plunged 50-100 times into a 50 mL centrifuge tube containing bursting solution. This technique appeared to yield the most repeatable results. Not only does this technique generate repeatable results, but even between regions of the same coverglass, all the sheets are treated in an identical manner.

Preparation of membrane sheets for Light Microscopy.

Cellulose was stained with a saturated Tinopal stock solution, diluted 1:10 in HEPES or

PBS washing medium at the time of use. Plasma membranes were stained with Vybrant

DiI (Molecular Probes) diluted 1:1000 just before use. Phase contrast and fluorescence

images of protoplasts and membrane sheets were captured on a Zeiss Universal

microscope equipped with an Optronics camera. Deconvolution images were made using

a Zeiss Axiovert Deconvolution microscope and Zeiss KS-400 software.

Treatment of plasma membrane sheets with UDPG-containing solutions for the

synthesis of cellulose in vitro

UDPG-containing solution A (USA) was used by Hirai *et al*. (1998) to synthesize beta-

glucans on tobacco BY-2 membrane sheets. This solution contained 5 mM UDP-glucose,

5 mM $MgCl_2$, 5 mM $CaCl_2$, 5 µM Taxol, and 10 mM HEPES/KOH (pH 7.0). UDPG-

containing solution B (USB) was developed in our lab and was used extensively to

synthesize cellulose (beta-1,4 glucans) specifically (Kudlicka *et al*., 1996). This solution

contained 10 mM UDPG, 200 mM cellobiose, 80 mM $MgCl_2$, 10 mM $CaCl_2$, 1 mM

cGMP, and 100 mM bis-tris-propane-HEPES (pH 7.6). For some studies, 1% CHAPS

was also added to these UDPG-containing solutions.

Preparation of membrane sheets for Electron Microscopy.

Protoplasts were glued to poly-L-lysine coated, carbon-covered grids. Protoplasts were

lysed by floating the grid on a drop of PIPES lysis medium for 1-2 minutes. Excess

PIPES was wicked away and the grid was washed by touching and wicking away 3 drops of HEPES and one drop of glass distilled water. Then the grid was touched to a drop of UA, excess wicked away, and air-dried. Other grids were air-dried and shadowed (unidirectionally or rotary) with platinum/carbon in an Edwards high vacuum evaporator equipped with a rotatilt stage.

Membrane sheets were also produced on glass coverslips, just as described for light microscopy, however, these sheets were dehydrated in graded ethanol (70, 95, absolute – 5 minutes each), HMDS (5 minutes), and then air-dried. The area of the coverglass containing the membrane sheets was cut out with a diamond scribe. This area was cut in half and one half was rotary replicated with platinum/carbon and one half was stuck to a steel puck for imaging by AFM. Membrane sheets were rotary-shadowed with platinum-carbon at 60 degrees and rotary-backed with pure carbon at 10 degrees. The platinum/carbon replica was removed from the glass by floating the replica onto full-strength hydrofluoric acid (HF). The replica was collected from the surface of the HF with a glass rod and washed 3x on glass-distilled water. The replica was then cleaned by floating on 50% sulfuric acid, 5% sodium dichromate (sulfochromic acid) for 30 minutes. The replica was then rinsed 3x on glass-distilled water and collected onto a thin-bar grid and examined in a Philips EM420 transmission electron microscope. Images were collected on a Gatan Bioscan camera.

Results

Isolation of plasma membrane sheets from *Arabidopsis* suspension culture cells

Plasma membrane sheets were isolated from protoplasts made from *Arabidopsis*

suspension culture cells. Using phase contrast microscopy, plasma membrane sheets are

easily seen (Figure A4.1A). Many of the features that characterize plasma membrane

sheets from *Arabidopsis* can be seen in Figure A4.1B. The plasma membrane sheet has a

relatively smooth, distinct edge. Many small, dark particles can be seen bound to the

plasma membrane sheet. This membrane sheet has been fixed with glutaraldehyde and

washed extensively. The region with the white halo near the center of the sheet is

probably cytoplasmic debris which became chemically linked to the membrane sheet

upon fixation with glutaraldehyde. Hints of fibrillar structures attached to the membrane

sheet can also be detected. These structures have little contrast and are very small and are

therefore difficult to see clearly here.

An image of a plasma membrane sheet from *Arabidopsis*, stained with Tinopal,

and imaged with a deconvolution microscope is shown in Figure A4.2. The exact identity

of the highly fluorescent spots attached to the membrane sheet is unknown. No cellulose

or fibrillar material of any kind can be seen.

Plasma membrane sheets are permeable to Tinopal

Plasma membrane sheets were stained with Tinopal and with the lipophilic dye, DiI. In

Figure A4.3A, the orange fluorescence corresponds to the DiI-labeled plasma

membranes. In Figure A4.3B, Tinopal-stained cellulose microfibrils can be seen under

the plasma membrane sheets. The size, shape, and location of the orange plasma membrane sheets are directly comparable to the blue fluorescence of the cellulose microfibrils.

In vitro synthesis of cellulose by isolated plasma membrane sheets of _Arabidopsis_

Plasma membrane sheets were isolated and incubated with UDPG (Figures 4.4C and D). Tinopal staining reveals the absence of significant production of fibrils compared to control membrane sheets fixed immediately after isolation (Figures 4.4A and B). Some plasma membranes appear to have a small amount of fibrils associated with them (Figure A4.4D); however, fibrils of a similar size and frequency can be seen on membrane sheets before UDPG treatment (Figure A4.4B).

The presence of Taxol-stabilized microtubules has no effect on the ability of plasma membrane sheets to synthesize cellulose _in vitro_

The inclusion of Taxol in the digestion, washing, and lysis solutions allows the visualization of large numbers of microtubules associated with the membrane sheets (Figure A4.5). Hyper-stabilized microtubules are visualized here by labeling with an anti-tubulin antibody conjugated to the fluorescent dye CY-3. The presence of these microtubules had no effect on the synthesis of cellulose by plasma membrane sheets.

Treatment of plasma membrane sheets with CHAPS has no effect on the synthesis of cellulose *in vitro*

Plasma membrane sheets were produced and incubated with 1% CHAPS + UDPG. Control membrane sheets were incubated in buffer solution only. The inclusion of the CHAPS had no apparent effect on the ability of plasma membrane sheets to synthesize cellulose in vitro (Figure A4.6). Plasma membrane sheets incubated in CHAPS had the same size and overall morphology as the control membrane sheets incubated in buffer solution only, indicating that this concentration of detergent did not solubilize the plasma membranes.

Plasma membrane sheets were also produced from protoplasts which had been allowed to recover for one hour in an iso-osmotic medium containing the cellulose synthesis inhibitor 2,6-dichlorobenzonitrile (DCB) (Delmer, 1999; Montezinos and Delmer, 1980). These protoplasts made an abnormal product and membrane sheets from them did not produce cellulose *in vitro* in the presence of UDPG.

Plasma membrane sheets were produced from protoplasts which had been digested in the presence of protease inhibitors. Protoplasts were lysed in protease inhibitors and incubated with UDPG + protease inhibitors. The inclusion of the protease inhibitors had no apparent effect on the ability of plasma membrane sheets to synthesize cellulose *in vitro*.

163

Immunocytochemical labeling of membrane sheets with anti-CesA

Plasma membrane sheets were prepared by the Sonobe method, fixed, and stained with either anti-CesA followed by an FITC-conjugated secondary antibody, or by secondary antibody only (Figure A4.7). A significant amount of FITC fluorescence was present on plasma membrane sheets incubated with secondary antibody only (Figure A4.7A). Interestingly, the same areas which bound the secondary antibody also took up Tinopal (Figure A4.7B), possibly indicating that the exposed cytoplasmic region of these membrane sheets is highly glycosylated. When the plasma membrane sheets were first treated with the primary antibody before exposure to the FITC-conjugated secondary antibody, the pattern of fluorescence observed was different (Figure A4.7C). A large number of fluorescent spots were observed in and around the plasma membrane sheets. It is unknown whether these are particulate. Of special note is the fact that the non-specific labeling of the membrane sheets with the secondary antibody is mirrored by the Tinopal, however, this is not the case with the punctate structures resulting from anti-CesA labeling (Figure A4.7D).

Synthesis of cellulose by intact protoplasts

Protoplasts which were transferred to an iso-osmotic, sucrose-containing medium synthesized cellulose (Figure A4.8). Protoplasts were made and isolated on a density gradient, as usual. At 0, 30, and 90 minutes, protoplasts were removed from the sucrose-containing, iso-osmotic "recovery" medium, placed onto a poly-L-lysine coated coverslip, burst (to yield plasma membrane sheets), and fixed. At time zero (Figure

164

A4.8A), short microfibrils can be seen under the plasma membrane sheets. After 30

minutes (Figure A4.8B), many microfibrils can be seen and their average length appears

to be greater than in those in Figure A4.8A. After 90 minutes of recovery, the length and

number of microfibrils has increased further.

Arabidopsis suspension cultures grown in NH4- medium were found to contain tracheary element-like cells

Arabidopsis cultures were transferred into NH4- medium. Cultures grew extremely

slowly. After two months, tracheary element-like cells were identified by polarization

microscopy (Figure A4.9A). These cells look exactly like those derived from *Zinnia*

suspension cultures (Fukuda and Komamine, 1980; Nakashima *et al*., 2004). The

birefringent bands were found to be lignified, based on their autofluorescence (Figure

A4.9B).

Electron Microscopic analysis of *Arabidopsis* plasma membrane sheets

Plasma membrane sheets of *Arabidopsis* have been prepared and imaged by shadowing

(Figures 4.10 and 4.11) and negative staining (Figure A4.12). On shadowed plasma

membrane sheets, the presence of microtubules and very large vesicles is apparent, as

well as the non-uniform surface texture of the sheet itself (Figure A4.10). In Figure

A4.11A, a large number of microtubules can be seen associated with the plasma

membrane sheets. The microtubules appear to be oriented in the same general direction,

however, they are not actually parallel. Furthermore, these microtubules are singular, not

bundled together. At higher magnification (Figure A4.11B), the surface of the membrane appears smooth. The microtubules can clearly be seen to be singular, not bundles. No cellulose microfibrils can be seen under the plasma membrane sheet.

Microtubule protofilaments imaged by negative staining

Microtubules can be seen associated with the plasma membrane by negative staining (Figure A4.12). At low magnification, the large number of microtubules associated with the plasma membrane sheet can be seen (Figure A4.12A). The individual protofilaments which comprise the microtubules are visible in Figures 4.12B. No cellulose microfibrils can be seen under the microtubule network by negative staining.

Cellulose microfibrils visible upon removal of plasma membrane lipids

The fact that cellulose microfibrils can clearly be seen under plasma membrane sheets on the fluorescence microscope but no microfibrils can be seen under plasma membrane sheets by either negative staining or platinum/carbon shadowing indicates that the cellulose microfibrils are present under the plasma membrane sheets but that the presence of the membrane is prohibiting the visualization of the cellulose microfibrils. Plasma membrane sheets were made on carbon-covered, PLL-coated TEM grids. The lipids of the plasma membrane sheets were removed with chloroform/methanol and the grids were negatively stained with UA. Copious cellulose microfibrils can be seen under plasma membrane sheet remnants (Figure A4.13). The size of this bundle may be due to aggregation of the cellulose microfibrils during treatment with the chloroform/methanol.

Cellulose microfibrils located under plasma membrane sheets with CBH I-gold

As demonstrated by the chloroform/methanol extraction of plasma membrane sheets (and previously by Tinopal staining), cellulose microfibrils are present under isolated plasma membrane sheets of *Arabidopsis*. Because the cellulose microfibrils cannot be directly imaged by negative staining or shadowing when the plasma membrane is intact, an indirect method for localizing cellulose microfibrils was developed. Protoplasts were allowed to regenerate for a short time following their removal from the cell wall-degrading enzymes. These protoplasts were incubated with CBH I-gold, bound to PLL-coated grids, lysed to yield plasma membrane sheets, and negatively stained. A linear trail of 10 nm gold particles can be seen under the plasma membrane sheet shown in Figure A4.14. Unfortunately, the negative stain does not reveal more of the surface structure of the membrane itself so these trails cannot be traced back to terminal complexes.

Electron microscopic observation of *Arabidopsis* protoplast surfaces

Protoplast of *Arabidopsis* were isolated and bound to glass coverslips with PLL. The protoplasts were fixed and carefully dehydrated. The dehydrated protoplasts were rotary replicated, backed with carbon, and the glass substrate was dissolved in HF. The replicas were cleaned in sulfochromic acid and household bleach to remove the protoplasts and the replicas were examined in the TEM. The replicated protoplasts appeared to be flattened and this flattening had caused the replica to shatter (Figure A4.15A). The

167

central region of the protoplast could still be observed. The surface of the protoplasts was very smooth with adhering particles of various sizes (Figure A4.15B). While some protoplasts did not display cellulose microfibrils, other protoplasts did have microfibrils (Figure A4.15C and D). The microfibrils appeared to have a non-uniform diameter and to have numerous bends and curves.

Discussion

Isolation of plasma membrane sheets from *Arabidopsis* suspension culture cells

Plasma membrane sheets from *Arabidopsis* suspension culture cells have been

successfully isolated (Figure A4.1A). Once the cells and as much adhering cytoplasmic

debris as possible has been removed from the sheet, a fixative is applied. The membrane

sheet in Figure A4.1B has been fixed with glutaraldehyde and washed rigorously. The

fact that this sheet did not become detached from the glass substrate indicates that

proteins in the membrane sheet have become covalently cross-linked to the poly-L-lysine

layer. The fibrillar structures seen associated with the membrane sheet are probably

cortical microtubules, based on later TEM analysis of similarly-prepared membrane

sheets from *Arabidopsis*.

Imaging plasma membrane sheets by deconvolution microscopy

Plasma membrane sheets always have some amount of cytoplasmic material associated

with them. Plasma membrane sheets must be washed thoroughly enough to remove the

cytoplasm but not so rigorously as to damage the sheets themselves. Certain cytoplasmic

structures may be covalently bound to, or physically a part of the inner surface of the

plasma membrane, making their removal unlikely. These structures include, but are not

limited to, cortical microtubules, vesicles (clathrin-coated and other types), endoplasmic

reticulum, cortical actin, transmembrane proteins and membrane-associated proteins, and

modified (e.g. glycosylated) membrane lipids. While the composition of these speckles is

uncertain, these sheets were made by a very gentle technique which may have been

169

insufficiently rigorous to remove all cytoplasmic remnants. The fluorescent stain Tinopal has a high affinity for cellulose; however, it has been observed to stain other structures and polysaccharides. Perhaps the brightly-stained particles seen in Figure A4.2 are in fact glycosylated membrane proteins and lipids. This would account for their intense staining by Tinopal. Of note is the fact that no fibrillar structures of any type can be seen. If present, cellulose should be stained by the Tinopal unless the Tinopal is being excluded from the microfibrils by the presence of the membrane sheet.

Correlation between plasma membrane sheets and Tinopal-stained microfibrils established

The plasma membrane of healthy, living plant cells is impermeable to molecules as small as glucose (Lodish *et al*.,1995). The fluorescent dye Tinopal is several times the size of a glucose molecule, therefore we questioned whether or not Tinopal could stain microfibrils located between isolated plasma membrane sheets and the coverglass. In Figure A4.3, plasma membrane sheets have been double-labeled with Tinopal and the lipophilic dye octadecyl indocarbocyanine (DiI). In Figure A4.3A, the orange fluorescence corresponds to the DiI-labeled plasma membranes. In Figure A4.3B, cellulose microfibrils can be seen under the plasma membrane sheets. This Figure clearly demonstrates that cellulose microfibrils can be labeled under a membrane sheet. It is possible that plasma membrane sheets develop holes during the cell-wounding/washing procedure. Alternatively, Tinopal may diffuse in from the edge of the plasma membrane sheet.

Synthesis of cellulose microfibrils *in vitro* by plasma membrane sheets

The terminal complex is a highly labile structure; therefore, isolated plasma membrane sheets which retained the ability to synthesize cellulose after the cell body had been torn away (i.e. in vitro) would be ideal for imaging terminal complexes. The synthesis of beta-glucans by isolated plasma membrane sheets from tobacco BY-2 cells has been reported (Hirai *et al.*, 1998). Thus, the first step of this project was to replicate these experimental findings using our *Arabidopsis* suspension culture system.

Plasma membrane sheets of *Arabidopsis* were incubated with two slightly different solutions, both of which were reported to allow the synthesis of cellulose *in vitro* in different experimental systems. In both solutions, UDPG is the cellulose precursor, however, the concentration of various other components is slightly different. UDPG-containing solution A (USA) was used by Hirai *et al.* (1998) to synthesize beta-glucans on tobacco BY-2 membrane sheets. UDPG-containing solution B (USB) was developed in our lab and was used extensively to synthesize cellulose (beta-1,4 glucans) specifically (Kudlicka *et al.*, 1996). As demonstrated by Figure A4.4, no convincing formation of any product was ever noted on any membrane sheet. There was no apparent difference between incubation in USA or USB. Many plasma membrane sheets display some cellulose microfibrils immediately following their removal from the density gradient isolation (Figure A4.3B). Therefore, the interpretation of these micrographs is complicated.

The role of Taxol-stabilized microtubules on cellulose synthesis investigated

Hirai *et al*. (1998) attempted to demonstrate a parallelism between in vitro-synthesized

beta-glucans and microtubule orientation. For this reason, all of the plasma membrane

sheets used in their experiments were prepared in the presence of Taxol. The nature of

the relationship between microtubules and cellulose biosynthesis has long been a subject

of debate for plant biologists. In order to rule out microtubule-mediated cellulose

synthesis inhibition, Taxol was used to hyper-stabilize cortical microtubules. The

inclusion of Taxol did cause the hyper-stabilization of microtubules on the membrane

sheets (Figure A4.5), but had no apparent effect on the ability of plasma membrane sheets

from *Arabidopsis* to make cellulose *in vitro*.

**Detergents added to UDPG do not increase cellulose synthesis by isolated plasma
membrane sheets**

The synthesis of cellulose by biochemically-isolated, detergent-solubilized membrane

fractions has been reported by several research groups (Lai-Kee-Him, *et al*., 2002;

Kudlicka *et al*., 1996). We thought that it might be possible to facilitate cellulose

synthesis on plasma membrane sheets by the inclusion of the same detergents used by

these researchers. The inclusion of 1% CHAPS in the UDPG-containing solutions had no

effect on the ability of plasma membrane sheets to synthesize cellulose. The inclusion of

detergents did, however, increase the rate of loss of membrane sheets from the

coverglass. Plasma membrane sheets were lost from the glass at a slow rate from all

PLL-isolated preparations. This rate was increased by including any detergents to the

media. The most likely cause of this accelerated loss is through interference of the electrostatic bonds between the PLL and the charged lipids in the plasma membrane by the detergent molecules.

Proteolytic deactivation of terminal complexes is not responsible for the inability of isolated plasma membrane sheets to synthesize cellulose

The cellulase solutions which are commonly used to make protoplasts from plant cells are notorious for also possessing protease activity. We speculated that this protease activity might be inactivating terminal complexes during protoplasts formation. Two approaches were used to answer this question. In one series of experiments, a protease inhibitor cocktail was included in the digestion, isolation, and *in vitro* synthesis solutions (Nakashima *et al.*, 2003). The inclusion of protease inhibitors was found to have no effect on the ability of membrane sheets to make cellulose *in vitro*.

In a second round of experiments, the cellulose synthesis inhibitor 2,6-dichlorobenzonitrile (DCB) was added to the washing solution following protoplast isolation on the density gradient. This might give the protoplasts time to make new terminal complexes and insert them into the plasma membrane. These new terminal complexes would then be capable of making cellulose *in vitro*. Protoplasts were allowed to recover in this solution for one hour before making membrane sheets. These protoplasts were found to have secreted a material, while not conventional fibrillar cellulose, still stained with Tinopal and made the evaluation of the production of *in vitro* product by membrane sheets impossible.

Protoplasts of *Arabidopsis* synthesize cellulose almost immediately after removal

of digesting enzymes. The speed (i.e. less than 10 minutes) that cellulose appears on the

protoplasts following removal from the density isolation solution suggests that even if all

of the terminal complexes are degraded by proteases during the digestion of the cell wall,

there are at least some active terminal complexes present in the plasma membrane by the

time the cells are removed from the protoplast isolation medium. Either these terminal

complexes were not degraded by proteases (endogenous or exogenous), or the rate of new

terminal complex insertion into the plasma membrane from the rough ER/Golgi is very

high.

Anti-CesA labeling of plasma membrane sheets

Antibodies to the catalytic region of cotton cellulose synthase were used to localize

terminal complexes on plasma membrane sheets from *Arabidopsis* and tobacco. There

was a very high background present in images of control plasma membrane sheets

incubated with the FITC-conjugated secondary antibody only. This background may be

due to non-specific binding of the secondary antibody to the membrane sheet, however,

the same area was stained by Tinopal. The significance of this dual-staining is unknown.

Perhaps the planar nature of these fluorophores allows their insertion into the

hydrophobic region of the large exposed plasma membrane bilayers. The inclusion of the

anti-CesA antibodies caused the appearance of punctate labeling which may possibly be

due to the binding of the anti-CesA antibodies to terminal complexes. These punctate

spots also appear over areas outside the boundaries of the plasma membrane sheets. This

may indicated that this type of labeling is due to non-specific interactions of the primary antibody with the membrane sheet or perhaps the PLL itself. It seems unlikely that these spots are due to the fluorescence of single FITC molecules, so therefore these are most likely aggregates. Another possible interpretation is that the primary antibody is truly labeling cellulose synthases present on the sheet and on the glass surface. In electron microscopic observations of plasma membrane sheet replicas, ribosomes can be seen bound to the glass surface in the area surrounding each plasma membrane sheet. The punctate spots observed here may be nascent cellulose synthase polypeptides still attached to ribosomes/polysomes which are themselves bound to the PLL. No cellulose microfibrils could be observed bound to the glass but not attached to a plasma membrane sheet; however, these nascent polypeptides would not be expected to be synthesizing cellulose yet. The non-specific association of the secondary antibody with the plasma membrane sheets can be directly correlated with the pattern of Tinopal binding. The punctate morphology generated by incubation with the anti-CesA primary antibody; however, is not also visualized by the Tinopal. Therefore, it can be said that the primary antibody is definitely labeling something different than what is bound by the secondary antibody.

Protoplasts synthesize cellulose microfibrils soon after wall-degrading enzymes are removed

Cell wall-degrading enzymes must be removed from the protoplasts before they can be adhered to PLL-coated surfaces. The presence of proteins in the medium coats the PLL

so that no protoplasts can stick to the coverslip. For *Arabidopsis*, protoplasts are separated from cell wall debris by floating on a density gradient composed of a three step sucrose/sorbitol layer system. This density gradient method, however, requires a significant amount of time to achieve separation of protoplasts from debris. This amount of time (5-10 minutes) is sufficient for the protoplasts to begin making new cellulose microfibrils. The images in Figure A4.8 prove that these protoplasts are capable of regenerating a cell wall after the removal of digestion medium. It is possible that the number of terminal complexes in the plasma membrane of protoplasts is depleted following isolation in the digestion medium; however, even at time zero there is some cellulose present on the surface of the protoplasts. It is possible that the tight binding of the plasma membrane lipids to the PLL is inhibiting the formation of cellulose by the terminal complexes in the membrane.

Characterization of plasma membrane sheets by electron microscopy

Plasma membrane sheets of *Arabidopsis* have been examined by TEM using platinum/carbon shadowing and negative staining. A plasma membrane sheet shadowed with platinum/carbon is shown in Figure A4.10. Cortical microtubules can be seen associated with the plasma membrane sheet. Also, a group of very large vesicles has remained bound to the plasma membrane sheet. These vesicles have not been seen before and may be a sign that this cell was dying or dividing when this membrane sheet was made. A large number of microtubules can be seen on the membrane sheet in Figure A4.11A. These microtubules appear to be oriented in the same direction. Interestingly,

176

none of these microtubules appear to be bundles. In fact, they do not seem to be in contact with each other at all and yet they are all oriented in roughly the same direction. The fact that these microtubules are singlets can be seen better in Figure A4.11B. Here also the structure of the plasma membrane can be seen to be very smooth in places and have rough "islands". This may indicate that the plasma membrane was partially extracted during the isolation or dehydration process. If the plasma membrane was being removed; however, the cellulose microfibrils should be imaged. Their absence leads to the conclusion that this sheet is intact but possibly covered in some type of contaminant which is partially obscuring some of the fine structure of the plasma membrane sheet's ultrastructure.

Protofilaments within intact microtubules imaged by negative staining

Microtubules can be seen on membrane sheets by negative staining. The microtubules shown in Figure A4.12 have been negatively stained. The stain has penetrated between the microtubule protofilaments, allowing them to be resolved. Images of microtubule protofilaments very similar to those shown in Figure A4.12 have been reported associated with plasma membrane sheets from tobacco (Van der Valk and Fowke, 1980). Several research groups have reported a direct correlation between the time when a protoplast begins to actively regenerate new cell wall components and the presence of microtubules associated with plasma membrane sheets (Marchant and Hines, 1979; Van Der Valk *et al.*, 1980). Therefore, the best chance of observing cellulose microfibrils and terminal complexes is on membrane sheets with extensive arrays of cortical microtubules.

177

Cellulose microfibrils imaged by negative staining chloroform/methanol-extracted plasma membrane sheets

Neither negative staining nor platinum/carbon shadowing revealed the presence of any cellulose microfibrils under plasma membrane sheets; however, Tinopal-stained cellulose is easily detected under plasma membrane sheets by fluorescence microscopy. Additionally, cellulose microfibrils can be seen on the surface of intact protoplasts on the TEM (Figure A4.15). If the lipids of the plasma membrane are removed by incubating the membrane sheets with chloroform/methanol, cellulose microfibrils can be seen (Figure A4.13). This indicates that cellulose microfibrils are likely present under other membrane sheets where cellulose microfibrils were not previously detected. The plasma membrane sheet is too thick, and the cellulose microfibrils too small, to be given contrast by negative staining or metal shadowing.

Cellulose microfibrils detected under intact plasma membrane sheets by CBH I-gold

The ultimate goal of this project is to develop a technique which will allow the imaging of the cytoplasmic domain of the terminal complex. Plasma membrane sheets have been isolated from *Arabidopsis* suspension culture cells and imaged by light and electron microscopy. Cellulose microfibrils have been identified under plasma membrane sheets by fluorescence microscopy and by TEM after chemically removing the plasma membrane lipids. The removal of plasma membrane lipids caused the aggregation of the protein components associated with the plasma membranes, hindering the identification

178

of terminal complexes. Ideally, terminal complexes will be identified by their association with the tips of nascent cellulose microfibrils. This technique was used by the first researchers to identify terminal complexes in freeze-fracture replicas (Brown and Montezinos, 1976; Mueller and Brown, 1980). Because cellulose microfibrils cannot be directly imaged under plasma membrane sheets either by negative staining or platinum/carbon shadowing, a method for identifying cellulose microfibrils was sought. CBH I is a cellulase enzyme secreted by the fungus *Trichoderma reesii* to digest cellulose (Nidetzky *et al.*, 1994). This enzyme has been purified and conjugated to 10 nm gold particles. These CBH I-gold conjugates retain their strong affinity for crystalline cellulose and can be used to identify cellulose in samples for electron microscopy. By labeling cellulose microfibrils on the surface of regenerating protoplasts with CBH I-gold before making membrane sheets, gold particles adhering to cellulose microfibrils became trapped between the plasma membrane and the glass substrate (Figure A4.14). The linear arrangement of gold particles indicates that they are in fact bound to a cellulose microfibril. Unfortunately, the binding of these gold particles to cellulose was found to be quite rare. It is possible that the CBH I enzymes retain some of their cellulase activity even when bound to the gold particles. Furthermore, some CBH I molecules may have completely disassociated from the gold particles all together. The presence of even minute quantities of cellulase may be sufficient to degrade the 5-10 nm microfibrils that are produced from a single TC. Therefore, what is shown in Figure A4.14 is most likely a bundle of microfibrils.

Protoplast surfaces by electron microscopy

Cellulose microfibrils under plasma membrane sheets have been imaged by Tinopal staining and by removing the plasma membrane and negatively staining the microfibrils that remain. Due to the presence of a non-trivial amount of background fluorescence, it is unlikely that Tinopal staining can reveal the presence of an isolated 36 member (5-8 nm) cellulose sub-microfibril produced from a single terminal complex. It is known that cellulose microfibrils combine into larger microfibrils soon after synthesis. What is probably being detected in Tinopal-stained specimens are these larger cellulose microfibrils generated as a result of the aggregation of several ~36 glucan sub-microfibrils. Furthermore, the imaging of cellulose present under the plasma membrane sheets by the chloroform/methanol extraction of lipids causes the cellulose microfibrils to undergo some amount of aggregation due to the removal of water bound to the surface of the microfibrils.

The presence of active terminal complexes in the plasma membrane sheet should coincide with the presence cellulose microfibrils on the outer surface of a regenerating protoplast. In order to see these microfibrils, protoplasts were produced, allowed to regenerate for a short time, and bound to PLL-coated coverslips in the same way as for the isolation of plasma membrane sheets. These protoplasts were then fixed and dehydrated without being lysed. Replicas of the surface of the protoplast were then prepared for TEM by rotary shadowing with platinum/carbon. Immediately apparent is the fact that the plasma membrane of these cells is much smoother from the outside than what is seen from the inside (Figures 4.15A and B). Furthermore, not every protoplast

had regenerated cellulose microfibrils at this time. The cellulose microfibrils which were imaged on the surface of protoplasts were irregular in nature (Figures 4.15C and D). The cellulose was not linear like what is usually seen in sections or freeze-fracture images, or what was imaged from these cells by negative staining chloroform/methanol-extracted plasma membrane sheets. The central region of the protoplasts is almost always seen to be devoid of cellulose microfibrils (Figures 4.15A and B). This may indicate that excessive thickness of shadow was used, burying the cellulose microfibrils. Another alternative is that the cellulose microfibrils were displaced from the top of the protoplasts during the fixation and dehydration procedures. This theory is made more convincing by the observation that the cellulose that is present is distorted in appearance and not linear, as usually seen. However, the fact that there is no visible cellulose on the top of the protoplasts where the deposition of shadow material would be expected to be the thickest seems to indicate that the thickness of the shadow is obscuring the cellulose microfibrils.

Conclusions

Arabidopsis suspension culture cells are suitable specimens for the isolation of plasma membrane sheets. Cellulose microfibrils are synthesized by protoplast rapidly following the removal of cell wall-degrading enzymes. Plasma membrane sheets isolated from these recovered protoplasts have cellulose microfibrils under them.

Plasma membrane sheets isolated from *Arabidopsis* suspension culture cells are not capable of synthesizing cellulose microfibrils in vitro. This inability to synthesize cellulose *in vitro* is not due to the proteolytic degradation of terminal complexes during

181

protoplast production or proteolysis on the membrane sheet itself. The ability to synthesize cellulose is not microtubule-dependent, nor can the presence of detergents restore function to the terminal complexes.

Although plasma membrane sheets with cellulose attached have been imaged, terminal complexes were not imaged on plasma membrane sheets isolated from *Arabidopsis* suspension culture cells. A method for simultaneously imaging the cytoplasmic domain of transmembrane proteins and their exocytoplasmic products has been developed using Tobacco BY-2 suspension culture cells (see Chapter 5). Terminal complexes have been imaged in plasma membrane sheets isolated from tobacco BY-2 protoplasts (see Chapter 6). Because plasma membrane sheets with attached cellulose microfibrils can be isolated from *Arabidopsis*, this technique may also be applied to *Arabidopsis* protoplasts from suspension cultures or possibly protoplast isolated from plant tissues. If possible, this would be a new way to answer questions about what types of proteins are part of the terminal complex and where the proteins are located that are responsible for certain types of cellulose synthesis mutants.
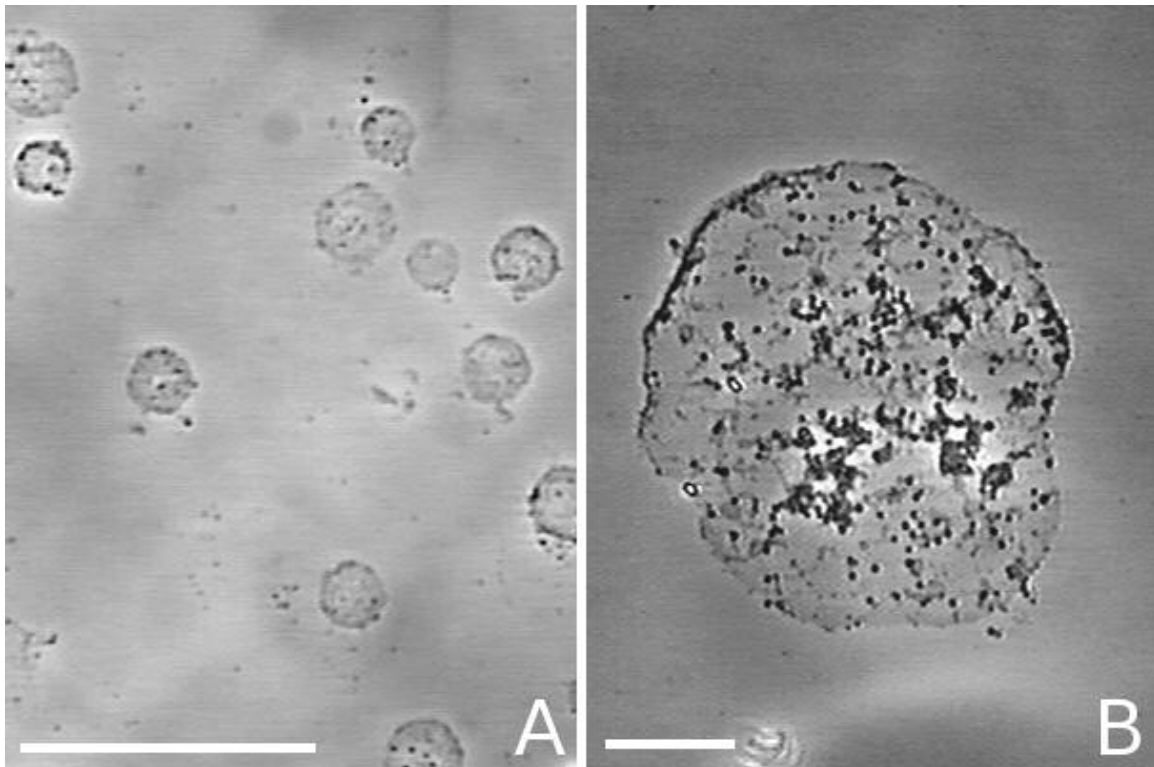
Figure A4.1. Plasma membrane sheets from *Arabidopsis* imaged by phase contrast.

(A) A preparation of plasma membrane sheets seen at low magnification. Scale bar = 50 μm.

(B) A plasma membrane sheet at higher magnification. This sheet has been fixed with 2.5% glutaraldehyde and rinsed vigorously. Many dark, spherical structures remain bound to the sheet. Also, a large region of the sheet is covered with cellular debris. The sheet has a very definite border. There are some hints of linear structures which may be cortical microtubules. Scale bar = 10 μm.
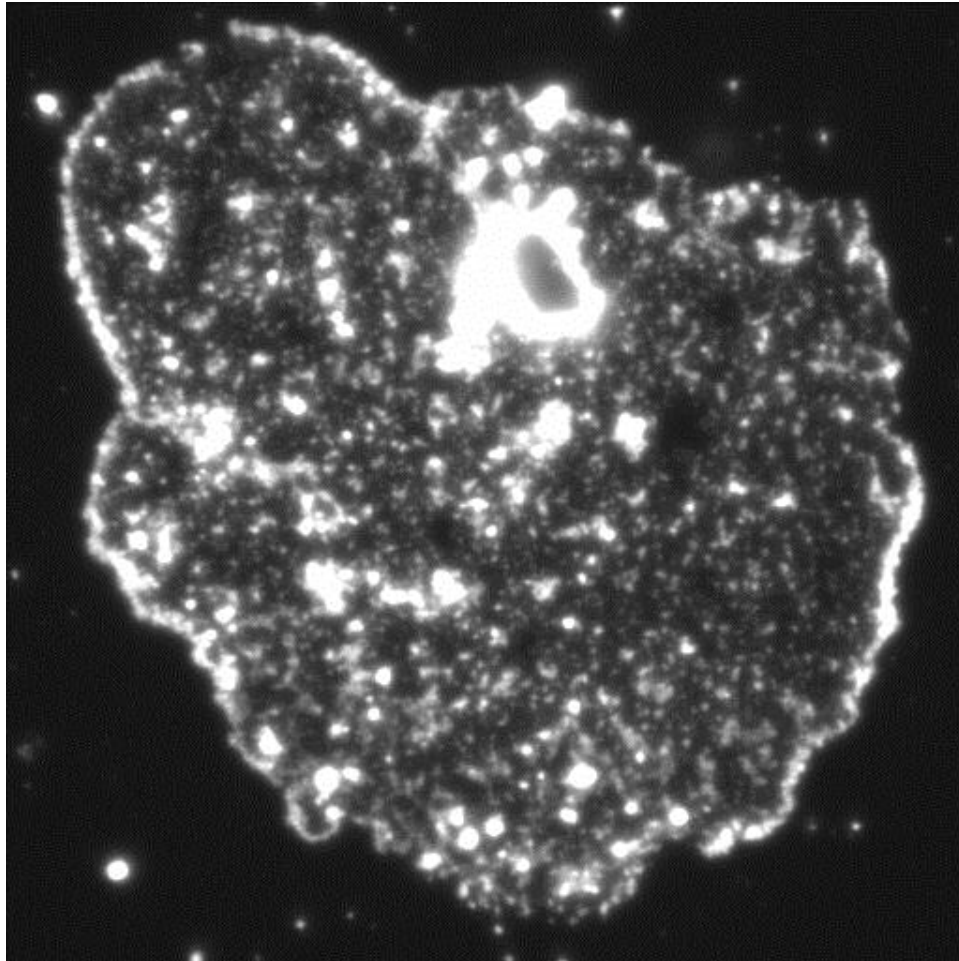
Figure A4.2. A plasma membrane sheet from *Arabidopsis* stained with Tinopal and viewed on a Zeiss deconvolution microscope.

Many brightly-stained particles of varying sizes can be seen attached to the membrane sheet. The fluorescence of these spots is due to the presence of Tinopal.
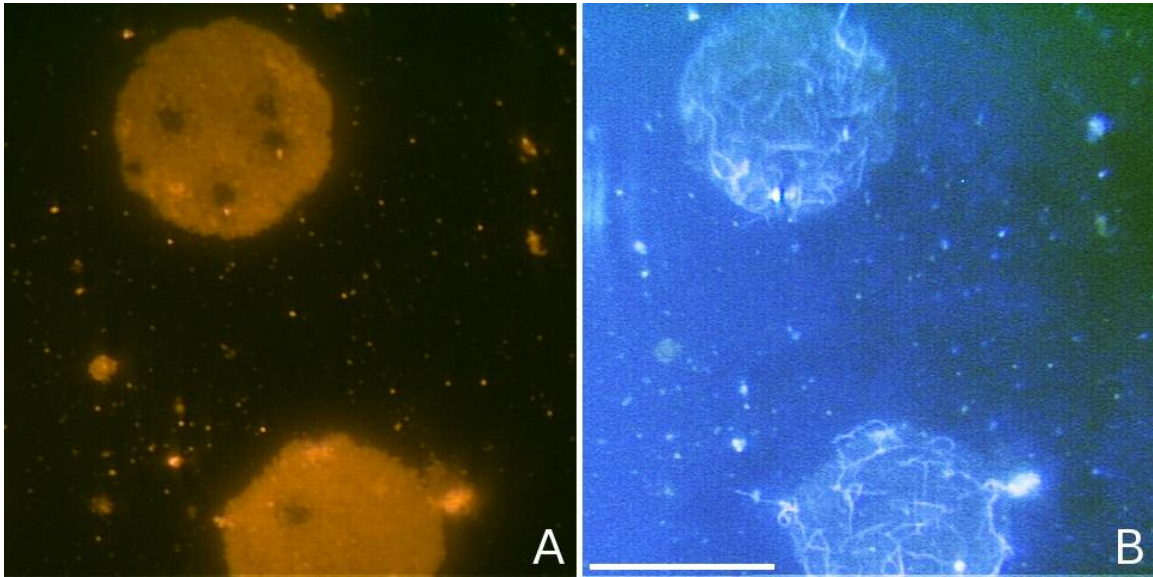
Figure A4.3. Plasma membrane sheets dual-stained with DiI (left) and Tinopal (right). Scale bar = 10 µm.

(A) The lipophilic dye DiI was used to fluorescently label the lipid component of the plasma membrane.

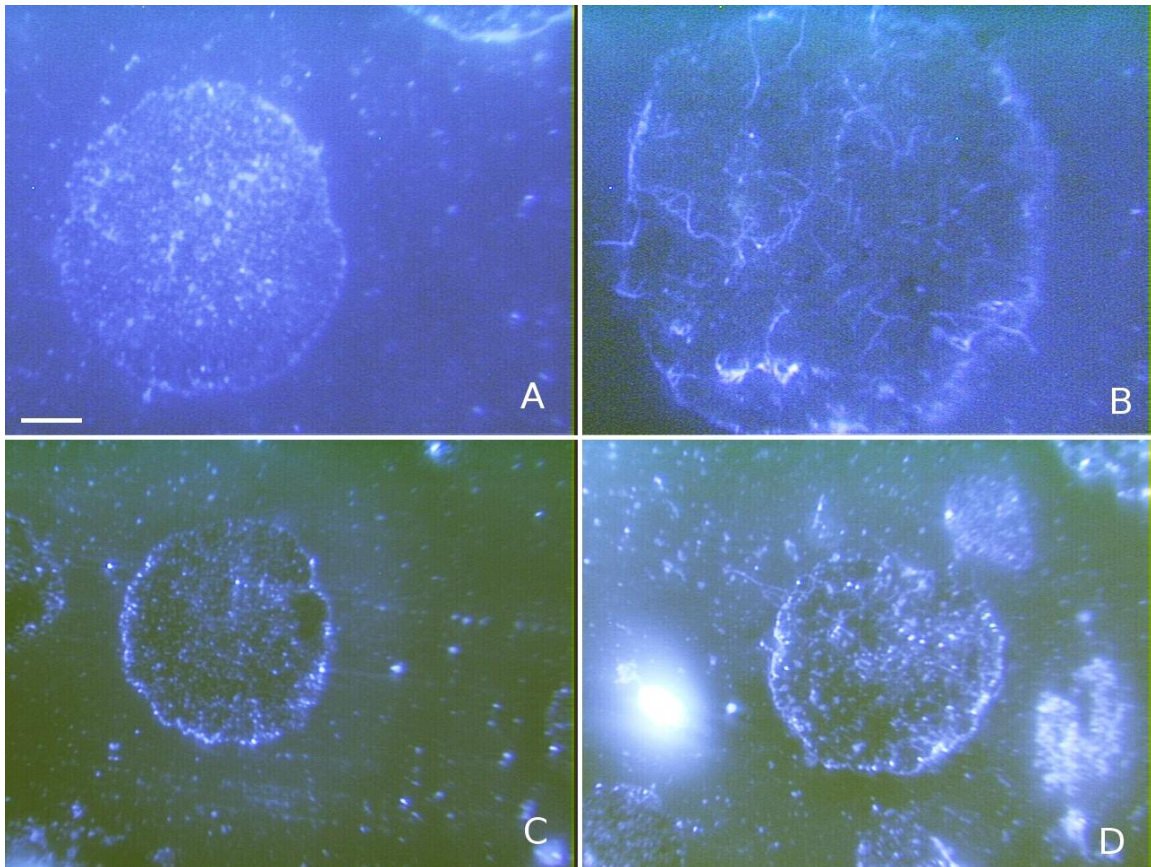(B) Tinopal-stained microfibrils are present under these membrane sheets.

Figure A4.4. Membrane sheets incubated in UDPG do not synthesize fibrillar cellulose.

Plasma membrane sheets were made fixed immediately (A and B) or incubated with UDPG-containing medium for 30 minutes. Scale bar = 10 μm.

(A) A membrane sheet at time zero showing punctate spots but very little fibrillar material.

(B) A membrane sheet from time zero showing fibrillar material but very little other fluorescence.

(C) A membrane sheet after a 30 minute incubation in UDPG-containing medium. No growth of fluorescent material, amorphous/punctate or fibrillar, can be detected.

(D) Another membrane sheet after a 30 minute incubation with UDPG. Some fibrillar structures can be seen, however, they could have been present before the incubation, as demonstrated in (B).
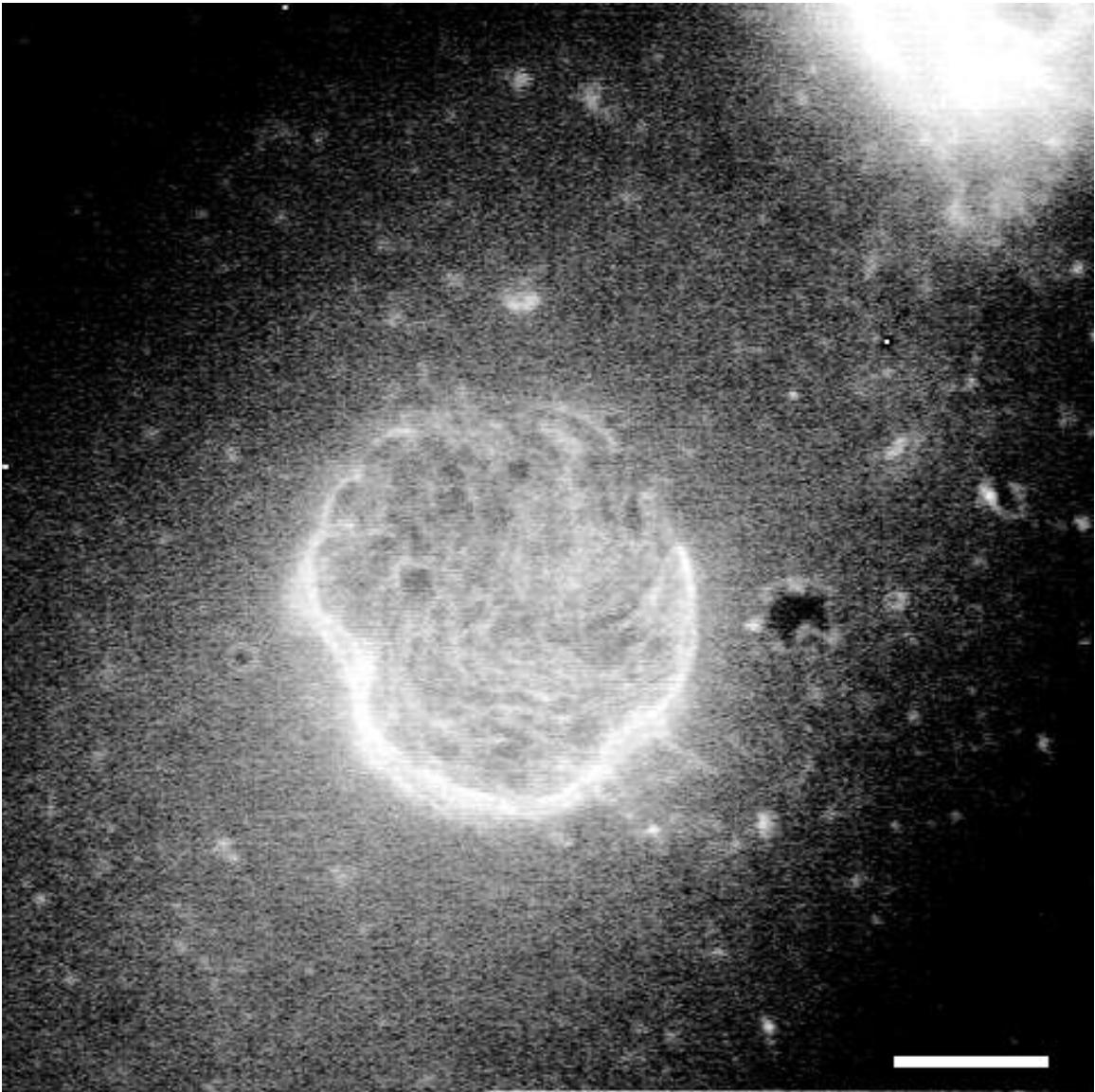
Figure A4.5. Taxol-stabilized microtubules labeled with anti-microtubule/CY-3

A large number of hyper-stabilized microtubules can be seen on Taxol-treated membrane sheets. Taxol-stabilization of microtubules had no effect on the ability of membrane sheets to synthesize cellulose *in vitro*. Scale bar = 10 μm.
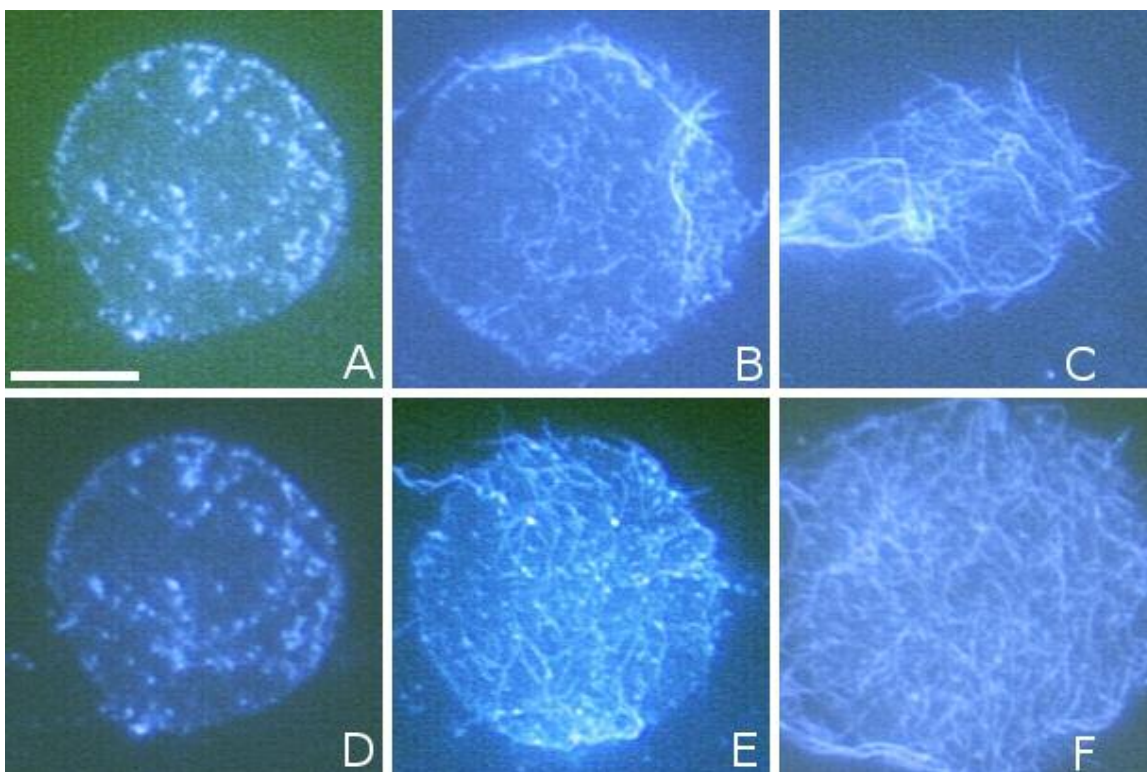
Figure A4.6. The addition of CHAPS has no effect of the ability of membrane sheets to synthesize cellulose *in vitro*. Scale bar = 10 μm.

(A-C) Membrane sheets incubated in buffer only showing the large variation in cellulose content/morphology.

(D-E) Membrane sheets incubated with 1% CHAPS + UDPG for 1.5 hours on a gyratory shaker at RT. A similar variation in the amount of cellulose and the appearance of the membrane sheets can be seen.

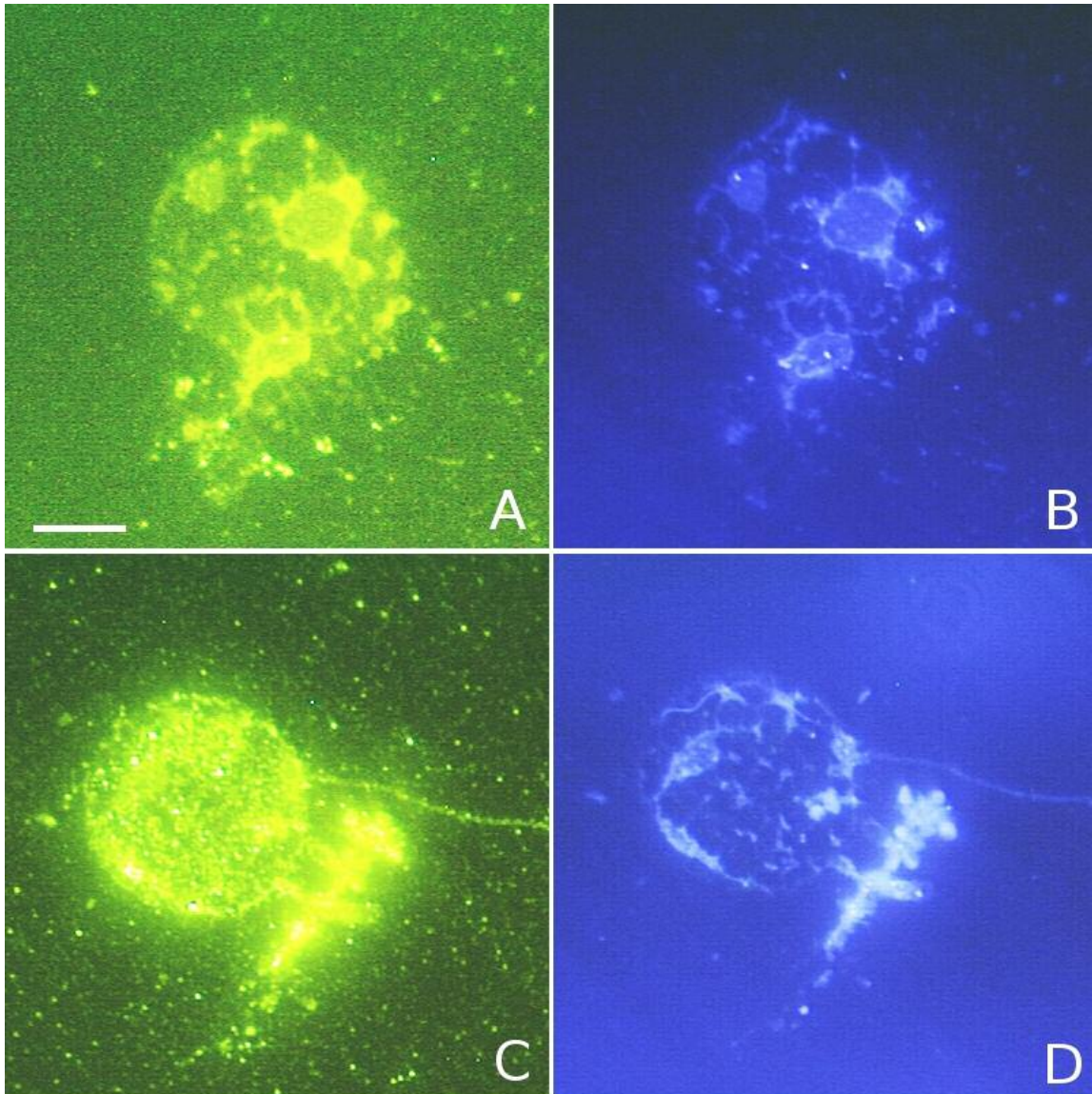**Figure A4.7.** Plasma membrane sheets labeled with anti-CesA antibodies.

Plasma membrane sheets prepared by the Sonobe method.   Scale bar = 10 μm.

(A) Plasma membrane sheets stained with the secondary antibody only.

(B) The plasma membrane sheet from (A) stained with Tinopal

(C) A Plasma membrane sheet stained with anti-CesA

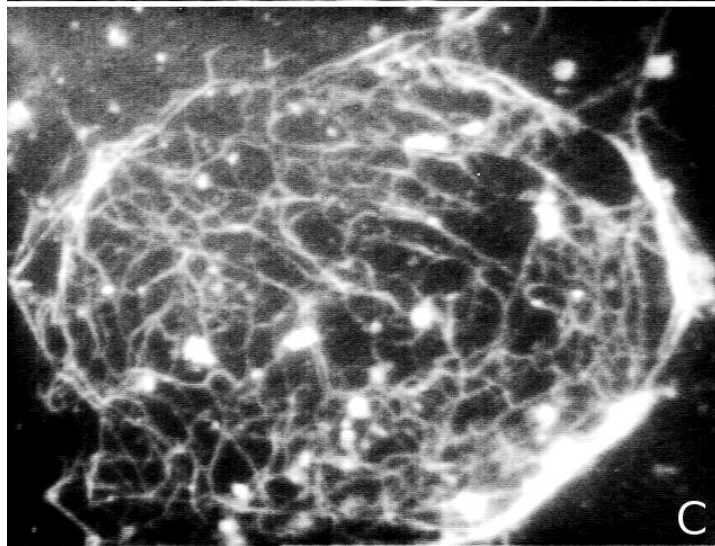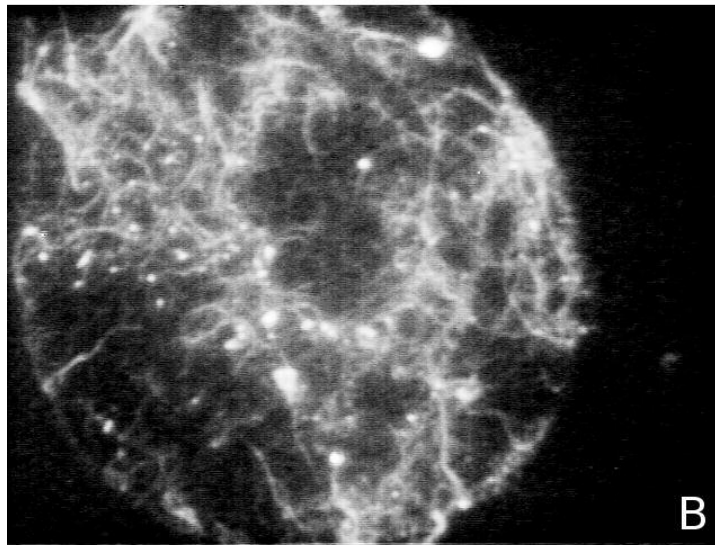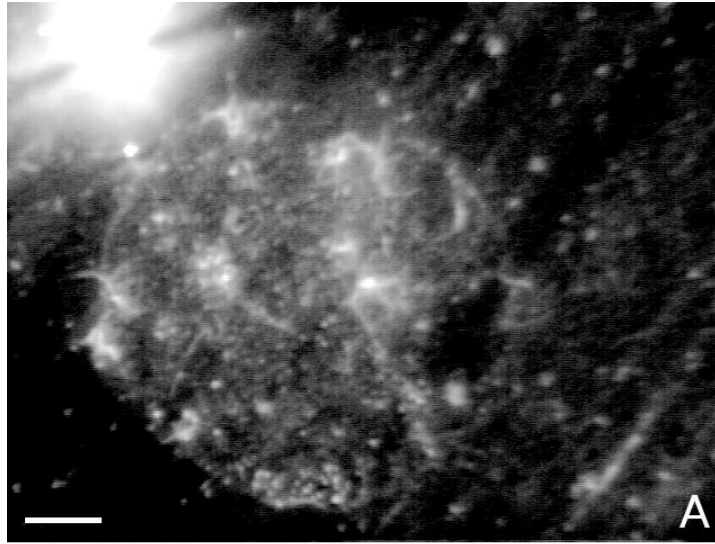(D) The plasma membrane sheet in (C) stained with Tinopal

Figure A4.8. Protoplasts left in density-isolation solution regenerate copious microfibrils.

Protoplasts were prepared and isolated on a sucrose/sorbitol density gradient. Protoplasts were collected and re-suspended in iso-osmotic medium containing sucrose for varying amounts of time. Protoplasts were then attached to poly-L-lysine coated coverslips, lysed to yield membrane sheets, fixed, and stained with Tinopal. Scale bar = 10 μm.

(A) Membrane sheets made immediately after resuspension in the sucrose-containing regeneration medium. At this time, small microfibrils can be detected at several places under the membrane sheet.

(B) After 30 minutes incubation in the sucrose-containing medium, a large number of cellulose microfibrils can be seen. The length of individual microfibrils has also increased.

(C) After 90 minutes in regeneration medium, both the length and number of microfibrils have further increased.
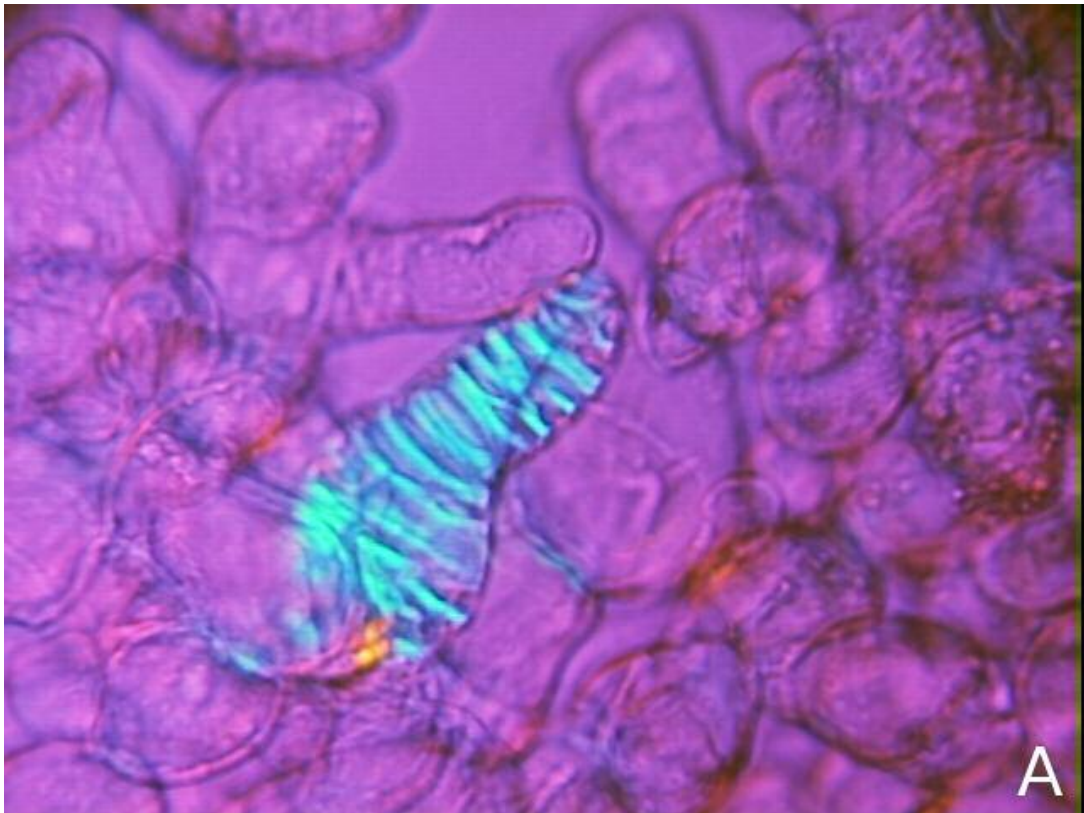
Figure A4.9. *Arabidopsis* suspension cultures were found to contain tracheary element-like cells.

(A) An aliquot of the *Arabidopsis* suspension culture was found to contain tracheary element-like cells by polarization microscopy.

(B) Tracheary element-like cells were found to contain lignin, as indicated by the autofluorescence of the bands of birefringent material.
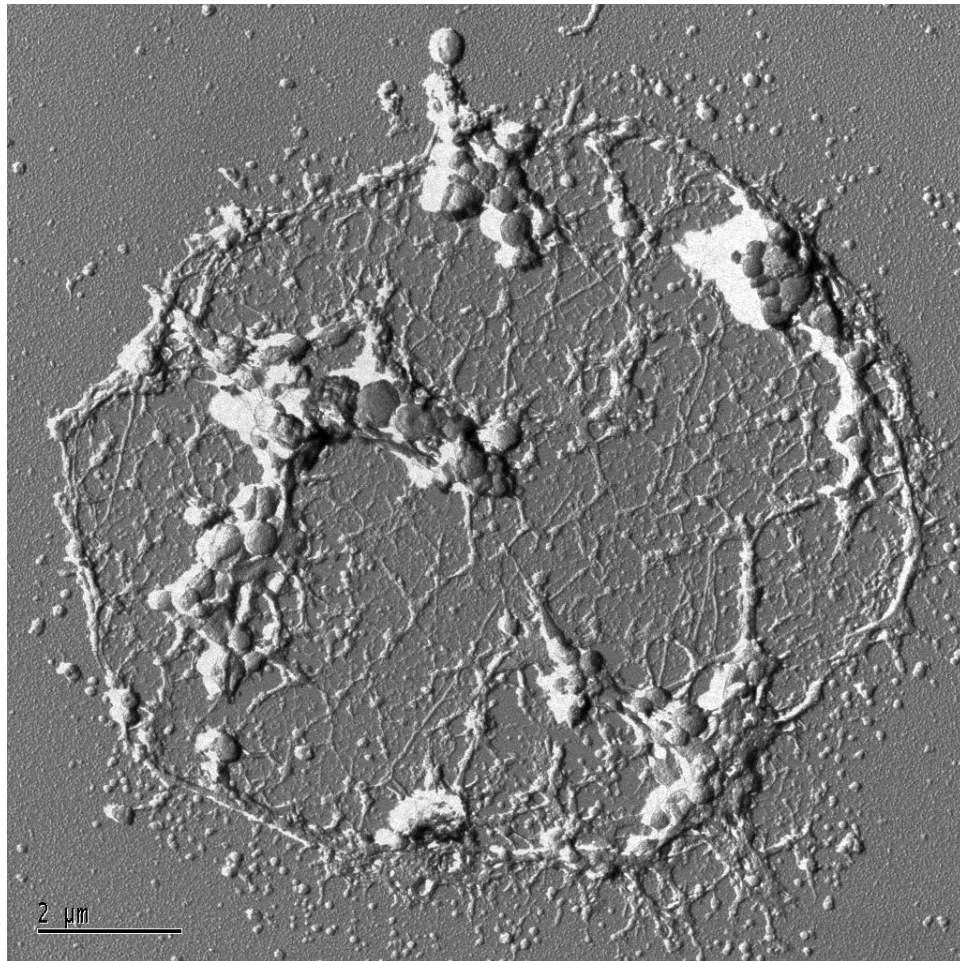
Figure A4.10. A plasma membrane sheet unidirectionally shadowed with Platinum/carbon.

The membrane sheets are roughly circular, just as seen by light microscopy. Many of the features seen with the light microscope can also be identified here. In several areas, large amounts of cytoplasmic components, including what appear to be large vesicles, remain bound to the membrane sheet. The presence of many cortical microtubules can be seen on all sectors of the sheet.
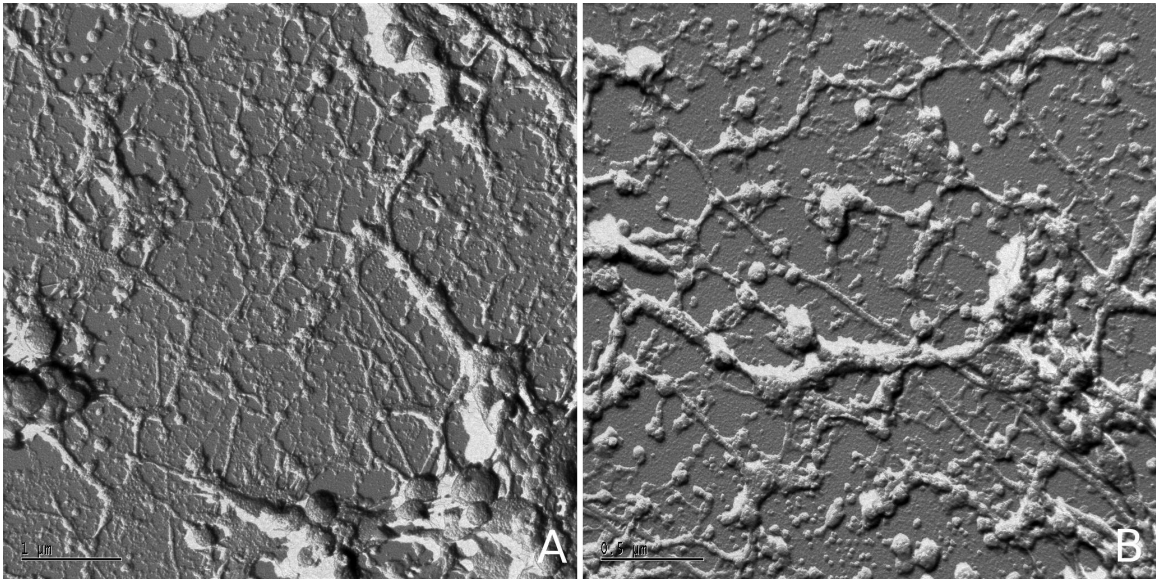
Figure A4.11. Cytoplasmic material and microtubules associated with platinum/carbon-shadowed plasma membrane sheets.

(A) A large number of microtubules can be seen associated with this plasma membrane sheet. Their orientations appear to be in the same general direction, however, they are not truly parallel.

(B) Microtubules can be seen with some large cytoplasmic structures lying over them. The surface of the membrane appears smooth but it is unclear whether this is the membrane or the surface of the glass under the plasma membrane. No cellulose microfibrils can be seen under the plasma membrane sheet.
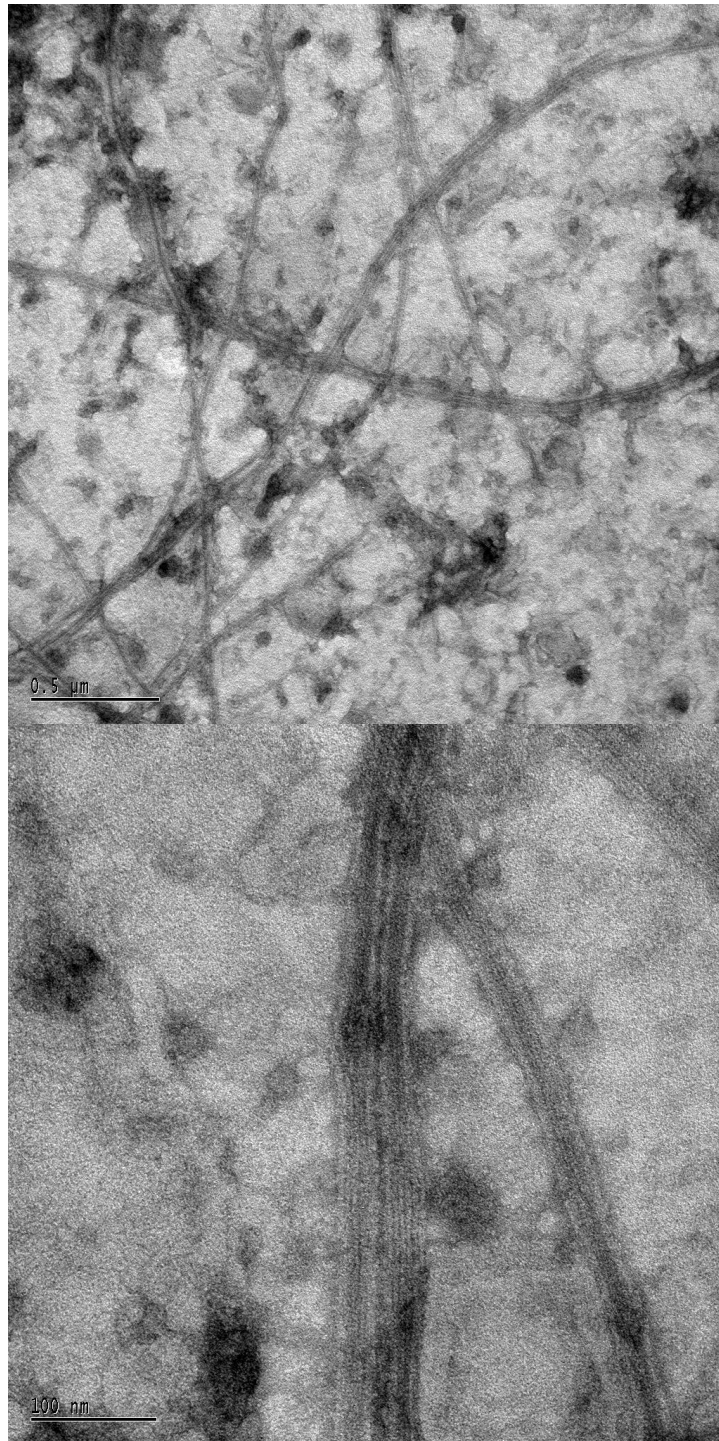
Figure A4.12. Cortical microtubules associated with a plasma membrane sheet.

(A) A randomly-oriented network of microtubules and microtubule bundles can be seen on this negatively-stained plasma membrane sheet.
(B) At higher magnification, the protofilaments within these microtubules are visible.
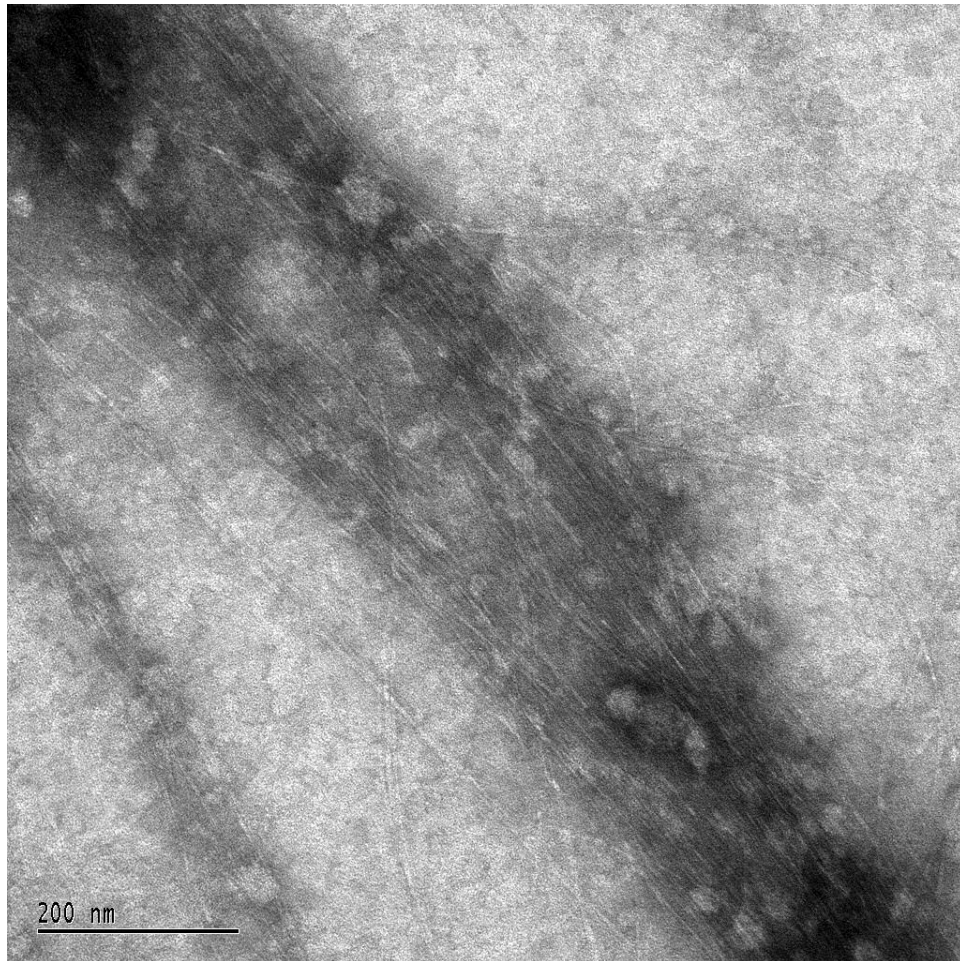
Figure A4.13. Cellulose microfibrils from *Arabidopsis* are visible after removal of the plasma membrane with chloroform/methanol.
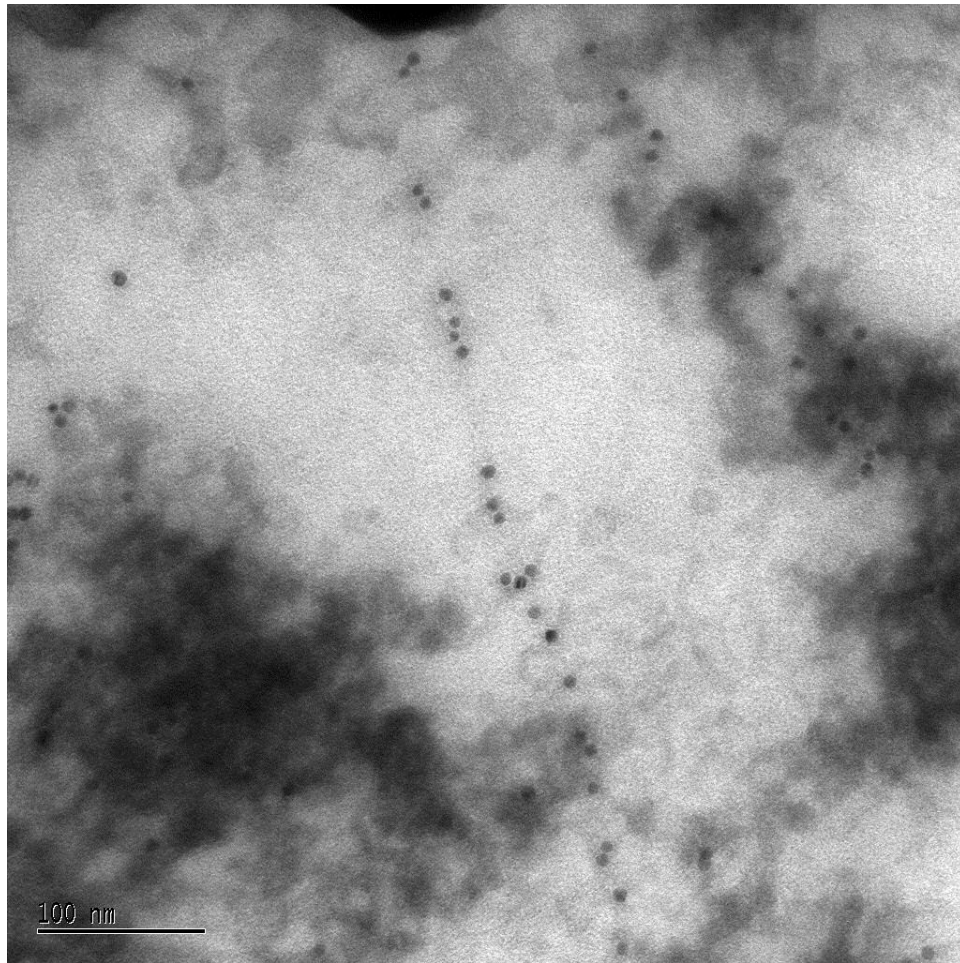
Figure A4.14. A plasma membrane sheet which has been labeled with CBH I-gold.

The gold particles are lined up in a linear fashion because they are adhering to a cellulose microfibril. The cellulose microfibril cannot be imaged directly because the plasma membrane is still intact.
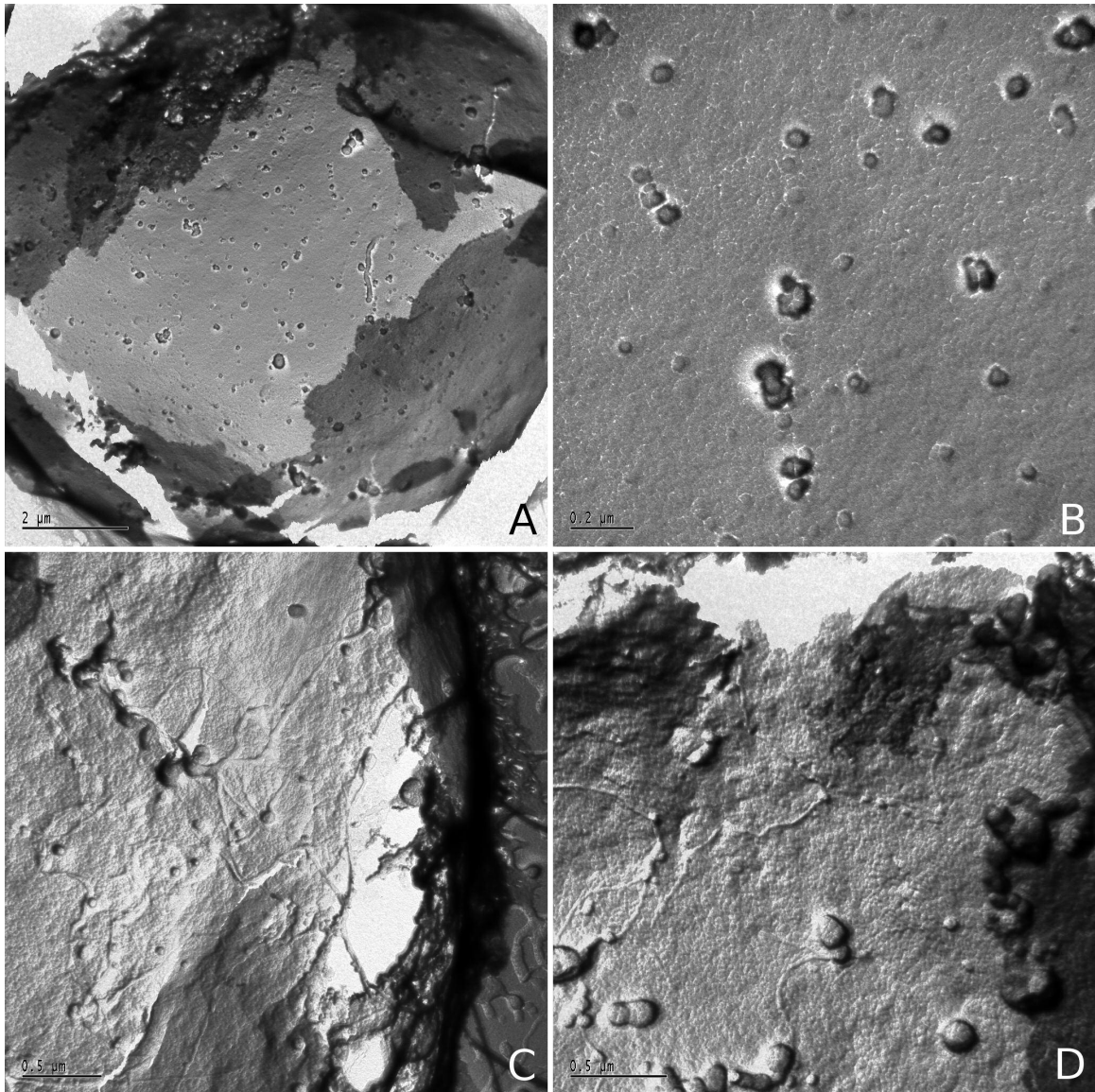
Figure A4.15. The surface of *Arabidopsis* protoplasts.

(A) An *Arabidopsis* protoplast that has been replicated. The drying of the replica has caused the protoplast replica to shatter.

(B) A higher magnification of view of (A). The surface of the plasma membrane is very smooth on the outside of the cell. Particles of various sizes can be seen adhering to the surface of the protoplast.

(C and D) On the surface of some protoplasts cellulose microfibrils can be seen.

Bibliography

Aggeler J, Werb Z. (1982). Initial events during phagocytosis by macrophages viewed from outside and inside the cell - membrane-particle interactions and clathrin. Journal of Cell Biology 94 (3): 613-623.

Amano Y, Shiroishi M, Nisizawa K, Hoshino E, Kanda T. (1996) Fine substrate specificities of four exo-type cellulases produced by *Aspergillus niger*, *Trichoderma reesei*, and *Irpex lacteus* on (1-3),(1-4)-β-D-glucans and xyloglucan. J. Biochem. 120, 1123-1129.

Amos L. (2000). Focusing-in on microtubules. Current Opinion in Structural Biology 10(2): 236-241.

Andrews SB, Gallant PE, Leapman RD, Schnapp BJ, Reese TS. (1993). Single kinesin molecules crossbridge microtubules in-vitro. Proceedings of the National Academy of Sciences of the United States of America 90 (14): 6503-6507.

Arioli T, Peng LC, Betzner AS, Burn J, Wittke W, Herth W, Camilleri C, Hofte H, Plazinski J, Birch R, Cork A, Glover J, Redmond J, Williamson RE. (1998). Molecular analysis of cellulose biosynthesis in *Arabidopsis*. Science 279 (5351): 717-720.

Böhm J, Frangakis AS, Hegerl R, Nickell S, Typke D, Baumeister W. (2000). Toward detecting and identifying macromolecules in a cellular context: Template matching applied to electron tomograms. Proceedings of the National Academy of Sciences of the United States of America 97: 14245-14250.

Bradford MM. (1976) A rapid and sensitive method for the quantitation of microgram quantities of protein utilizing the principle of protein-dye binding. Anal Biochem 72, 248-54.

Bradley DE. (1965). Replica and shadowing techniques, in: Techniques for electron microscopy, 2nd edition, D.H. Kay, ed. (Blackwell, Oxford), p. 96.

Brown D, Zeef L, Ellis J, Goodacre R, Turner S. (2005). Identification of novel genes in *Arabidopsis* involved in secondary cell wall formation using expression profiling and reverse genetics. The Plant Cell (Early release).

Brown Jr RM, Montezinos D. (1976). Cellulose microfibrils: visualization of biosynthetic and orienting complexes in association with the plasma membrane.

Proceedings of the National Academy of Sciences of the United States of America 73: 143–147.

Brown Jr RM, Saxena IM. (2000). Cellulose biosynthesis: A model for understanding the assembly of biopolymers. Plant Physiology and Biochemistry 38: 57-67.

Brown Jr RM. (1996). The biosynthesis of cellulose. Journal of Macromolecular Science —Pure and Applied Chemistry A33: 1345–1373.

Brown Jr RM, Haigler CJ, Suttie J, White AR, Roberts E, Smith C, Itoh T, and Cooper K. (1983) The biosynthesis and degradation of cellulose. J. App. Polymer Sci. 37, 33-78.

Brown Jr RM, Haigler CJ, Cooper K. (1982) Experimental induction of altered nonmicrofibrillar cellulose. Science 218, 1141-1142.

Brown Jr RM, Montezinos D. (1976). Cellulose microfibrils: visualization of biosynthetic and orienting complexes in association with the plasma membrane. Proc Nat Acad Sci USA 73:143-147.

Buchanan CM, Hyatt JA, and Lowman D. W (1989) Supramolecular structure and microscopic conformation of cellulose esters. J. Am. Chem. Soc. 111, 7312-7319.

Chanzy, H., Henrissat, B., Vuong, R., and Schülein, M. (1983). The action of 1,4-β-D-glucan cellobiohydrolase on *Valonia* cellulose microcrystals. FEBS Lett. 153(1), 113-118.

Clarke M, Schatten G, Mazia D, Spudich JA. (1975). Visualization of actin fibers associated with cell-membrane in amebas of *Dictyostelium-discoideum*. Proceedings of the National Academy of Sciences of the United States of America 72 (5): 1758-1762.

Cousins SK, Brown Jr RM. (1995). Cellulose I microfibril assembly: computational molecular mechanics energy analysis favours bonding by van der Waals forces as the initial step in crystallization. Polymer 36: 3885–3888.

Cousins SK, Brown Jr RM. (1997). X-ray diffraction and ultrastructural analyses of dye-altered celluloses support van der Waals forces as the initial step in cellulose crystallization. Polymer 38: 897–902.

Cousins SK, Brown Jr RM. (1997) Photoisomerization of a dye-altered β-1,4 glucan sheet induces the crystallization of a cellulose-composite. Polymer 38, 903-912.

Delmer DP. (1999). Cellulose biosynthesis: exciting times for a difficult field of study. Annual Reviews of Plant Physiology and Plant Molecular Biology 50: 245–276.

Divne C, Ståhlberg J, Reinikainen T, Ruohonen L, Pettersson G, Knowles CKJ, Teeri TT, Jones TA. (1994) The three-dimensional crystal structure of the catalytic core of cellobiohydrolase I from *Trichoderma reesei*. Science 265, 524-528.

Divne C, Ståhlberg J, Teeri TT, Jones TA. (1998) High-resolution crystal structures reveal how a cellulose chain is bound in the 50 Å long tunnel of cellobiohydrolase I from *Trichoderma reesei*. J. Mol. Biol, 275, 309-325.

Doblin MS, Kurek I, Jacob-Wilk D, Delmer DP. (2002). Cellulose biosynthesis in plants: from genes to rosettes. Plant Cell Physiology 43: 1407–1420.

Eskandari S, Wright EM, Kreman M, Starace DM, Zampighi GA. (1998). Structural analysis of cloned plasma membrane proteins by freeze-fracture electron microscopy. Proceedings of the National Academy of Sciences of the United States of America 95 (19): 11235-11240.

Feng R, Brown Jr RM. (2000). A novel cotton ovule culture: induction, growth, and characterization of submerged cotton fibers (Gossypium Hirsutum L.). in vitro Cell Dev Biol - Plant 36: 293-299.

Fisher DD, Cyr RJ. (1998). Extending the microtubule/microfibril paradigm - Cellulose synthesis is required for normal cortical microtubule alignment in elongating cells. Plant Physiology 116 (3): 1043-1051.

Fujimoto K. (1995). Freeze-fracture replica electron microscopy combined with SDS digestion for cytochemical labeling of integral membrane proteins. Application to the immunogold labeling of intercellular junctional complexes Journal of Cell Science 108: 3443-3449.

Fukuda H, Komamine A. (1980). Establishment of an experimental system for the study of tracheary element differentiation from single cells isolated from the mesophyll of Zinnia elegans. Plant Physiology 65: 57-60.

Gardner KH, Blackwell J. (1974). The structure of native cellulose. Biopolymers 13: 1975-2001.

Giddings Jr TH, Staehelin LA. (1991). Microtubule-mediated control of microfibril deposition: a re-examination of the hypothesis. In: Lloyd CW, ed. The cytoskeletal basis of plant growth and form. London: Academic Press, 85–99.

Gilkes NR, Jervis E, Henrissat B, Tekant B, Miller Jr RC, Warren RAJ, Kilburn DG. (1992). The adsorption of a bacterial cellulase and its two isolated domains to crystalline cellulose. J. Biol. Chem. 267(10), 6743-6749.

Glauert A, Lewis P. (1998). Biological specimen preparation for transmission electron microscopy. Princeton University Press, Princeton, NJ.

Gould JH, Palmer RL, Dugger WM. (1986). Isolation and culture of anucleate protoplasts from cotton fiber: assessment of viability and analysis of regenerated wall polymers. Plant Cell Tissue Organ Cult 6: 61-72.

Green PB. (1980). Organogenesis – a biophysical view. Annual Reviews in Plant Physiology 31: 51-82.

Grout BWW. (1975). Cellulose microfibril deposition at the plasmalemma surface of regenerating tobacco mesophyll protoplasts: A deep-etch study. Planta 123: 275-282.

Ha MA, Apperley DC, Evans BW, Huxham M, Jardine WG, Vietor RJ, Reis D, Vian B, Jarvis MC. (1998). Fine structure in cellulose microfibrils: NMR evidence from onion and quince. Plant Journal 16 (2): 183-190.

Haigler CH, Brown Jr RM, Benziman M. (1980). Calcofluor White ST alters the in vivo assembly of cellulose microfibrils. Science 210: 903–906.

Haigler CH, Chanzy H. (1988) Electron diffraction analysis of the altered cellulose synthesized by Acetobacter xylinum in the presence of fluorescent brightening agents and direct dyes. Journal of Ultrastructure and Molecular Structure Research 98, 299-311.

Haigler CH, Brown Jr RM, Benziman M. (1980) Calcofluor White ST alters the in vivo assembly of cellulose microfibrils. Science 210, 903-906.

Hanley SJ, Revol J, Godbout L, Gray D. (1997) Atomic force microscopy and transmission electron microscopy of cellulose from *Micrasterias denticulata*; evidence for a chiral helical microfibril twist. Cellulose 4, 209-220.

Harris JR. (1997). Negative Staining and Cryoelectron Microscopy: The Thin Film Techniques. Microscopy Handbook No. 35, BIOS Scientific Publishers, Oxford.

Henriksson H, Jonsson S, Isaksson R, Pettersson G. (1995) Chiral separation based on immobilized intact and fragmented cellobiohydrolase II (CBH II): A comparison with cellobiohydrolase I (CBH I). Chirality 7, 415-424.

Herth W. (1983). Arrays of plasma-membrane rosettes involved in cellulose microfibril formation of Spirogyra. Planta 159 (4): 347-356.

Heuser J. (1981). Preparing biological samples for stereomicroscopy by the quick-freeze, deep-etch, rotary-replication technique. Methods in Cell Biology 22: 97-122

Heuser, J. (2000). The production of 'cell cortices' for light and electron microscopy. Traffic 1 (7): 545-552.

Himmelspach R, Wiliamson RE, Wasteneys GO. (2003). Cellulose microfibril alignment recovers from DCB-induced disruption despite microtubule disorganization. The Plant Journal 36: 565-575.

Hirai N, Sonobe S, Hayashi T. (1998). In situ synthesis of beta-glucan microfibrils on tobacco plasma membrane sheets. Proceedings of the National Academy of Sciences of the United States of America 95 (25): 15102-15106.

Hirai A, Tuji M, Horii F. (2000) Cellulose assemblies produced by Acetobacter xylinum under different conditions (Abstract) 219th ACS National Meeting, San Francisco, CA. March, 2000.

Irwin DC, Spezio M, Walker LP, Wilson DB. (1993) Activity studies of eight purified cellulases: specificity, synergism, and binding domain effects

Itoh T, O'Neil R, Brown RM Jr. (1983). The Assembly of Cellulose Microfibrils in Selected Siphonocladalean Algae. Journal of Cell Biology 97: A416-A416.

Itoh T. (1989). Biogenesis of cellulose microfibrils and the role of microtubules in green algae. In: Lewis NG & Paice MG, (ed), Plant Cell Wall Polymers, Biogenesis and Biodegradation, Vol 399, American Chemical Society Symposium Series (pp. 258–277). Amer. Chem. Soc., Washington, DC.

Jarvis M. (2003). Chemistry - Cellulose stacks up. Nature 426 (6967): 611-612.

Jervis, E. J., Haynes, C. A., Kilburn, D. G. (1997) Surface diffusion of cellulases and their isolated binding domains on cellulose. J. Biol. Chem. 272(38), 24016-24023.

Kimura S, Laosinchai W, Itoh T, Cui X, Linder CR, Brown Jr RM. (1999). Immunogold labeling of rosette terminal cellulose-synthesizing complexes in the vascular plant Vigna angularis. Plant Cell 11: 2075–2085.

Kondo, T. Togawa, E., and Brown, JR. R. M. (2000) Molecular images of glucan chains revealed in a new supermolecular structure of cellulose . Biomacromolecules (submitted)

Kudlicka K, Brown Jr RM. (1997). Cellulose and Callose Biosynthesis in Higher Plants (I. Solubilization and Separation of (1->3)- and (1->4)-[beta]-Glucan Synthase Activities from Mung Bean). Plant Physiology 115(2):643-656.

Kudlicka K, Wardrop A, Itoh T, Brown Jr RM. (1987). Further evidence from sectioned material in support of the existence of a linear terminal complex in cellulose synthesis. Protoplasma 136: 96–103.

Kuga S, Brown Jr RM. (1988). Silver labeling of the reducing ends of bacterial cellulose. Carb. Res. 180, 345-350.

Lai-Kee-Him J, Chanzy H, Muller M, Putaux JL, Imai T, Bulone V. (2002). in vitro versus in vivo cellulose microfibrils from plant primary wall synthases: structural differences. J Biol Chem 277: 36931-36939.

Lee I, Evans BR, Woodward J. (2000) The mechanism of cellulose action of cotton fibers: evidence from atomic force microscopy. Ultramicroscopy 82, 213-221.

Linder M, Salovuori I, Ruohonen L, Teeri TT. (1996). Characterization of a double cellulose-binding domain. J. Biol. Chem. 271(35), 21268-21272.

Lodish H, Baltimore D, Berk A, Zipursky SL, Matsudaira P, Darnell J (1995). Transport across cell membranes. In Molecular Cell Biology. American Scientific Books, New York, 3rd edition, pp 633-667.

Marchant HJ. (1978). Microtubules associated with the plasma membrane isolated from protoplasts of the green alga Mougeotia. Exp Cell Res 115: 25-30.

Marchant HJ, Hines ER. (1979). Role of microtubules and cell-wall deposition in elongation of regenerating protoplasts of Mougeotia. Planta 146 (1): 41-48.

Mazia D, Schatten G, Sale W. (1975). Adhesion of cells to surfaces coated with polylysine: applications to electron microscopy. J Cell Biol 66: 198-200.

Mazia D. (1975). Adhesion of cells to surfaces coated with polylysine. Applications to electron microscopy. Journal of Cell Biology 66: 198-200.

Mizuta S, Harada T. (1991). Formation of Cellulose Microfibrils on an Isolated Plasma Membrane of the Coenocytic Green Alga, Boergesenia forbesii. Botanica Marina 34: 411-415.

Montezinos D, Delmer DP. (1980). Characterization of inhibitors of cellulose synthesis in cotton fibers. Planta 148: 305-311.

Mueller SC, Brown Jr RM. (1980). Evidence for an intramembrane component associated with a cellulose microfibril synthesizing complex in higher plants. Journal of Cell Biology 84: 315–326.

Nagata T, Kumagai F. (1999). Plant cell biology through the window of the highly synchronized tobacco BY-2 cell line. Methods in Cell Science 21(2-3):123-127.

Nakashima J, Endo S, Fukuda H. (2004). Immunocytochemical localization of polygalacturonase during tracheary element differentiation in Zinnia elegans. Planta 218: 729-739.

Nakashima J, Laosinchai W, Cui XJ, Brown RM. (2003). New insight into the mechanism of cellulose and callose biosynthesis: proteases may regulate callose biosynthesis upon wounding. Cellulose 10 (4): 369-389.

Nidetzky B, Steiner W, Hayn M, Claeyssens M. (1994). Cellulose hydrolysis by the cellulases from *Trichoderma reesei*: a new model for synergistic interaction. Biochemical Journal 298, 705-710.

Nogales E, Whittaker M, Milligan RA, Downing KH. (1999). High-resolution model of the microtubule. Cell 96: 79-88.

Pear JR, Kawagoe Y, Schreckengost WE, Delmer DP, Stalker DM. (1996). Higher plants contain homologs of the bacterial celA genes encoding the catalytic subunit of cellulose synthase. Proceedings of the National Academy of Sciences of the United States of America 93 (22): 12637-12642.

Perrin RM. (2001). Cellulose: how many cellulose synthases to make a plant? Current Biology 11: R213–R216.

Persson S, Wei H, Milne J, Page G, Somerville C. (2005). Identification of genes required for cellulose synthesis by regression analysis of public microarray data sets. Proceedings of the National Academy of Sciences of the United States of America 102 (24): 8633-8638.

Ranby BG. (1952). Acta Chem. Scand. 6: 128.

Reiss HD, Schnepf E, Herth W. (1984). The plasma-membrane of the Funaria caulonema tip cell – Morphology and distribution of particle rosettes, and the kinetics of cellulose synthesis. Planta 160 (5): 428-435.

Ritcey AM, Gray DG. (1988). Induced CD provides evidence for helical solution conformation in cellulosic chains. Biopolymers 27, 479-491.

Robards AW. (1969). Particles associated with developing plant cell walls. Planta 88: 376-379.

Roberts E, Seagull RW, Haigler CH, Brown Jr RM. (1982). Alteration of cellulose microfibril formation in eukaryotic cells: Calcofluor White interferes with microfibril assembly and orientation in *Oocystis apiculata*. Protoplasma 113, 1-9.

Roelofsen A. (1958). Cell wall structure as related to surface growth. Acta Botanica Neerlandica 7: 77-89.

Roland JC, Vian B. (1991). General preparation and staining of thin sections. In: Hall JL, Hawes C (eds) Electron Microscopy of Plant Cells. Academic Press, San Diego, pp. 1-66.

Ruben, G. C. and Bokelman, G. H. (1987) Triple-stranded, left-hand-twisted cellulose microfibril. Carb. Res. 160, 434-444.

Ruben GC, Bokelman GH, Krakow W. (1989). Triple-stranded left-hand helical cellulose microfibril in Acetobacter xylinum and in Tobacco primary cell wall. Plant Cell Wall Polymers 20, 279-298.

Rudolph U, Gross H, Schnepf E. (1989). Investigations of the turnover of the putative cellulose-synthesizing particle rosettes within the plasma-membrane of Funaria-Hygrometrica protonema cells. 2. Rosette structure and the effects of cycloheximide, actinomycin-D, 2,6-dichlorobenzonitrile, Biofluor, heat-shock, and plasmolysis. Protoplasma 148 (2-3): 57-69.

Rudolph U, Schneph E. (1988). Investigations of the turnover of the putative cellulose-synthesizing particle rosettes within the plasma-membrane of Funaria-Hygrometrica protonema cells. 1. Effects of monensin and cytochalasin-B. Protoplasma 143 (1): 63-73.

Saxena IM, Brown Jr RM. (2005). Cellulose Biosynthesis: Current views and evolving concepts. Annals of Botany 96: 9-21.

Saxena IM, Lin FC, Brown Jr RM. (1990). Cloning and sequencing the cellulose synthase catalytic subunit gene of *Acetobacter xylinum*. Plant Molecular Biology 15 (5): 673-683.

Scheible WR, Eshed R, Richmond T, Delmer D, Somerville C. (2001). Modifications of cellulose synthase confer resistance to isoxaben and thiazolidinone herbicides in *Arabidopsis* Ixr1 mutants. Proceedings of the National Academy of Sciences of the United States of America 98 (18): 10079-10084.

Scheible WR, Pauly M. (2004). Glycosyltransferases and cell wall biosynthesis: novel players and insights. Current opinion in plant biology 7 (3): 285-295.

Seagull RW. (1990). Tip growth and transition to secondary wall synthesis in developing cotton hairs. In IB Heath, eds, Tip Growth in Plant and Fungal Cells. Academic Press, San Diego, pp 261-284.

Segui-Simarro JM, Austin JR, White EA, Staehelin LA. (2004). Electron tomographic analysis of somatic cell plate formation in meristematic cells of *Arabidopsis* preserved by high-pressure freezing. The Plant Cell 16: 836-856.

Shiroishi M, Amano Y, Nisizawa K, Hoshino E, Kanda T. (1997) Hydrolysis of various celluloses, (1,3),(1,4)-β-D-glucans and xyloglucan by three endo-type cellulases. Mokuzai Gakkaishi 43, 178-187.

Sild V, Ståhlberg J, Pettersson G, Johansson G (1996). Effect of potential binding site overlap to binding of cellulase to cellulose: a two-dimensional simulation. . FEBS Lett. 378(1), 51-56.

Somerville C, Bauer S, Brininstool G, Facette M, Hamann T, Milne J, Osborne E, Paredez A, Persson S, Raab T, Vorwerk S, Youngs H. (2004). Toward a systems approach to understanding plant-cell walls. Science 306 (5705): 2206-2211.

Sonobe S, Takahashi S. (1994). Association of microtubules with the plasma-membrane of tobacco by-2 cells in-vitro. Plant and cell physiology 35 (3): 451-460.

Sonobe S. (1990). ATP-dependent depolymerization of cortical microtubules by an extract in tobacco BY-2 cells. Plant Cell Physiology 31: 1147-1153.

Srisodsuk M, Lehtio J, Linder M, Margolles-Clark E, Reinikainen T, Teeri TT. (1997). *Trichoderma reesei* cellobiohydrolase I with an endoglucanase cellulose-binding domain: Action on bacterial microcrystalline cellulose. J. Biotech. 57, 49-57.

Ståhlberg J, Johansson G, Pettersson G. (1993). *Trichoderma reesei* has no true exo-cellulase: all intact and truncated cellulases produce new reducing end groups on cellulose. Biochem. J. 298, 705-710.

Sugiyama J, Harada H, Fujiyoshi Y, Uyeda N. (1985).. Lattice images from ultrathin sections of cellulose microfibrils in the cell wall of Valonia macrophysa Kutz. Planta 166, 161-168.

Taylor NG, Howells RM, Huttly AK, Vickers K, Turner SR. (2003). Interactions among three distinct CesA proteins essential for cellulose synthesis. Proceedings of the National Academy of Sciences of the United States of America 100 (3): 1450-1455.

Teeri TT, Koivula A, Linder M, Wohlfahrt G, Divne C, Jones TA. (1998). *Trichoderma reesei* cellobiohydrolases: why so efficient on crystalline cellulose? Biochem Soc Trans. 26, 173-8.

Tomme P, Warren RAJ, Gilkes NR. (1995). Cellulose hydrolysis by bacteria and fungi. Adv. Microbial Physiol. 37: 1-81.

Vacquier VD. (1975). The isolation of intact cortical granules from sea urchin eggs: calcium ions trigger granule discharge. Developmental Biology 43:62-74.

Väljamäe P, Sild V, Pettersson G, Johansson G. (1998). The initial kinetics of hydrolysis by cellobiohydrolases I and II is consistent with a cellulose surface - erosion model. Eur. J. Biochem., 253 469-475.

Van der Valk P, Fowke LC. (1981). Ultrastructural aspects of coated vesicles in tobacco protoplasts. Can J Bot 59: 1307-1313.

Van der Valk P, Rennie PJ, Connolly JA, Fowke LC. (1980). Distribution of cortical microtubules in tobacco protoplasts - an immunofluorescence microscopic and ultrastructural-study. Protoplasma 105 (1-2): 27-43.

Westafer JM, Brown Jr RM. (1976). Electron-microscopy of cotton fiber – New observations on cell-wall formation. Cytobios 15 (58-5): 111-138.

White AR, Brown Jr RM. (1981). Enzymatic hydrolysis of cellulose: visual characterization of the process. Proc. Natl. Acad. Sci. USA 78(2), 1047-1051.

Williamson FA, Fowke LC, Weber G, Constabel F, Gamborg O. (1977). Microfibril deposition on cultured protoplasts of *Vicia hajastana*. Protoplasma 91: 213-219.

Willison JHM, Rowe AJ. (1980). Replica, shadowing and freeze- etching techniques. In: Practical Methods in Electron Microscopy, vol 8 (ed. A. M. Glauert). Amsterdam, New York, Oxford: North-Holland Publishing Company.

Willison JHM, Cocking EC. (1975). Microfibril synthesis at the surfaces of isolated tobacco mesophyll protoplasts, a Freeze-etch study. Protoplasma 84: 147-159.

Wood TM, Garcia-Campayo V. (1990). Enzymology of cellulose degradation. Biodegradation 2, 147-161.

Zhong RQ, Burk DH, Morrison WH, Ye ZH. (2002). A kinesin-like protein is essential for oriented deposition of cellulose microfibrils and cell wall strength. Plant Cell 14 (12): 3101-3117.

VITA

Andrew Jason Bowling was born in Kansas City, Missouri on August 18, 1975, the son of LaDona Beth and John Walter Bowling. He attended James E. Taylor High School in Katy, Texas and received a Bachelor of Science in Botany from the University of Texas at Austin in December 1997. He was a teaching assistant for two semesters for Laboratory experience in Cell Biology and ten semesters for Laboratory experience in Genetics. He was awarded an Outstanding Teaching Assistant award in 2001. He published a paper entitled "Rotation of cellulose ribbons during degradation with fungal cellulase" in Cellulose 8, 91-97, 2001.

Permanent Address: 4817 Harmon Avenue, Austin, Texas 78751

This dissertation was typed by the author.